DISSERTATION

ASSESSING LONG-TERM CONSERVATION OF GROUNDWATER RESOURCES IN THE OGALLALA AQUIFER REGION USING HYDRO-AGRONOMIC MODELING

Submitted by

Zaichen Xiang

Department of Civil and Environmental Engineering

In partial fulfillment of the requirements

For the Degree of Doctor of Philosophy

Colorado State University

Fort Collins, Colorado,

Spring 2022

Doctoral Committee:

Advisor: Ryan T. Bailey

Jeffrey Niemann
Aditi Bhaskar
Jordan Suter

ABSTRACT

ASSESSING LONG-TERM CONSERVATION OF GROUNDWATER RESOURCES IN THE OGALLALA AQUIFER REGION USING HYDRO-AGRONOMIC MODELING

Groundwater is vital for domestic use, municipalities, agricultural irrigation, industrial processes, etc. Over the past century, excessive groundwater depletion has occurred globally and regionally, notably in arid and semi-arid regions, often due to providing irrigation water for crop cultivation. The High Plains Aquifer (HPA) is the largest freshwater aquifer in the United States and has experienced severe depletion in the past few decades due to excessive pumping for agricultural irrigation. There is a need to determine management strategies that conserve groundwater, thereby allowing irrigation for coming decades, while maintaining current levels of crop yield within the context of a changing climate. Numerical models can be useful tools in this effort. Hydrologic models can be used to assess current and future storage of groundwater and how this storage depends on system inputs and outputs, whereas agronomic models can be used to assess the impact of water availability on crop production. Linking these models to jointly assess groundwater storage and crop production can be helpful in exploring management practices that conserve groundwater and maintain crop yield under future possible climate conditions. The objectives of this dissertation are: i) to develop a linked modeling system between DSSAT, an agronomic model, and MODFLOW, a groundwater flow model to be used for evaluating long-term impacts of climate and management strategies on water use efficiency and farm profitability of agricultural systems while managing groundwater sustainably; ii) to use the DSSAT-MODFLOW modeling system in a global sensitivity analysis framework to

determine the system factors (climate, soil, management, aquifer) that control crop yield and groundwater storage in a groundwater-stressed irrigated region, thereby pointing to possibilities of efficient management; and iii) to quantify the effect of groundwater conservation strategies and climate on crop yield and groundwater storage to identify irrigation and planting practices that will maintain adequate crop yield while minimizing groundwater depletion. These three objectives are applied to the hydro-agronomic system of Finney County, Kansas, which lies within the HPA.

Major findings include: 1) climate-related parameters significantly affect crop yields, especially for maize and sorghum, and soybean and winter wheat yields are sensitive to a combination of cultivar genetic parameters, soil-related parameters, and climate-related parameters; 2) Climatic parameters account for 44%, 29%, 40%, and 36% variation in yield of maize, soybean, winter wheat, and sorghum; 3) Hydrogeologic parameters (aquifer hydraulic conductivity, aquifer specific yield, and riverbed conductance) have a relatively low influence on crop yields; 4) water table elevation, recharge, and irrigation pumping are considerably sensitive to soil- and climate-related parameters, while ET, river leakage, and groundwater/aquifer discharge are highly influenced by hydrogeological parameters (e.g., riverbed conductance, and specific yield); 5) the best management practice is the combination of implementing drip irrigation and planting quarter plots under both dry and wet future climate conditions. Other irrigation systems (sprinkler) and planting decisions (half-plots) can also be implemented without severe groundwater depletion. If crop yield is to be maintained in this region of the HPA, groundwater depletion can be minimized but not completely prevented. Results highlight the need for implementing new irrigation technologies, and likely changing crop type decisions (e.g.,

limiting corn cultivation) in coming decades in this region of the HPA. Results from this dissertation can be used in other groundwater-irrigated regions facing depletion of groundwater.

ACKNOWLEDGEMENTS

This work was supported by the National Institute of Food and Agriculture, U.S. Department of Agriculture, under award number 2016-68007-25066, “Sustaining agriculture through adaptive management to preserve the Ogallala aquifer under a changing climate."

TABLE OF CONTENTS

CHAPTER 1 - INTRODUCTION AND OBJECTIVES

1.1 INTRODUCTION

Groundwater resources are used for domestic use, municipalities, agricultural irrigation, industrial processes, etc. Groundwater provides drinking water for 30% of the world's population and 47% of the rural population. Of the groundwater used globally, 43% is for crop irrigation and 24% is for industrial applications. Over the past century, groundwater resources have declined rapidly, notably in arid and semi-arid regions due to over-extraction for irrigation and lack of other viable water sources for irrigation and drinking water. Groundwater globally depleted by about 4,500 km^3 during 1900 – 2008, with depletion rates of 126 $km^3\ yr^{-1}$ in 1960 to 283 $km^3\ yr^{-1}$ in 2000 and, regionally, 1000 km^3 in the United States during 1900 – 2008; 170.3 km^3 in North China Plain during 1900 – 2008; 91.3 km^3 in north-central Middle East during 2003 – 2009; and 1.5 km^3 in the Nairobi aquifer, Kenya since 1950.

The High Plains Aquifer (HPA) is the largest fresh groundwater resources in the U.S. to provide 30% of total crop and animal production nationally. Due to excessive pumping for agricultural irrigation, the HPA has experienced severe depletion in the past few decades. Between 1960 and 2008, groundwater storage has decreased by 360 km^3, accounting for 36% of total groundwater depletion in U.S.A, while the change in water table elevation varies from a decline of 78 m (256 ft) to a rise of 26 m (85 ft), with an average of 5 m (16 ft) in decline, accounting for 9% of the area-weighted average saturated thickness. Declines have taken place mainly in Eastern Colorado, Southwest Kansas, the Panhandle of Oklahoma, and Northwest Texas. Increases have occurred in Central Nebraska due to higher precipitation rates,

composition of soil layer (e.g., the sandy soils that allow more infiltration and percolation) and the presence of streams for surface water irrigation. Besides exhausting a valuable resource, and therefore limiting future use of groundwater for irrigation and crop production, groundwater depletion can result in many negative issues, such as land subsidence and associated damage to infrastructure, wetland degradation, lowering well pumping capacity, increase in pumping costs, and reduction or cessation of groundwater discharge to streams.

Land management strategies are needed to conserve groundwater in the High Plains Aquifer. These strategies must be implemented in accordance with expected changes in future climate patterns in the region. As the aquifer region covers a broad area of the United States, strategies must be adapted for local conditions. Spatially distributed, physically based hydro-agronomic models can be a key tool in assessing the impacts of climate, land management, and local cultivation practices and conditions, to 1) enhance understanding of the interplay between cultivation, crop growth, climate, and groundwater resources and 2) identify strategies that can provide the highest degree of groundwater conservation while maintaining crop yield (i.e. economic prosperity) in the region.

1.2 OBJECTIVES

Hydrologic models can be used to assess current and future storage of groundwater and how this storage depends on system inputs and outputs, whereas agronomic models can be used to assess the impact of water availability on crop production. Linking these models to jointly assess groundwater storage and crop production can be helpful in exploring management practices that conserve groundwater and maintain crop yield with future climate conditions.

This dissertation aims to:

1. develop a linked modeling system between DSSAT, an agronomic model, and MODFLOW, a groundwater flow model to be used for evaluating long-term impacts of climate and management strategies on water use efficiency and farm profitability of agricultural systems while managing groundwater sustainably;
2. use the DSSAT-MODFLOW modeling system in a global sensitivity analysis framework to determine the system factors (climate, soil, management, aquifer) that control crop yield and groundwater storage in a groundwater-stressed irrigated region; and
3. quantify the effect of groundwater conservation strategies and climate on crop yield and groundwater storage to identify irrigation and planting practices that will maintain adequate crop yield while minimizing groundwater depletion.

These three objectives are applied to the hydro-agronomic system of Finney County, Kansas, which lies within the Ogallala Aquifer Region. As with many areas within the Ogallala Aquifer Region, Finney County has experienced significant groundwater depletion in recent decades due to irrigation practices, and future economic prosperity depends on future groundwater conservation.

Each objective forms the basis for a journal article. The first objective has been summarized in a paper published in Agricultural Water Management: "DSSAT-MODFLOW: A new modeling framework for exploring groundwater conservation strategies in irrigated areas", *Agricultural Water Management* 232 (2020) (Xiang et al., 2020). The second objective has been summarized in a manuscript submitted to *Journal of Hydrology*: "Using DSSAT-MODFLOW to Determine the Controls of Groundwater Storage and Crop Yield in Groundwater-Based Irrigated Regions". The third objective is summarized in a manuscript that will be submitted to *Water Resources Research*.

REFERENCES

Xiang, Z., Bailey, R.T., Nozari, S., Husain, Z., Kisekka, I., Sharda, V., Gowda, P., 2020. DSSAT-MODFLOW: A new modeling framework for exploring groundwater conservation strategies in irrigated areas. Agricultural Water Management 232. https://doi.org/10.1016/j.agwat.2020.106033

CHAPTER 2 - DSSAT-MODFLOW: A NEW MODELING FRAMEWORK FOR EXPLORING GROUNDWATER CONSERVATION STRATEGIES IN IRRIGATED AREAS[1]

2.1 INTRODUCTION

Excessive groundwater depletion occurs in various regions of the world (Konikow and Kendy, 2005), principally due to intensive use of groundwater for irrigation in arid and semi-arid regions. According to a recent global study using hydrologic models, total global groundwater depletion had increased from 126 $km^3\ yr^{-1}$ in 1960 to 283 $km^3\ yr^{-1}$ in 2000 (Wada et al., 2010). In the first 8 years of the 21st century, total groundwater consumption was more than 1100 km^3, approximately one-fourth the entire depletion experienced during the 20th century (Konikow, 2011). Groundwater depletion has led to decreasing well yields, increased pumping costs, land subsidence and associated damage to infrastructure, wetland degradation, reduction in groundwater discharge to streams, and seawater intrusion in coastal areas (Aeschbach-Hertig and Gleeson, 2012; Famiglietti, 2014; Konikow and Kendy, 2005; Motagh et al., 2008; Varela-Ortega et al., 2011; Werner, 2010; Zhang et al., 2014)

Although groundwater sustainability, i.e. the use of groundwater without causing a decrease in groundwater storage, may not be possible for many arid and semi-arid regions, land and water management strategies can be pursued to minimize groundwater depletion while maintaining adequate crop yield for local populations and export. Often, numerical models are use[1]d to explore the impact of various management strategies on groundwater storage and crop yield. These modeling approaches can be classified into three broad modeling groups: 1) groundwater-based, 2) agronomic-based, and 3) linked agronomic-groundwater-based models.

[1] This paper has been published in Agricultural Water Management: "DSSAT-MODFLOW: A New Modeling Framework for Exploring Groundwater Conservation Strategies in Irrigated Areas", *Agricultural Water Management* 232 (2020)

Groundwater-based approaches use numerical groundwater flow models to simulate groundwater head, groundwater flow, and groundwater storage under a variety of management scenarios. Examples include Ebraheem et al. (2003), Dawoud et al. (2005), Mao et al. (2005), and Mylopoulos (2007), who used process-based groundwater flow models to investigate the impact of groundwater management options on groundwater storage and conservation in southwest Egypt, the Nile River Valley, northern China, and northern Greece, respectively. Models used in these studies include MODFLOW (Harbaugh, 2005), a finite difference groundwater flow model, and TRIWACO (Dawoud et al., 2005), a finite element groundwater flow model. Management strategies include reduction in pumping, new irrigation canals, irrigation patterns, and increase in irrigation efficiency. MODFLOW with the Farm Process (MF-FMP) (Schmid et al., 2006), which includes routines for plant consumptive use of water, was employed by Hanson et al. (2010) to evaluate sources of irrigation water for Central Valley, California. A recent study (Wada et al., 2012) linked global-scale hydrological land surface (PRC-GLOBWB) and groundwater (MODFLOW) models to simulate changes in global groundwater storage due to climate and groundwater pumping. These groundwater-based approaches, while successfully simulating groundwater energy and flow in aquifers, neglect the effect of groundwater management strategies on crop yield.

In contrast, agronomic-based approaches simulate the effect of the interactions between genetics, weather and management (e.g. irrigation management) on crop growth, but do not account for the impact of groundwater availability on irrigation capacity and associated crop yield. Yang et al. (2006) used the DSSAT crop growth model (Jones et al., 2003) to optimize water use during the stages of leaf and ear growth of wheat, to minimize groundwater depletion in the north China Plains while Kisekka et al. (2015) used DSSAT to assess effects of various

irrigation management strategies on maize in western Kansas. Other agronomic models that have been used to explore irrigation impact on crop yield include EPIC (Williams et al., 1989), the SIMDualKc model (Rolim et al., 2006; Rosa and Paredes, 2011; Wu et al., 2015), AquaCrop (Raes et al., 2009), and APSIM (Keating et al., 2003). These models typically are applied to one-dimensional soil profiles to represent field-scale dynamics.

A third approach links two or more single-domain models to form an integrated agronomic-hydrologic modeling system. The developers of these integrated models strive to assess impacts of water management strategies on both groundwater storage and crop yield. The Soil and Water Assessment Tool (SWAT) (Arnold et al., 1998) simulates land surface hydrology and crop yield for a collection of hydrologic response units (HRUs) within a watershed, and has manual irrigation or auto-irrigation routines tied to both surface water sources and groundwater. However, groundwater flow in the aquifer and groundwater discharge to streams is simulated using simplistic flow and lagging equations, without consideration of aquifer heterogeneity or regional groundwater flow patterns. Cai et al. (2003) and Bulatewicz et al. (2010) developed specialized hydrologic-agronomic-economic modeling systems for irrigated river basins, with the latter using the EPIC model for crop yield simulation and the Analytical Element Model (Strack, 1989) for groundwater flow. Xu et al. (2012) linked MODFLOW with SWAP (Soil-Water-Atmosphere-Plant) to provide a modeling system that estimates recharge and evapotranspiration fluxes in groundwater systems, but did not apply it to groundwater management scenarios. Varela-Ortega et al. (2011) applied a linked WEAP-economic model to the Upper Guadiana basin in central Spain to analyze effects of water and agricultural policies; however, the modeling system did not use process-based groundwater flow. Hadded et al. (2013) developed the decision support system WEAP (Water Evaluation and Planning)-MODFLOW for

groundwater management in Tunisia, with WEAP passing water use to MODFLOW to simulate pumping and groundwater levels. Pokhrel et al. (2015) modified a global Land Surface Model (LSM) to include groundwater dynamics, groundwater pumping, irrigation, and crop growth to simulate groundwater depletion at the global scale and also for specific aquifers in the USA. More recently, Bailey et al. (2016) published a linked SWAT-MODFLOW, but the modeling system has not yet been applied to groundwater management scenarios in irrigated regions.

Typically, the modeling systems in this third approach are designed for large (river basin, global) spatial and temporal scales, without consideration of field-scale crop yield, strategies, and conditions (e.g., soil, depth to water table, pumping depth, etc.). There is a need for a modeling framework that addresses field-scale cropping conditions while accounting for groundwater availability in space and time throughout the aquifer system. To assess groundwater storage and crop yield simultaneously over time under various management strategies, groundwater pumping should be dependent on crop water demand, and applied irrigation depths and timing should be constrained by available groundwater volumes and actual pumping rates (i.e., well capacity).

The objective of this chapter is to present a linked agronomic-hydrological modeling system that can be used to evaluate alternative management strategies conducive to both groundwater management and crop production sustainability in groundwater-based irrigated regions. The modeling framework links the DSSAT model with MODFLOW, with one DSSAT simulation for each cultivated field within the MODFLOW aquifer modeling domain. Linkage occurs on an annual basis, with DSSAT-simulated irrigation depths and deep percolation converted to pumping rates and recharge for MODFLOW, respectively. For the following season, saturated thickness simulated by MODFLOW constrains pumping rates, irrigation

depths, and timing for each pumping well. The scheme is demonstrated for Finney County, Kansas, a portion of the Ogallala aquifer region experiencing severe groundwater depletion due to extensive groundwater pumping for irrigation. Whereas this paper focuses on the presentation of the model and a demonstration example, future studies can focus on assessing and quantifying the impact of conservation strategies on both groundwater storage and crop yield.

2.2 DEVELOPMENT OF DSSAT-MODFLOW MODELING SYSTEM

2.2.1 MODEL OVERVIEW

2.2.1.1 DECISION SUPPORT SYSTEM FOR AGROTECHNOLOGY TRANSFER (DSSAT)

The Decision Support System for Agrotechnology Transfer (DSSAT) is a software application program that comprises crop simulation models for over 40 crops. DSSAT is supported by data base management programs for soil, weather, crop management and experimental data, and by utilities and application programs. The crop simulation models simulate growth, development and yield as a function of the soil-plant-atmosphere dynamics. DSSAT and its crop simulation models have been used for many applications ranging from on-farm and precision management to regional assessments of the impact of climate variability and climate change. The crop models require daily weather data, soil surface and profile information, and detailed crop management as input (e.g., irrigation schedules). Crop genetic information is defined in a crop species file that is provided by DSSAT and cultivar or variety information that is provided by the user. Simulations are initiated either at planting or prior to planting through the simulation of a bare fallow period. The simulations are conducted at a daily time step and, in some cases, at an hourly time step depending on the process and the crop model. At the end of the day the plant and soil water, nitrogen and carbon balances are updated, as well as the crop's vegetative and reproductive development stage. DSSAT integrates the effects of soil, crop

cultivar, weather and management options, and allows users to ask "what if" question by conducting virtual simulation experiments.

DSSAT also provides for evaluation of crop model outputs with experimental data, thus allowing users to compare simulated outcomes with observed results. This is critical prior to any application of a crop model, especially if real-world decisions or recommendations are based on modeled results. Crop model evaluation is accomplished by inputting the user's minimum data, running the model, and comparing outputs with observed data. DSSAT includes improved application programs for seasonal, spatial, sequence and crop rotation analyses that assess the economic risks and environmental impacts associated with irrigation, fertilizer and nutrient management, climate variability, climate change, soil carbon sequestration, and precision management (Hoogenboom et al., 2019)

2.2.1.2 MODFLOW

The MODFLOW (Harbaugh, 2005) is a physically-based, spatially-distributed groundwater flow model that solves the groundwater flow equation for spatial- and time-dependent groundwater hydraulic head using the finite difference method. It can be used to simulate groundwater flow in both confined and unconfined aquifers. The aquifer model domain is discretized into cells laterally and vertically, with uniform properties of the aquifer (e.g., hydraulic conductivity, specific storage, and specific yield) within a grid cell. The MODFLOW can be run for steady-state or transient conditions, with the latter simulating groundwater head for each grid cell at each time step of the simulation period. The time domain is divided into stress periods, with each stress period divided into time steps. A stress period is a length of simulation time over which all groundwater stresses (e.g., recharge, pumping) remain constant.

2.2.2 DSSAT-MODFLOW MODELING SYSTEM

The linked DSSAT-MODFLOW modeling system developed in this study is based on a simulation loop that passes data between DSSAT and MODFLOW on an annual basis. This system therefore assumes that crop growth is not dependent on the position of the water table, as there is no feedback between MODFLOW and DSSAT during the growing season. The current version of the model therefore may not be applicable regions with shallow water tables. The linkage process and annual simulation loop are summarized in the schematic shown in Fig. 2-1.

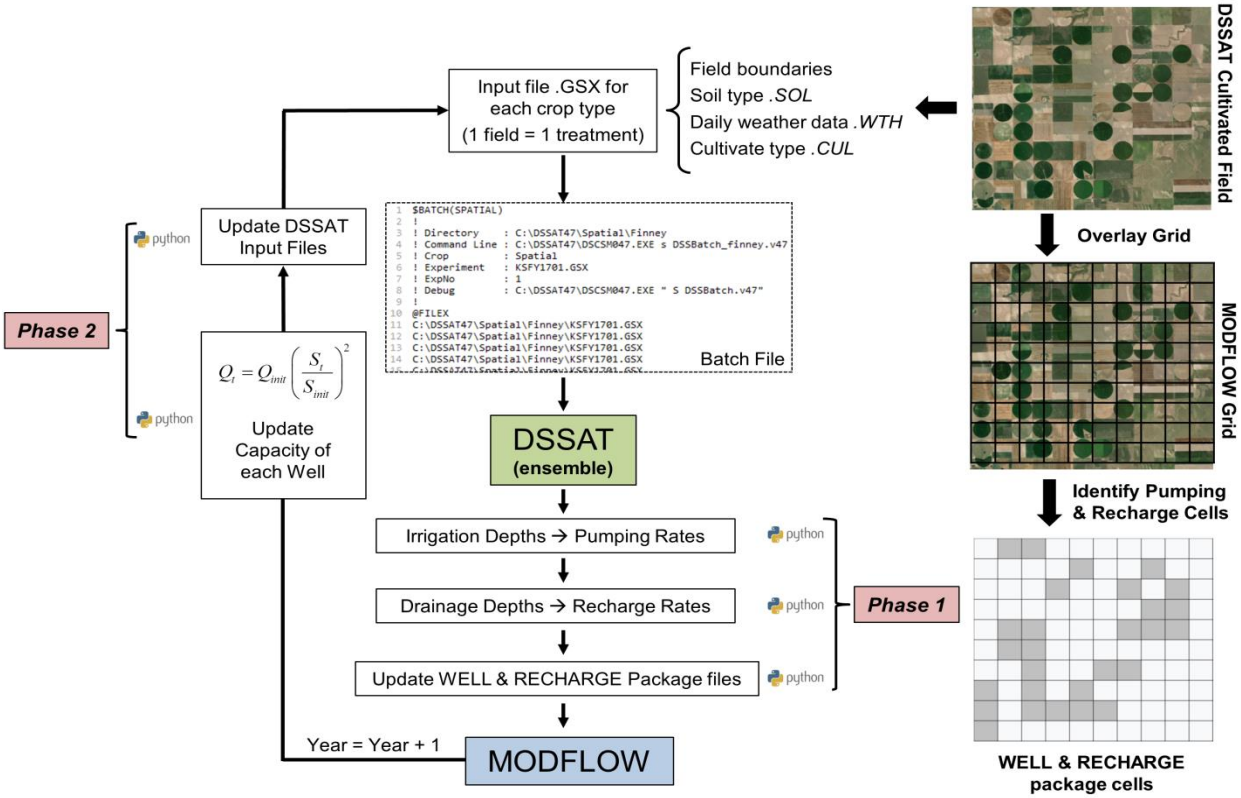

Fig. 2-1. Schematic showing the procedure of linking multiple DSSAT simulations with a MODFLOW model. The modeling framework consists of a batch of DSSAT simulations, a MODFLOW model, and two Python scripts to transfer data between the models.

For a selected model domain, one DSSAT model is run for each cultivated field according to field boundaries (to calculate total cultivated area), soil type, daily weather data, and cultivar type. Mapping DSSAT output to MODFLOW, and vice versa, is explained in the following sub-sections.

Step 1: Ensemble of DSSAT Simulations

The DSSAT model is used to simulate crop yield and water use. The Spatial module/utility with a batch file is used to simulate the ensemble of DSSAT field simulations within the model domain. The batch file contains a list of all main .GSX input files (*see Fig. 2-S1 in Appendices for example*), with one .GSX input file for each crop type within the model domain. Within each .GSX file, weather data, soil type, cultivar type, planting schedule, and irrigation method, are specified for each field of that crop type (*see Fig. 2-S2 in Appendices for example*). Within each simulation, DSSAT calculates the applied irrigation depths/amount (mm) throughout the growing season for each field.

Step 2: Linkage Phase 1 (DSSAT → MODFLOW)

Phase 1 in the linkage process converts DSSAT output to MODFLOW input, using a Python script. Pumped groundwater volumes are mapped to MODFLOW's grid cells (rows and columns) (see gray cells on the MODFLOW grid in Fig. 2-1) using the intersected portion of each field in each grid cell, and then written to a text file for MODFLOW's Well package, which lists the rate and corresponding layer, row, and column of each pumping cell active during the current growing season. As irrigation occurs only for a fraction of days during the growing season, consequently most daily pumping rates are 0. For the case of a field containing multiple irrigation wells, water use is proportionally distributed to each irrigation well according to the ratio of authorized withdrawal quantity of each singe well.

Recharge volumes for each grid cell are written to a text file for MODFLOW's Recharge package. Total recharge includes precipitation recharge and irrigation return recharge. As DSSAT simulations account for precipitation, precipitation recharge is estimated only for cells that do not contain a cultivated field, or for cultivated field cells during the non-growing season. Precipitation recharge can be estimated using a number of techniques. For the application shown

in this paper (Section 2.3), precipitation recharge is computed using a power function (Liu et al., 2010). For cells that contain a cultivated field, recharge from irrigation events is assumed to be equal to the daily deep percolation from the bottom of the soil profile, as simulated by DSSAT. The depth of deep percolation is multiplied by the field area to provide a daily volumetric flow rate, and then mapped to the intersected grid cells. The volume of recharge for each cell is then divided by the cell area, to provide a rate in L/T for inclusion in MODFLOW's Recharge package. (*see Fig. 2- S3 in Appendices for one year example*)

Step 3: MODFLOW Simulation

Following the conclusion of annual DSSAT runs and the conversion of irrigation depths to pumping rates, the MODFLOW simulation is run for the year to simulate groundwater hydraulic head (i.e., water table elevation for unconfined aquifers) for each finite difference grid cell. Daily stress periods are used to account for daily pumping rates provided by DSSAT. The groundwater head values at the end of the year are used to compute saturated thickness (i.e., groundwater head - bedrock elevation), which is used to update well capacity for each pumping well, as discussed in Step 4. The final groundwater head values at the end of the year are used as initial conditions for the simulation of the following year.

Step 4: Linkage Phase 2 (MODFLOW → DSSAT)

Phase 2 of the linkage process has two main purposes: (1) compute a new well capacity for each pumping well, and (2) update irrigation parameters in the DSSAT simulations that rely on the well capacity. The impact of groundwater decline expressed in the form of well capacity on grain yield and a producer's irrigation decisions were demonstrated in Araya et al. (2018) and Rouhi Rad et al. (2019), respectively. In this study, well capacity is defined as the maximum rate at which the well can reasonably operate, given the local saturated thickness of the aquifer.

Well capacity Q_t [L^3/T] is updated (see Figure 1) using the following relationship for unconfined aquifers (Harman, 1966):

$$Q_t = Q_{init}\left(\frac{S_t}{S_{init}}\right)^2 \quad (2\text{-}1)$$

Where Q_{init} and S_{init} are the pumping rate [L^3/T] and aquifer saturated thickness [L] at some designated time $t = 0$, and S_t is the aquifer saturated thickness [L] after t years. Saturated thickness S_t is calculated for each grid cell as the difference between the MODFLOW-simulated groundwater head (approximately equivalent to the water table in unconfined aquifers) and the bedrock elevation, with the latter often specified as the bottom of the lowest layer in the MODFLOW model.

The IFREQ (Irrigation Frequency) and IRAMT (Irrigation Application Depth) parameters control irrigation application in DSSAT simulations. The IFREQ parameter relates to the minimum number of days between irrigation events, which is equal to the time (days) required to irrigate the field, and IRAMT (mm) is the irrigation management depth. These parameters are listed in the .GSX input files of DSSAT. The values for these two parameters are constrained by the rate at which the groundwater can be extracted from the aquifer, i.e., the well capacity of the pumping well supplying the groundwater as well as the amount of area irrigated. In this way, the updated well capacity of each pumping well as provided by MODFLOW is used to constrain the irrigation capacity simulated by DSSAT for each irrigated field in the model domain. To update IFREQ for each field, an assumption is made that 2.54 cm (1 inch) of water is supplied to the entire field. The time required to apply irrigation is then calculated by dividing the volume of water applied to the field by the well capacity Q_t for the pumping well that provides water to the field. If IFREQ is calculated to be longer than 14 days, which is assumed to

be the longest time for a single irrigation event, then IFREQ is set to 14 days and instead the depth of irrigation IRAMT is re-calculated to provide a depth < 2.54 cm (1.0 inch).

Step 5: Multiple-Year Simulation

Multiple-year simulations are feasible through a batch file (*see Fig. 2-S4 in Appendices for one year example*) that contains a series of command-lines for looping simulations under the environment of DOS, OS/2, or Microsoft Windows. Command-lines in the batch are divided into blocks in terms of year, since the linked model exchange information annually, which is user-friendly to prepare a batch file for the simulations of the linked model.

2.2.3 Model CAPABILITIES AND LIMITATIONS

Although not performed in this current study, the DSSAT-MODFLOW modeling system as explained in Section 2.2.2 can be used to explore alternative groundwater conservation strategies in irrigated areas, with both crop yield (on a field-by-field basis) and water table elevation and saturated thickness (on a cell-by-cell basis) tracked each year in the simulation period. The model can also be run under varying climate patterns to investigate the impact of climate on management scenarios. The variation of water table elevation and simulated crop yields are dynamically linked together through pumping rates and irrigation application timing and depth, which is conducive to making comprehensive sustainable groundwater use plans.

Currently, the linked model does not simulate water movement in the vadose zone, i.e., between the bottom of the soil layer and the top of water table. In the current system, deep percolation from the bottom of the soil profile, as simulated by DSSAT, and precipitation-based recharge, as simulated by a power function, are assumed to reach the water table instantaneously. Future versions of the modeling system could use the UZF (Unsaturated Zone Flow) package of MODFLOW to route the near-surface percolation water to the water table.

2.3 APPLICATION OF DSSAT-MODFLOW: FINNEY COUNTY, KANSAS

2.3.1 STUDY REGION

The Ogallala aquifer (also often referred to as the High Plains Aquifer) underlies approximately 45,000 km^2 and portions of South Dakota, Wyoming, Nebraska, Colorado, Kansas, Oklahoma, New Mexico, and Texas (Fig. 2-2), providing water for about one fifth of all irrigated cropland in the USA and 30% of total crop and animal production in the USA (Guru and Horne, 2001; Rosenberg et al., 1999). The composition of aquifer material includes poorly sorted clay, silt, sand, and gravel, while the composition of bedrock unit is siltstone, shale, loosely to moderately cemented clay and silt, chalk, limestone, dolomite, conglomerate, claystone, gypsum, anhydrite, and bedded salt. The elevation of the aquifer bedrock is from 366 m (1200 ft) to 1829 m (6000 ft) above NGVD 29 (Gutentag et al., 1984).

Approximately 88% of the water pumped from the Ogallala aquifer is used for irrigated agriculture, in comparison with 60% of agricultural irrigation that is dependent on groundwater overall in the USA (Gollehon and Winston, 2013; Scanlon et al., 2012). The agricultural area makes up 41% of total land area in the Ogallala Aquifer Region (OAR), which contain 53% row crops, 33% small grains, and 14% pasture, alfalfa, and fallow lands. Furthermore, the agricultural land use supplies a large percentage of the total crop and animal production for the United States, including 19% of wheat, 19% of cotton, 15% of corn, 3% of sorghum, and about

18% of cattle and swine production ("USGS High Plains Aquifer WLMS: Physical/Cultural Setting," n.d.).

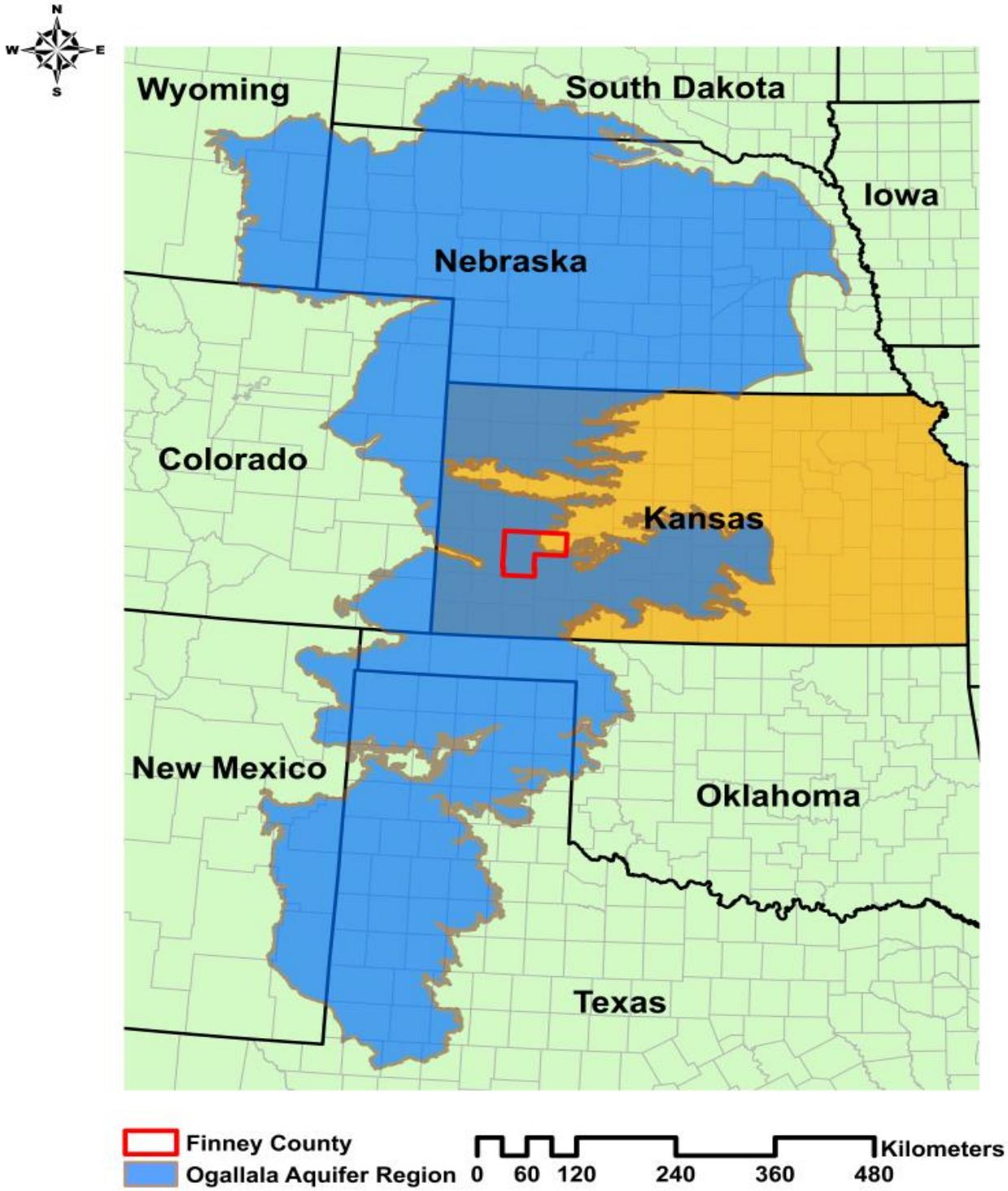

Fig. 2-2. Map of study region of Finney County in the Ogallala Aquifer. The area of Finney County is enclosed with the red contour line. The blue domain is the Ogallala Aquifer, and the states are separated by black lines.

Due to excessive pumping for irrigation, the rate of groundwater depletion has increased from 2.6 km^3 yr^{-1} during 1900 – 2000 to 12.5 km^3 yr^{-1} during 2003-2013 (Famiglietti, 2014), with 6% of the amount of groundwater storage decreased from the predevelopment period (1950s) during the 20^{th} century (McGuire et al., 2003). The change in water table elevation from predevelopment to 2015 ranges from a decline of 78 m (256 ft) to a rise in 26 m (85 ft), with an average of 5 m (16 ft) decline (McGuire, 2014). Declines occur primarily in eastern Colorado, southwest Kansas, Oklahoma, and Texas, and rises in central Nebraska. Saturated thickness ranges from > 305 m (1,000 ft) in central Nebraska to < 15 m (50 ft) in large regions of eastern Colorado, western Kansas, and west Texas. According to Haacker et al. (2016), current rates of decline in parts of the southern and central High Plains regions may result in a near-complete depletion of groundwater in the next 20-30 years and an associated cessation of irrigation.

Finney County, Kansas (see Fig. 2-2 for county outline) is selected as the study area for the DSSAT-MODFLOW application (Fig. 2-2) due to its high dependence on groundwater for irrigation (roughly 97% of the total groundwater withdrawals) and a resulting 15-meter (50-feet) average decline in water table elevation in the majority of the county since 1950. Groundwater is used to irrigate 105,218 hectares (260,000 acres), using 1629 irrigation wells.

Fig. 2-3A shows a map of average water table elevation (m) during the 1997-2007 period, obtained by interpolating between 522 observation wells in the county. Water table elevation values for the wells were obtained from the Kansas Geological Survey's (KGS) Water Well Levels Database (WIZARD) and the KGS Water Well Completion Records Database (WWC5). About 10% of the point values were not involved in interpolation for calculating the interpolation error. The Ordinary Kriging method under Geostatistical Analyst Extension in ArcMap was used to make the interpolated surface of water table elevation maps for different years. Fig. 2-3B

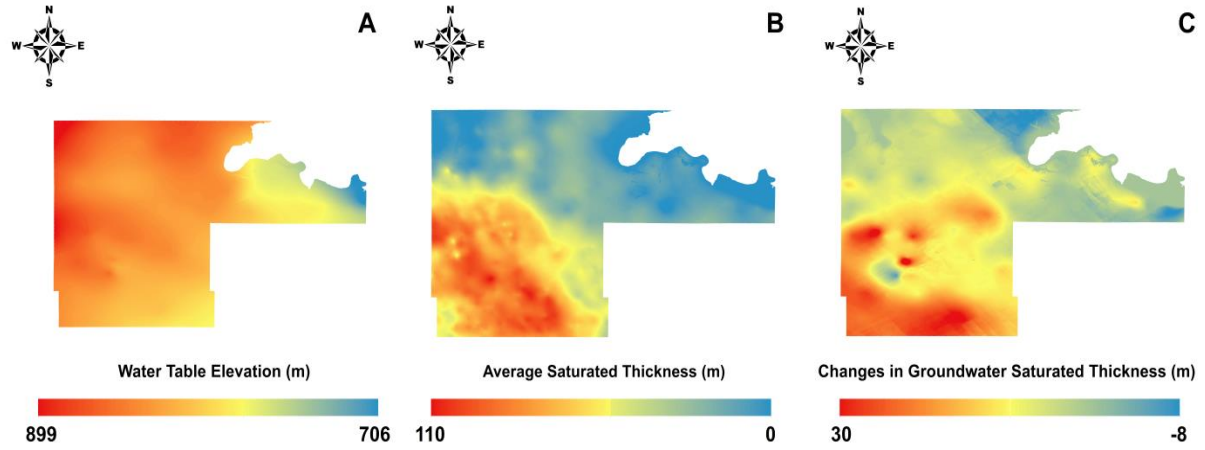

Fig. 2-3. Map of groundwater conditions in the Finney County. A) Average water table elevation in Finney County between 1997 and 2007; B) Average groundwater saturated thickness between 1997 and 2007; and C) The change in groundwater saturated thickness between 1997 and 2007.

shows an average saturated thickness (m) during 1997-2007 period. Saturated thickness was calculated as the difference between the water table elevation and the bedrock elevation. The bedrock elevation raster was derived from the well log data of drilled wells of WWC5 using the Ordinary Kriging method. Fig. 3C shows a change in saturated thickness between 1997 and 2007, with negative values indicating an increase in water table elevation. As seen in Fig. 2-3C, the southern part of the county has experienced the highest water table decline, with some areas up to 30 m (99 ft) over the time period, due to an initially high saturated thickness and an imbalance between pumping and recharge.

2.3.2 DSSAT-MODFLOW MODEL SETUP

2.3.2.1 INITIAL DATA PROCESSING

The fields and associated irrigation pumping wells in Finney County used for the DSSAT-MODFLOW model application are shown in Fig. 2-4. The spatial extent of each field was delineated using the National Agricultural Imagery Program (NAIP) aerial photo for 2015, resulting in rectangular and circular croplands within the county. Only fields with groundwater irrigation were included in the modeling system. These were identified using information from the state of Kansas' Water Information Management and Analysis System (WIMAS) and the

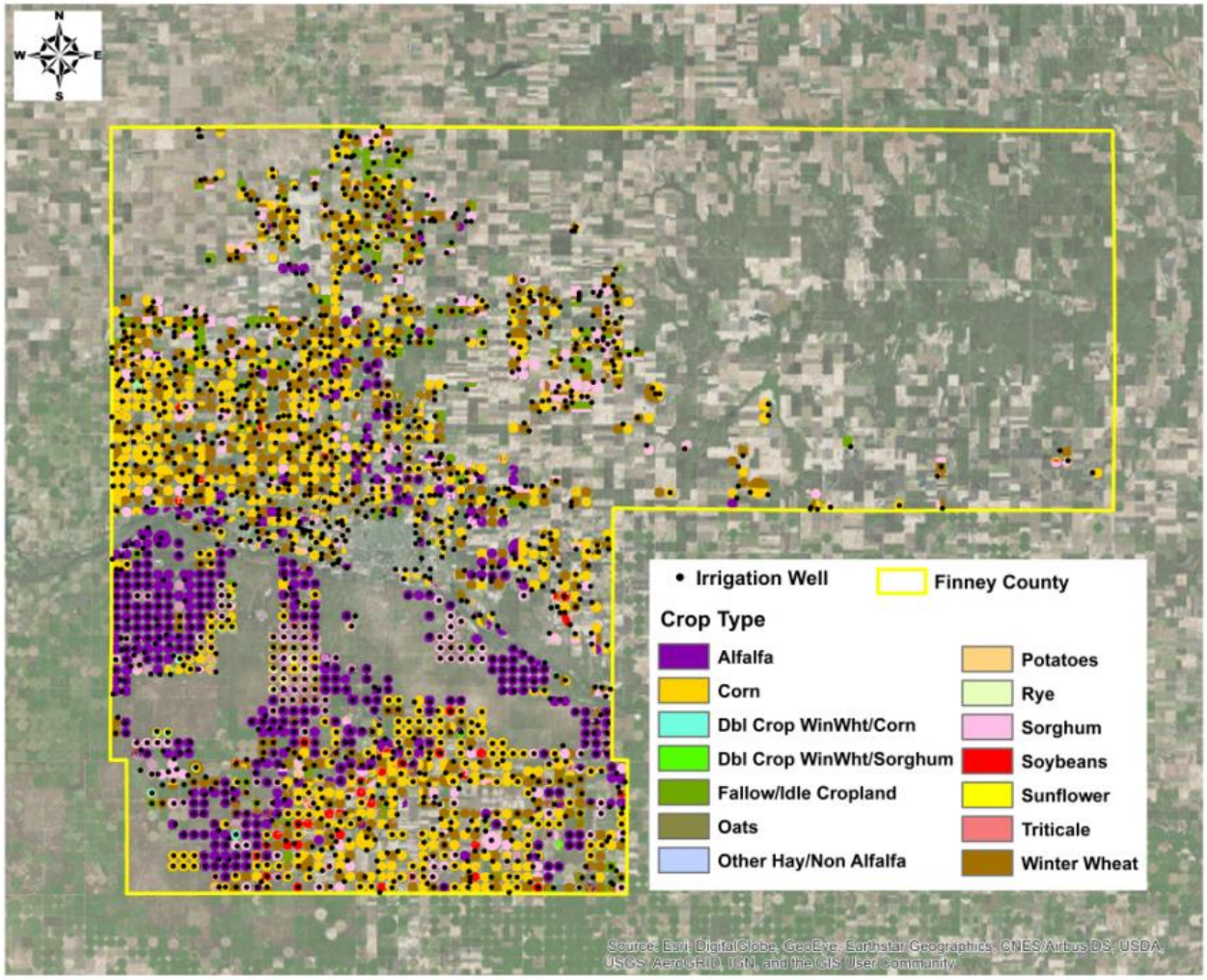

Fig. 2-4. Map of irrigation wells and crop types. In the Finney County, there are five major crop types, including corn, winter wheat, soybeans, sorghum, and triticale.

Public Land Survey System (PLSS), with the latter dividing the land into sections and quarter sections. If one or more irrigation wells are in a quarter section, then the parcel is classified as irrigated land. If there are no wells in the quarter section, but the quarter section includes a center pivot, and an irrigation well is located within a certain radial distance from the field, then the parcel is also considered as irrigated. Using this method, 1332 groundwater-irrigated field and 1629 irrigation pumping wells were located within the county (see Fig. 2-4). Authorized groundwater withdrawal quantity for each parcel, obtained from WIMAS, was used to determine the number of fields serviced by each pumping well, with the well's authorized quantity proportionally partitioned to the fields according to field spatial area.

2.3.2.2 ENSEMBLE OF DSSAT SIMULATION

The DSSAT model was previously calibrated and tested for the study area using experimental data, with cultivar parameters and associated calibrated values provided for corn, wheat, and grain in Araya et al. (2017). One DSSAT simulation was run for each of the 1332 fields shown in Fig. 2-4 according to properties of fields (e.g., soil type, crop type, soil water content, etc.), planting management (e.g. planting schedule, irrigation method, etc.), weather information, cultivar type, etc. All input information were organized into files according to DSSAT input file format, including Soil Input File (.SOL), Daily Weather Data (.WTH), Cultivar Input File (.CUL), Spatial Execution File (.GSX). Operations and management were summarized in the MgmtEvents.OUT.

As mentioned in section 2.3.2.1, all croplands in the same quarter section are considered as a whole parcel (field). To determine dominant soil and crop type (in 2015) for the groundwater-based irrigated parcels, the Soil Survey Geographic Database (SSURGO) and USDA's Cropland Data Layer (CDL) were utilized, respectively. The Zonal Statistics Tool in ArcMap was applied to determine dominant soil and crop type (in 2015) for each irrigated field. Since the SSURGO maps include a vast variety of soil types and to facilitate the DSSAT simulation, the dominant soil types of fields were merged into the seven specific soil groups, including Beeler silt loam, Las clay loam, Manter fine sandy loam, Richfield silt loam, Satanta loam, Ulysses silt loam, and Valent fine sand. Six major crops such as corn, winter wheat, soybeans, sorghum, and triticale on 564, 484, 28, 206, and 50 fields, respectively, in Finney County (Fig. 2-4) were simulated with the DSSAT model.

Historical weather data for 2000-2007 period was collected from a weather station located within the Finney County (39^{o} N, 100^{o} W) for DSSAT simulations. Weather data include

latitude (LAT), longitude (LONG), elevation (ELEV), air temperature average (TAV), air temperature amplitude (AMP), height of temperature measurements (REFHT), height of wind measurements (WNDHT), date (DATE), solar radiation (SRAD), maximum air temperature (TMAX), minimum air temperature (TMIN), precipitation (RAIN), and optional model parameters, such as dew-point temperature (DEWP), wind velocity (WIND), photosynthetic active radiation (PAR), respectively (Jones and Singels, 2008; Tsuji et al., 1994) (*see Fig. 2-S5 in Appendices*).

2.3.2.3 MODFLOW MODEL

The calibrated MODFLOW model for southwest Kansas Groundwater Management District No.3 (GMD3), developed by the Kansas Geological Survey (KGS) (Liu et al., 2010), was used for linkage with the DSSAT model. The domain area of the MODFLOW model is 161 kilometers by 241 kilometers (100 miles by 150 miles) with a rectangular expanse that contains GMD3 and extends approximately 9.7 kilometers (6 miles) to the north, east, south, and west (Fig. 2-5A). The dimensions of each grid cell are 1.61 kilometers by 1.61 kilometers (1 mile by 1 mile). The KGS MODFLOW model contains two main phases, i.e., a steady-state simulation for the predevelopment period (1944-1946), and a transient simulation for the periods between 1947 and 2007. Time-varying specified-head and time-varying flux boundaries were applied along the northern and southern side of the model domain and the western and eastern edges of the model area, respectively. The top of the Permian and Cretaceous bedrock was considered as a no-flow boundary for the lower boundary of the model, while land surface was treated as the upper boundary of the model. Hydraulic conductivity (K) and specific yield (S_y) were dynamically updated through the observed water levels to take into account the influence of the decline in water table during transient periods; therefore, the calibrated model was divided

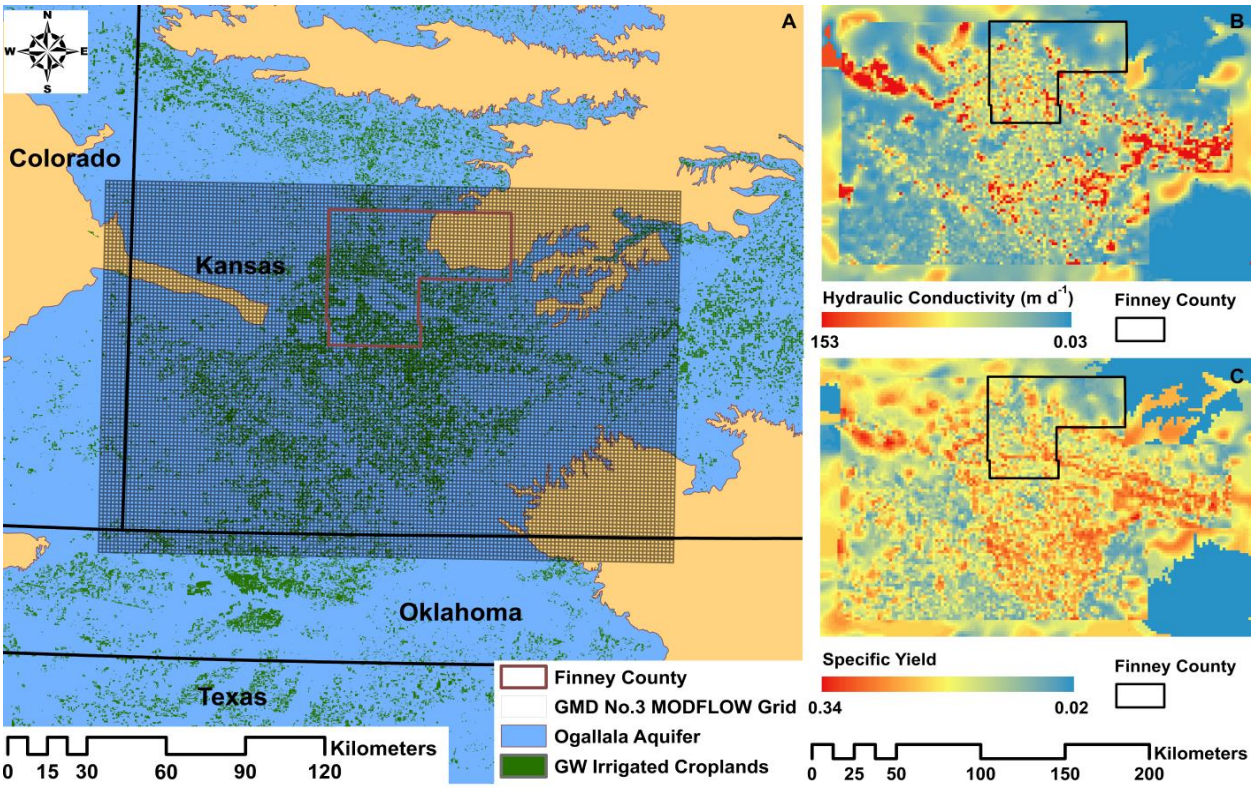

Fig. 2-5. Map of the domain area of KGS MODFLOW mode, hydraulic conductivity, and specific yield. A) the domain area of MODFLOW model with total size of 161 kilometers by 241 kilometers (100 miles by 150 miles) and the size of 1.61 kilometers by 1.61 kilometers (1 mile by 1 mile) grid cell; B) the horizontal distribution of hydraulic conductivity in the KGS model area, with range from 0.03 to 153 m d^{-1}, and in the Finney County enclosed within the black contour line; C) the horizontal variation in specific yield in the model are, with range from 0.02 to 0.34, and in the Finney County enclosed within the black contour line.

into six periods, including predevelopment, predevelopment-1966, 1967-1976, 1977-1986, 1987-1996, and 1997-2007. Fig. 2-5B and 2-5C show cell-by-cell values of K and S_y used in the aquifer during the 1997-2007 simulation period. The pumped volumes from the Ogallala aquifer for the model were obtained from reported water-use records during 2000 - 2007 period (Liu et al., 2010).

Recharge to the water table occurs through precipitation recharge and irrigation return (deep percolation). Precipitation recharge was computed by a power-function relationship, and irrigation return recharge was calculated depending on the irrigation method. The model simulated stream-aquifer interaction using the stream package (STR), with 18 segments and 764 reaches in the three major streams (i.e., Arkansas River, Cimarron River, and Crooked Creek),

depending on stream stage calculated by the Manning equation with the assumption of a rectangular channel.

The stress period of the original KGS model is monthly, whereas the DSSAT simulations provide daily-based irrigation depths that are converted to daily pumping rates. As pumping simulated by the Well package is a stress for MODFLOW, the MODFLOW model was converted to daily stress periods, requiring changes to the Discretization file (.DIS), the Recharge Package file (.RCH), the Time-Variant Specified-Head Package file (.CHD), and the Stream Package file (.STR). The Well Package and Recharge Package input files were updated through the Phase 1 Python Code (see Figure 2-1), using depths of applied irrigation and deep percolation simulated by DSSAT for each cultivated field.

2.3.2.4 LINKED DSSAT-MODFLOW MODEL FOR FINNEY COUNTY, KANSAS

The linked DSSAT-MODFLOW modeling system for Finney County follows the data flow shown in Fig. 2-1. Following 1332 DSSAT simulations for the first year, with one simulation for each field, the DSSAT-simulated irrigation depths were converted to daily pumping rates for the 1629 pumping wells and mapped to the MODFLOW Well package. Similarly, recharge rates from precipitation and from DSSAT-simulated deep percolation were converted to daily recharge rates for each grid cell. The MODFLOW model was then run for that year, providing updated water table elevation and saturated thickness for each grid cell within the county boundary. The MODFLOW model for the entire GMD3 was run, with pumping rates only modified for the grid cells within the Finney County boundary.

Updated saturated thickness was used to update well capacity using Equ. 2-1. To do so, the initial well capacity Q_{init} for each pumping well and the initial saturated thickness S_{init} for each grid cell must be specified. Based on the KGS Water Well Completion Records Database

(WWC5), the well capacity value was available for only 503 irrigation wells in Finney County. Since the well capacity was measured during the 1975-1978 period for the majority of these irrigation wells, this period was selected to create an interpolated surface (raster) of well capacity in Finney County with the available values. The Geostatistical Analyst Extension in ArcMap was used to make the interpolated surface using Ordinary Kriging. By creating the interpolated surface of well capacity, the well capacity values were estimated for all irrigation pumping wells in the county during 1975-1978, which was considered as Q_{init}. Results are shown in Fig. 2-6A, with well capacity ranging from 1,499 to 16,566 $m^3\ d^{-1}$ (275 to 3,039 gal min^{-1}). S_{init} values for the 1975-1978 period were calculated using water table elevation measurements from the KGS Water Well Level Database (WIZARD). Measurements from 1975 to 1978 were interpolated annually in the same way as for the Q_{init} values. Using the lithologic log information of the drilled wells in Finney County (as obtained from WWC5), the approximate location of the aquifer's base was located and the bed-rock elevation was estimated at 2281 borehole locations. Subsequently, an interpolated surface of bed-rock elevation was created for the county by using the same interpolation method. The saturated thickness raster was created by subtracting the bed-rock elevation raster from the water table elevation raster. The mean saturated thickness raster, considered as S_{init}, was created in ArcMap for the period of 1975 to 1978 as the initial saturated thickness (Fig. 2-6B).

The simulation was made for the 2000 - 2007 period, with simulation results compared against observed groundwater levels and estimated county-wide crop yield for corn, sorghum, winter wheat, and soybeans. A scenario without pumping was also simulated to quantify the influence of pumping on groundwater levels in the county.

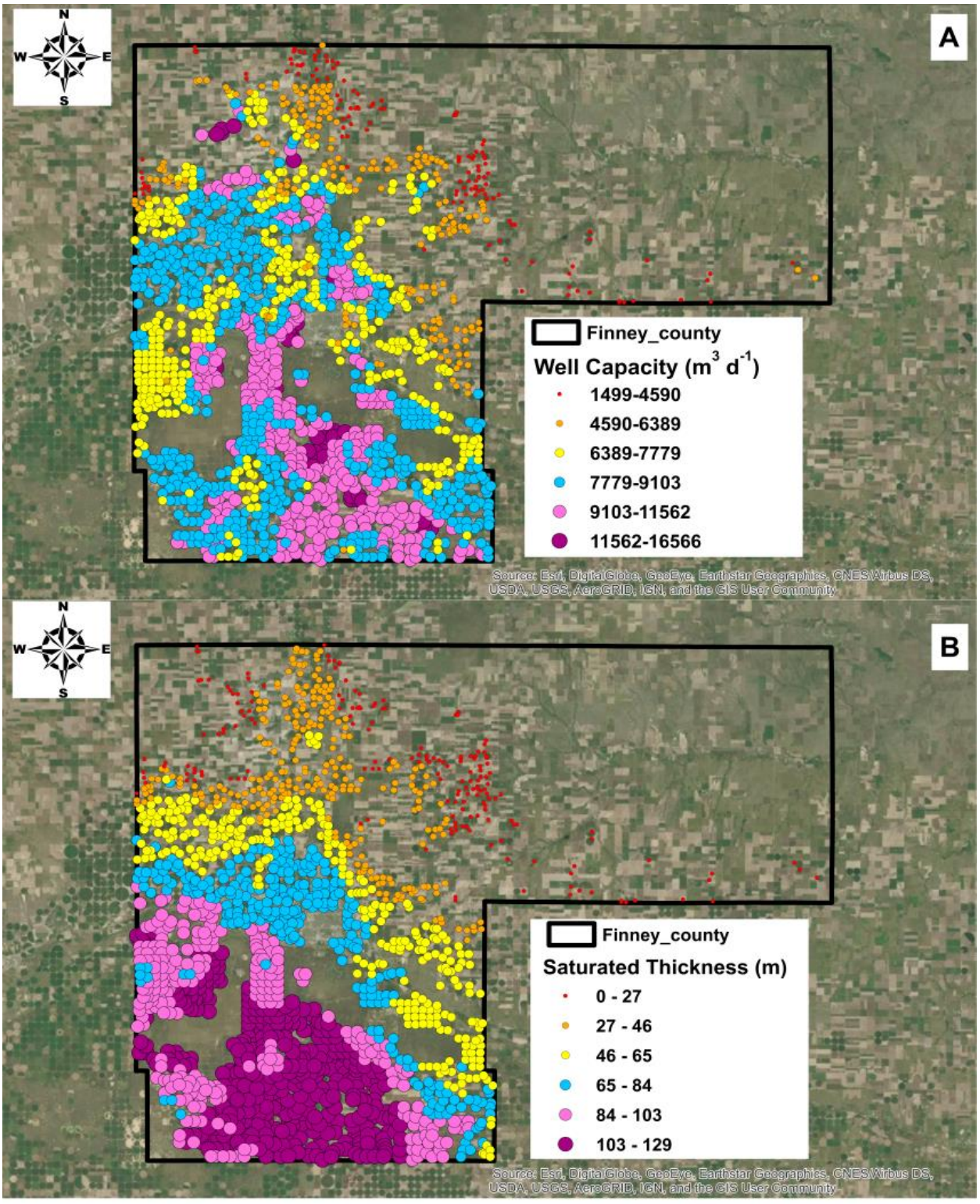

Fig. 2-6. Map of initial well capacity and saturated thickness in Finney County. A) Initial well capacity in Finney County during 1975 to 1978; B) Initial saturated thickness in Finney County that is averaged between 1975 and 1978.

2.3.2.5 SCENARIO ANALYSIS

A simple model application was performed to demonstrate the use of the DSSAT-MODFLOW modeling system. An end-member analysis was performed for assessing the effects of 1) pumping at the current rates of 2000-2007, and 2) cessation of all pumping, for the 2000-2007 time period. Crop yield for both scenarios were also assessed. Future studies can use the DSSAT-MODFLOW system to explore and quantify the effects of irrigation technology and management practices.

2.3.3 RESULTS AND DISCUSSION

2.3.3.1 WATER TABLE ELEVATION

The comparison between observed and simulated water table elevation (WTE) for both the original MODFLOW model and the linked DSSAT-MODFLOW model is shown in Fig. 2-7A and 7B, respectively. As seen in the figures, the points for both models are scattered along the 1:1 line, with no apparent pattern for either model, and average errors for the original MODFLOW and the linked model are -8.5 m (-28 ft) and -8.7 m (-29 ft), respectively. Fig. 2-7C shows the results from both models plotted against each other, showing a strong similarity in groundwater head output from the two models, with NSCE of 0.99 and scaled RMSE of 0.01637 (1.637 %). This is an especially important result, as this indicates that the DSSAT-MODFLOW modeling system is able to provide pumping rates comparable to the reported pumping rates used in the original MODFLOW model. Therefore, DSSAT can be used as a "pumping rate simulator" for MODFLOW models in groundwater-irrigated regions.

Fig. 2-8A shows the cell-by-cell WTE values (m) in the end of 2007 due to continuous pumping for the 2000-2007 periods, with high water tables in the northern and western edges of the county. Fig. 2-8B shows the same plot for the scenario without pumping, and Fig. 2-8C

shows the difference in WTE between the two scenarios (i.e., groundwater drawdown). For the latter, as expected large differences occur in the regions of densely-located irrigation well (see Fig. 2-4).

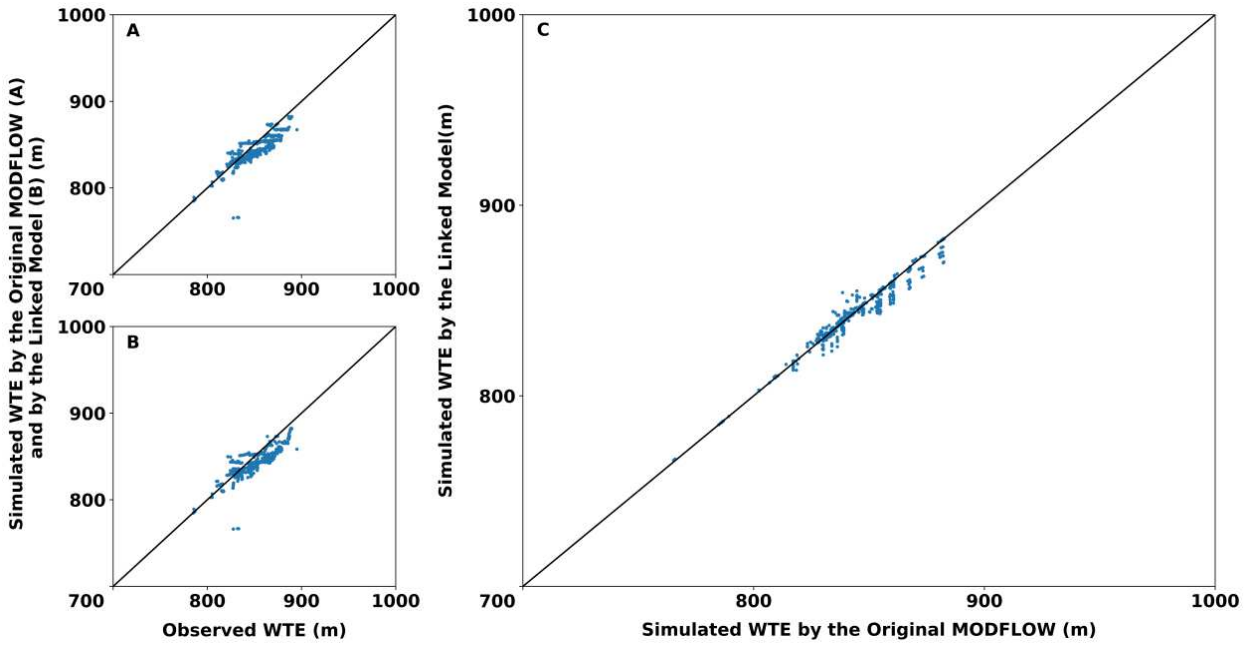

Fig. 2-7. The comparison of simulated water table elevation (WTE) and observed water table elevation and the comparison of simulated water table elevation between MODFLOW model and the linked model. A) the comparison of observed and simulated water table elevation by the original MODFLOW model; B) the comparison of observed and simulated water table elevation by the linked DSSAT-MODFLOW model; C) the comparison of simulated water table elevation between MODFLOW model and the linked DSSAT-MODFLOW model.

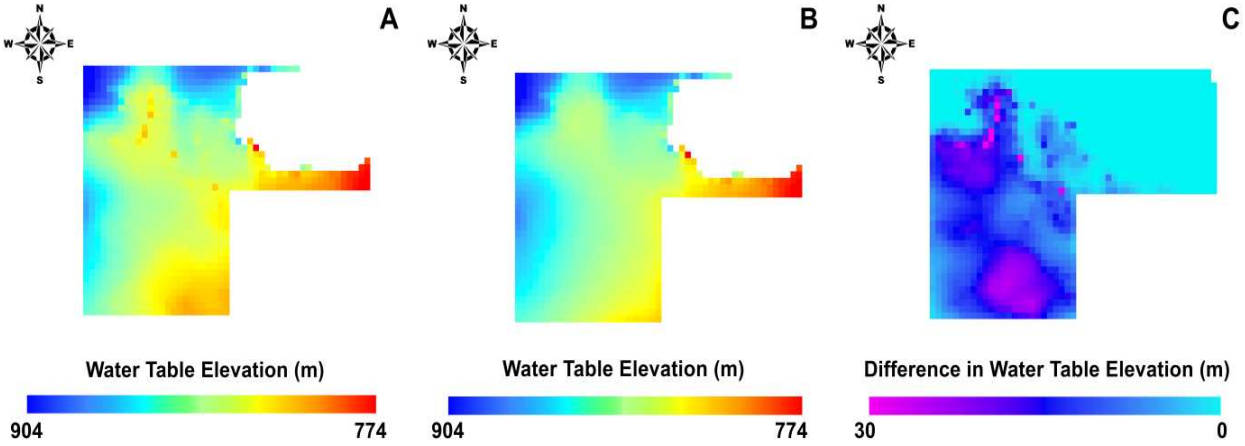

Fig. 2-8. The water table elevation with pumping and without pumping and the groundwater drawdown in Finney County during 2000-2007 simulated by the linked DSSAT-MODFLOW model. A) Water table elevation in the Finney County with pumping; B) Water table elevation in the Finney County without pumping; C) Groundwater drawdown due to pumping in the Finney County during 2000 – 2007.

2.3.3.2 CROP YIELD

Estimates of county-wide observed and simulated crop yield for 2002 and 2007 are presented in Fig. 2-9 for corn, sorghum, winter wheat, and soybean. Results are shown for the

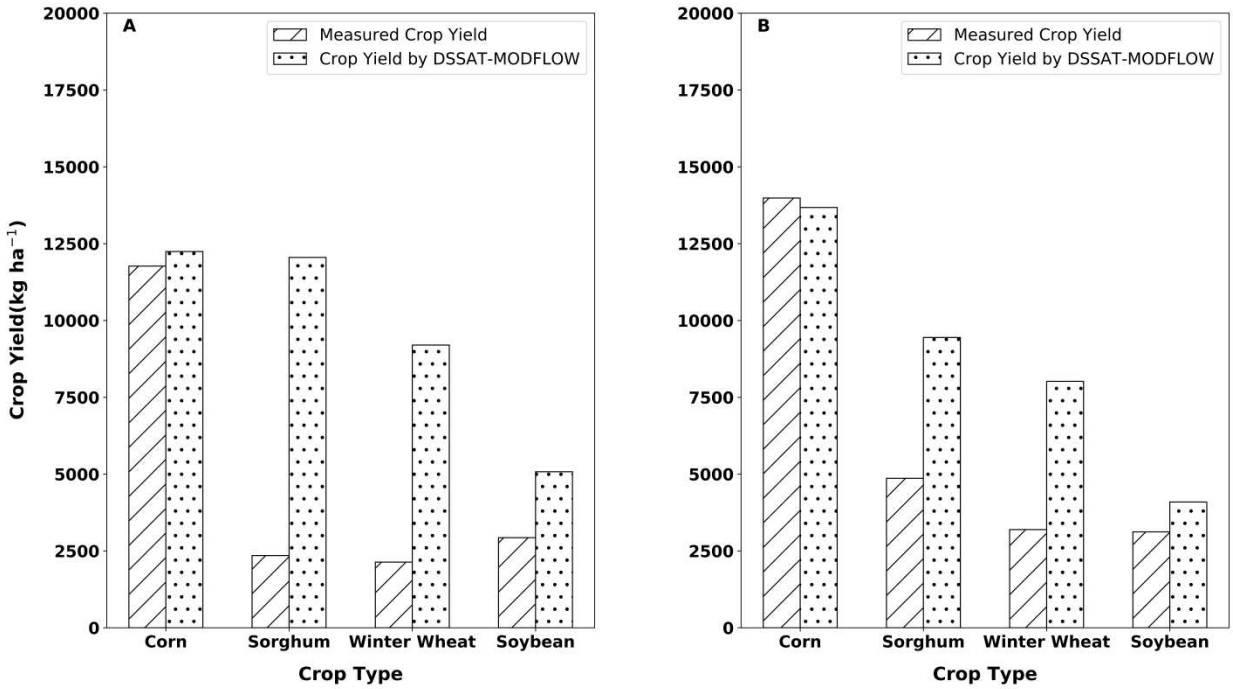

Fig. 2-9. Comparison between measured crop yield and simulated crop yield. A) Comparison between average measured crop yield and simulated crop yield by the DSSAT-MODFLOW linkage in 2002. Standard error mean are 0.003, 0.2, 0.3, 16 kg ha^{-1} for simulated corn, sorghum, winter wheat, soybean, respectively. B) Comparison between average measured crop yield and simulated crop yield by the DSSAT-MODFLOW linkage in 2007. Standard error mean are 0, 0.06, 0.5, 8 kg ha^{-1} for simulated corn, sorghum, winter wheat, soybean, respectively.

county-based measurements and the linked DSSAT-MODFLOW model, with results from measurements and the linked model using a method: calculating a weighted average of crop yield using the area of each field. In 2002, simulated yield for the crops are extremely high (12,052 kg ha^{-1} and 9200 kg ha^{-1} for sorghum and winter wheat, respectively) compared to the measured values (2,349 kg ha^{-1} and 2,137 kg ha^{-1} for sorghum and winter wheat, respectively), possibly due to uncertainty in the weather data input into the DSSAT simulations. In addition, measured values include fields for the entire county, whereas model results are only for groundwater-irrigated fields. Other fields may not have as high of crop yield, due to dependence on surface water or reliance on rainfall in the case of dryland farming, thereby decreasing the overall

average crop yield. Also, it could be due to the reason that the modeled crop yield does not account for pest/weed pressure. Furthermore, for sorghum and winter wheat, which show a large difference between simulated and measured values, the reason could be an inadequate calibration for southwest Kansas. In general, simulated yields will be difficult to match county average yields for sorghum and winter wheat because these crops are either not irrigated or under deficit irrigation, so there exists a wide standard deviation around the mean yield. In 2007, the measured value for corn (13,980 kg ha^{-1}) is a little higher than the simulated value (13,677 kg ha^{-1}), and the measured and simulated values for soybean are 3,120 kg ha^{-1} and 4,092 kg ha^{-1}, respectively.

2.3.3.3 Well Capacity and Saturated Thickness

Well capacity should be tracked through time to determine feasibility of future pumping in the region. The relationship between well capacity (m^3 d^{-1}) for each pumping well and

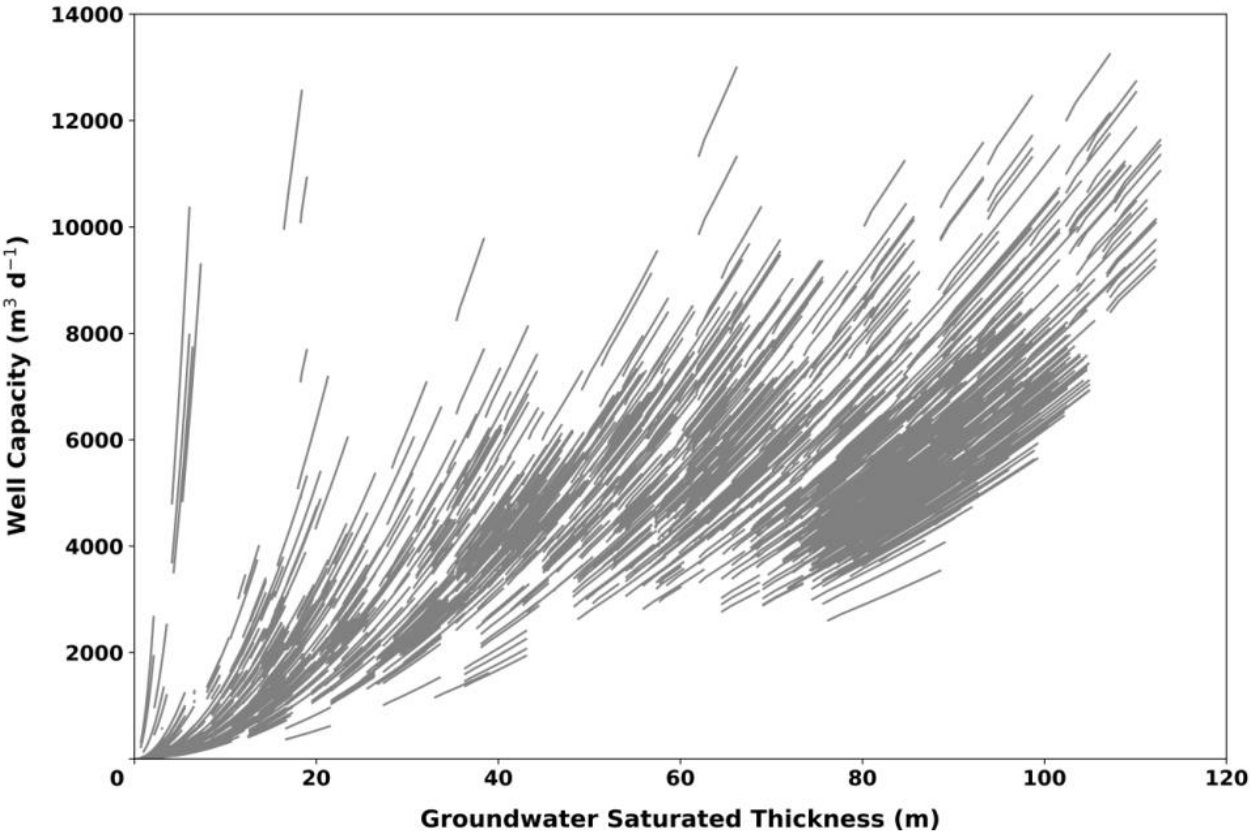

Fig. 2-10. The relationship between well capacity (m^3 d^{-1}) and groundwater saturated thickness (m) for each pumping well in Finney County. The relationship is tracked during the 2000-2007 time period, with well capacity decreasing as saturated thickness decreases. For some wells, well capacity approached 0 as the groundwater is completely depleted in the local area.

groundwater saturated thickness in the local area of the pumping well (i.e., the grid cell in which the pumping well resides) is shown in Fig. 2-10. There is one trend line for each pumping well, showing the decrease in well capacity during the 2000-2007 time periods due to decrease in saturated thickness. Each segment trends to 0, with several wells reaching 0 well capacity due to a complete depletion of groundwater in the local area around the pumping well. For areas with a large saturated thickness (> 76 m), well capacities are not significantly sensitive to the change in saturated thickness, whereas areas with small saturated thickness (< 18 m) exhibit a strong sensitivity of well capacity to saturated thickness. Similarly, well capacity is sensitive to saturated thickness for wells with high pumping rates (> 8000 m^3 d^{-1}), not for wells with low pumping rates. The trend in well capacity, of course, could be reversed if pumping ceases.

2.3.3.4 PERCENT CHANGE IN WELL CAPACITY

The percent change in well capacity for each pumping well during the 2000-2007 period in Finney County is shown in Fig. 2-11. Well capacity changes spatially in terms of crop type, which dictates pumping rates, and aquifer characteristics, which dictate saturated thickness. Dark and light blue dots represent wells that increased capacity due to replenishment of groundwater. However, the majority of Finney County experiences a decline in well capacity. The highest changes in well capacity (>60%) occurred in the north region of the Finney County in which corn and winter wheat were grown (see Fig. 2-4), due to low well capacity and small initial saturated thickness (see Fig. 2-3B and Fig. 2-6). Moderate changes in well capacity (20%-40%), and high changes (> 40%) occurs in the southern area, again related to initial well capacity and initial saturated thickness.

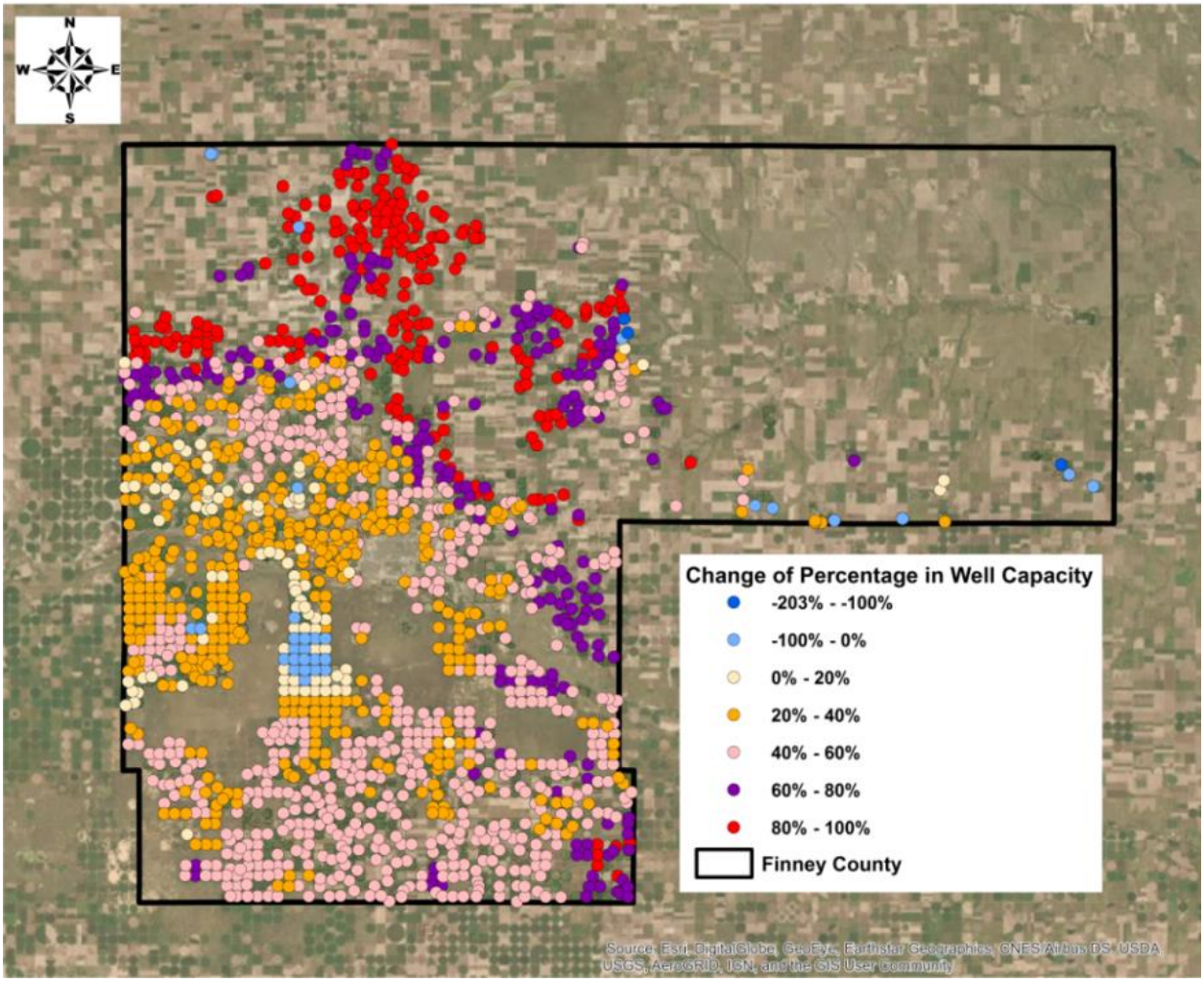

Fig. 2-11. The change in well capacity in Finney County during the simulated 2000-2007 period, expressed as a percentage. Negative values indicate an increase in well capacity.

2.3.3.5 RESULTS OF PUMPING VS. NO PUMPING

Considering all cell-by-cell results from Finney County, average water table elevation gradually depletes during the 2000-2007 period. This is shown in Fig. 2-12, which shows the pre-development water table elevation (WTE), the elevation of the bedrock, and the WTE with full irrigation (i.e., the baseline model used in this study) (Fig. 2-12A). The average crop yields (kg ha^{-1}) are also shown for this scenario (Fig. 2-12B). Results from the second scenario, in which no groundwater pumping occurs during the 1997-2007 period, are also shown, along with average crop yield. As seen from the results, no irrigation during the decadal period increases average WTE from 846 m to 848 m (2,775 ft to 2,782 ft), with the change in WTE ranging from

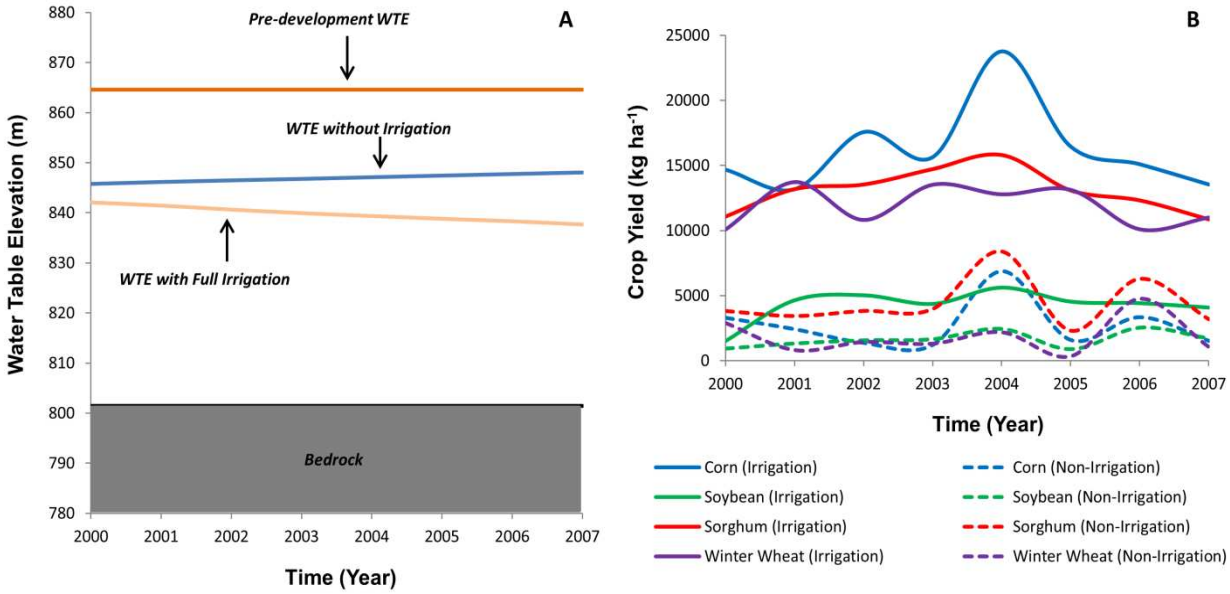

Fig. 2-12. Water table elevation (WTE) and crop yield under the scenarios of 1) full pumping and 2) no pumping) from 2000-2007. The WTE of the pre-development period (pre-1946) and the bedrock elevation also are shown.

a decline of 2 m (6 ft) to a rise of 9 m (29 ft). However, this increase is at the expense of crop yields, which are decreased from 16238 kg ha^{-1} (Corn), 4277 kg ha^{-1} (Soybean), 13071 kg ha^{-1} (Sorghum), and 11892 kg ha^{-1} (Winter Wheat) for the full irrigation scenario to 2705 kg ha^{-1} (Corn), 1632 kg ha^{-1} (Soybean), 4405 kg ha^{-1} (Sorghum), and 1851 kg ha^{-1} (Winter Wheat) for the non-irrigation scenario, with a decrease of crop yields by 83%, 62%, 66%, 84% for corn, soybean, sorghum, and winter wheat, respectively.

Therefore, management strategies are sought that balance between conserving groundwater and maintaining crop yield for future decades, i.e., that can decrease the gap between the "full pumping" and "no pumping" scenarios while also preserving adequate crop yield for the local economy. Such strategies may include implementing irrigation technology to increase irrigation efficiency, optimized irrigation scheduling, and crop selection. The linked DSSAT-MODFLOW model presented in this paper can assist in assessing the influence of these management strategies. The influence of future climate patterns on these impacts can also be estimated using the linked model.

2.4 SUMMARY AND CONCLUSION

This chapter presents a linked DSSAT-MODFLOW modeling framework and applied it to the Ogallala aquifer within Finney County, Kansas, a region experiencing significant groundwater depletion due to irrigation practices. The linkage between the models occurs on an annual time step, with irrigation depths from an ensemble of field-scale DSSAT simulations (DSSAT version 4.7) converted to pumping rates for the MODFLOW simulation (MODFLOW 2000). The MODFLOW simulates groundwater head, which can be used to update saturated thickness and thereby well capacities for each pumping well in the model domain. Well capacities are then used to constrain irrigation application in the DSSAT simulations during the following growing season. Python scripts are used to pass information between the two models and prepare input files. Batch files for DSSAT are used to run the ensemble of simulations for each year. Model results are tested against water table elevation and crop yield.

This chapter focuses on the presentation and demonstration of the DSSAT-MODFLOW modeling system, whereas future studies can focus on assessing future conditions under changes in climate and management practices. The DSSAT-MODFLOW modeling system can be a valuable tool in assessing groundwater conservation strategies in groundwater-irrigated regions, since it tracks jointly groundwater resources (groundwater head, saturated thickness), pumping conditions (well capacity), and crop yield. Therefore, any strategy used to conserve groundwater can also be assessed in terms of resulting crop yield to determine feasibility for local economies. The model can be used to assess changes in irrigation technology, crop selection, and climate change. In addition, in areas where pumping rates are not readily available, the DSSAT portion of the linked model can be used to estimate pumping rates, based on DSSAT's crop growth routines and associated irrigation depths.

REFERENCES

Aeschbach-Hertig, W., Gleeson, T., 2012. Regional strategies for the accelerating global problem of groundwater depletion. Nat. Geosci. 5, 853–861. https://doi.org/10.1038/ngeo1617

Araya, A., Kisekka, I., Gowda, P.H., Prasad, P.V.V., 2017. Evaluation of water-limited cropping systems in a semi-arid climate using DSSAT-CSM. Agric. Syst. 150, 86–98. https://doi.org/10.1016/j.agsy.2016.10.007.

Araya, A., Kisekka, I., Gowda, P.H., Prasad, P.V.V., 2018. Grain sorghum production functions under different irrigation capacities. Agric. Water Manag. 203, 261–271. https://doi.org/10.1016/j.agwat.2018.03.010.

Arnold, J.G., Srinivasan, R., Muttiah, R.S., Williams, J.R., 1998. Large area hydrologic modeling and assessment part I: model development 1. JAWRA J. Am. Water Resour. Assoc. 34, 73–89.

Bailey, R.T., Wible, T.C., Arabi, M., Records, R.M., Ditty, J., 2016. Assessing regional-scale spatio-temporal patterns of groundwater–surface water interactions using a coupled SWAT-MODFLOW model. Hydrol. Process. 30, 4420–4433. https://doi.org/10.1002/hyp.10933

Bulatewicz, T., Yang, X., Peterson, J.M., Staggenborg, S., Welch, S.M., Steward, D.R., 2010. Accessible integration of agriculture, groundwater, and economic models using the Open Modeling Interface (OpenMI): Methodology and initial results. Hydrol. Earth Syst. Sci. 14, 521–534. https://doi.org/10.5194/hess-14-521-2010

Cai, X., McKinney, D.C., Lasdon, L.S., 2003. Integrated hydrologic-agronomic-economic model for river basin management. J. Water Resour. Plan. Manag. 129, 4–17. https://doi.org/10.1061/(ASCE)0733-9496(2003)129:1(4)

Dawoud, M.A., Darwish, M.M., El-Kady, M.M., 2005. GIS-based groundwater management model for Western Nile Delta. Water Resour. Manag. 19, 585–604. https://doi.org/10.1007/s11269-005-5603-z

Ebraheem, A.M., Garamoon, H.K., Riad, S., Wycisk, P., Seif El Nasr, A.M., 2003. Numerical modeling of groundwater resource management options in the East Oweinat area, SW Egypt. Environ. Geol. 44, 433–447. https://doi.org/10.1007/s00254-003-0778-1

Famiglietti, J.S., 2014. The global groundwater crisis. Nat. Clim. Chang. 4, 945–948. https://doi.org/10.1038/nclimate2425

Gollehon, N., Winston, B., 2013. Groundwater Irrigation and Water Withdrawals: The Ogallala Aquifer Initiative 15. https://doi.org/10.1787/261513543751

Guru, M., Horne, J., 2001. The Ogallala Aquifer. Prog. Water Resour. 48, 321–328.

Gutentag, E.D., Heimes, F.J., Krothe, N.C., Luckey, R.R., Weeks, J.B., 1984. Geohydrology of the High Plains aquifer in parts of Colorado, Kansas, Nebraska, New Mexico, Oklahoma, South Dakota, Texas, and Wyoming (USGS, USA, groundwater). US Geol. Surv. Prof. Pap. 1400 B.

Haacker, E.M.K., Kendall, A.D., Hyndman, D.W., 2016. Water Level Declines in the High Plains Aquifer: Predevelopment to Resource Senescence. Groundwater 54, 231–242. https://doi.org/10.1111/gwat.12350

Hadded, R., Nouiri, I., Alshihabi, O., Maßmann, J., Huber, M., Laghouane, A., Yahiaoui, H., Tarhouni, J., 2013. A Decision Support System to Manage the Groundwater of the Zeuss Koutine Aquifer Using the WEAP-MODFLOW Framework. Water Resour. Manag. 27, 1981–2000. https://doi.org/10.1007/s11269-013-0266-7

Hanson, R.T., Schmid, W., Faunt, C.C., Lockwood, B., 2010. Simulation and analysis of conjunctive use with MODFLOW's farm process. Ground Water 48, 674–689. https://doi.org/10.1111/j.1745-6584.2010.00730.x

Harbaugh, A.W., 2005. MODFLOW-2005, the US Geological Survey modular ground-water model: the ground-water flow process. US Department of the Interior, US Geological Survey Reston, VA.

Harman, W.L., 1966. An economic evaluation of irrigation water use over time on Texas High Plains farms with a rapidly diminishing water supply. Master's thesis, Texas A&M University. Available electronically from http : / /hdl .handle .net /1969 .1 /ETD -TAMU -1966 -THESIS -H287.

Hoogenboom, G., Porter, C.H., Shelia, V., Boote, K.J., Singh, U., White, J.W., Hunt, L.A., Ogoshi, R., Lizaso, J.I., Koo, J., Asseng, S., Singels, A., Moreno, L.P., Jones, J.W., 2019. DSSAT v4.7 Released | DSSAT.net [WWW Document]. URL https://dssat.net/2435 (accessed 8.29.19).

Jones, J.W., Hoogenboom, G., Porter, C.H., Boote, K.J., Batchelor, W.D., Hunt, L.A., Wilkens,

P.W., Singh, U., Gijsman, A.J., Ritchie, J.T., 2003. The DSSAT cropping system model, European Journal of Agronomy. https://doi.org/10.1016/S1161-0301(02)00107-7

Jones, M., Singels, a, 2008. DSSAT v4. 5-Canegro Sugarcane Plant Module: user documentation. … , South Africa Int. Consort. Sugarcane … 1–58.

Keating, B.A., Carberry, P.S., Hammer, G.L., Probert, M.E., Robertson, M.J., Holzworth, D., Huth, N.I., Hargreaves, J.N.G., Meinke, H., Hochman, Z., McLean, G., Verburg, K., Snow, V., Dimes, J.P., Silburn, M., Wang, E., Brown, S., Bristow, K.L., Asseng, S., Chapman, S., McCown, R.L., Freebairn, D.M., Smith, C.J., 2003. An overview of APSIM, a model designed for farming systems simulation. Eur. J. Agron. 18, 267–288. https://doi.org/10.1016/S1161-0301(02)00108-9

Kisekka, I., Aguilar, J.P., Rogers, D., Holman, J., O'Brian, D., Klock, N., 2015. Assessing deficit irrigation strategies for corn using simulation, in: 2015 ASABE/IA Irrigation Symposium: Emerging Technologies for Sustainable Irrigation-A Tribute to the Career of Terry Howell, Sr. Conference Proceedings. American Society of Agricultural and Biological Engineers, pp. 1–28.

Konikow, L.F., 2011. Contribution of global groundwater depletion since 1900 to sea-level rise. Geophys. Res. Lett. 38, 1–5. https://doi.org/10.1029/2011GL048604

Konikow, L.F., Kendy, E., 2005. Groundwater depletion: A global problem. Hydrogeol. J. 13, 317–320. https://doi.org/10.1007/s10040-004-0411-8

Liu, G., Wilson, B., Whittemore, D., Jin, W., and Butler, J. (2010), Ground-water model for southwest Kansas Groundwater Management District No. 3. Kansas Geological Survey Open File Report 2010-18, University of Kansas, Lawrence, Kansas, USA.

Mao, X., Jia, J., Liu, C., Hou, Z., 2005. A simulation and prediction of agricultural irrigation on groundwater in well irrigation area of the piedmont of Mt. Taihang, North China. Hydrol. Process. 19, 2071–2084. https://doi.org/10.1002/hyp.5667

McGuire, V.L., 2014. Water-level changes and change in water in storage in the High Plains aquifer, predevelopment to 2013 and 2011-13, Scientific Investigations Report. Reston, VA. https://doi.org/10.3133/sir20145218

McGuire, V.L., Johnson, M.R., Schieffer, R.L., Stanton, J.S., Sebree, S.K., Verstraeten, I.M., 2003. Water in storage and approaches to ground-water management, High Plains Aquifer, 2000. US Geol. Surv. Circ. 1–51.

Motagh, M., Walter, T.R., Sharifi, M.A., Fielding, E., Schenk, A., Anderssohn, J., Zschau, J., 2008. Land subsidence in Iran caused by widespread water reservoir overexploitation. Geophys. Res. Lett. 35, 1–5. https://doi.org/10.1029/2008GL033814

Mylopoulos, N., Mylopoulos, Y., Tolikas, D., Veranis, N., 2007. Groundwater modeling and management in a complex lake-aquifer system. Water Resour. Manag. 21, 469–494. https://doi.org/10.1007/s11269-006-9025-3

Pokhrel, Y.N., Koirala, S., Yeh, P.J., Hanasaki, N., Longuevergne, L., Kanae, S., Oki, T., 2015. Incorporation of groundwater pumping in a global L and S urface M odel with the representation of human impacts. Water Resour. Res. 51, 78–96.

Raes, D., Steduto, P., Hsiao, T.C., Fereres, E., 2009. AquaCrop – The FAO crop model to simulate yield response to water AquaCrop Reference Manual. Ref. Man.

Rad, M.R., Brozović, N., Foster, T., Mieno, T., 2019. Effects of instantaneous groundwater availability on irrigated agriculture and implications for aquifer management. Resour. Energy Econ. 59, 101129. https://doi.org/10.1016/j.reseneeco.2019.101129.

Rolim, J., Godinho, P., Sequeira, B., Rosa, R., Paredes, P., Pereira, L.S., 2006. SIMDualKc, a software tool for water balance simulation based on dual crop coefficient, in: Computers in Agriculture and Natural Resources, 23-25 July 2006, Orlando Florida. American Society of Agricultural and Biological Engineers, p. 781.

Rosa, R.D., Paredes, P., 2011. The SIMDualKc Model: Software application for water balance computation and irrigation scheduling using the dual crop coefficient approach. CEER-Biosystems Eng. Inst. Agron. Tech. Univ. Lisbon, Lisbon, Port.

Rosenberg, N.J., Epstein, D.J., Wang, D., Vail, L., Srinivasan, R., Arnold, J.G., Northwest, P., 1999. POSSIBLE IMPACTS OF GLOBAL WARMING ON THE HYDROLOGY OF THE OGALLALA AQUIFER REGION 1 . Introduction The Ogallala or High Plains aquifer underlies about 450 , 000 km 2 of the states of South Dakota , Wyoming , Colorado , Nebraska , Kansas , Oklahoma , Texa. Source 677–692.

Scanlon, B.R., Faunt, C.C., Longuevergne, L., Reedy, R.C., Alley, W.M., McGuire, V.L., McMahon, P.B., 2012. Groundwater depletion and sustainability of irrigation in the US High Plains and Central Valley. Proc. Natl. Acad. Sci. U. S. A. 109, 9320–9325. https://doi.org/10.1073/pnas.1200311109

Schmid, W., Hanson, R.T., Maddock, T.I., Leake, S.A., 2006. User Guide for the Farm Process

(FMP1) for the User Guide for the Farm Process (FMP1) for the U. S. Geological Survey's Modular Three-Dimensional Finite-Difference Ground-Water Flow Model, MODFLOW-2000. U.S. Geol. Surv. Tech. Methods.

Strack, O.D.L., 1989. Groundwater mechanics. Prentice Hall.

Tsuji, G., Uehara, G., Balas, S., 1994. DSSAT version 3, Transfer.

USGS High Plains Aquifer WLMS: Physical/Cultural Setting [WWW Document], n.d. URL https://ne.water.usgs.gov/ogw/hpwlms/physsett.html (accessed 8.29.19).

Varela-Ortega, C., Blanco-Gutiérrez, I., Swartz, C.H., Downing, T.E., 2011. Balancing groundwater conservation and rural livelihoods under water and climate uncertainties: An integrated hydro-economic modeling framework. Glob. Environ. Chang. 21, 604–619. https://doi.org/10.1016/j.gloenvcha.2010.12.001

Wada, Y., Van Beek, L.P.H., Bierkens, M.F.P., 2012. Nonsustainable groundwater sustaining irrigation: A global assessment. Water Resour. Res. 48. https://doi.org/10.1029/2011WR010562

Wada, Y., Van Beek, L.P.H., Van Kempen, C.M., Reckman, J.W.T.M., Vasak, S., Bierkens, M.F.P., 2010. Global depletion of groundwater resources. Geophys. Res. Lett. 37, 1–5. https://doi.org/10.1029/2010GL044571

Werner, A.D., 2010. A review of seawater intrusion and its management in AustraliaUne étude de l'intrusion d'eau de mer en Australie et de sa gestionUna revisión de la intrusión de agua de mar y su gestión en Australia**澳大利**亚海水入侵及其**管理的**综述Análise da intrusão salina e sua gestão na. Hydrogeol. J. 18, 281–285. https://doi.org/10.1007/s10040-009-0465-8

Williams, J.R., Jones, C.A., Kiniry, J.R., Spanel, D.A., 1989. EPIC crop growth model. Trans. Am. Soc. Agric. Eng. 32, 497–511.

Wu, Y., Liu, T., Paredes, P., Duan, L., Pereira, L.S., 2015. Water use by a groundwater dependent maize in a semi-arid region of Inner Mongolia: EVAPOTRANSPIRATION partitioning and capillary rise. Agric. Water Manag. 152, 222–232. https://doi.org/10.1016/j.agwat.2015.01.016

Xu, X., Huang, G., Zhan, H., Qu, Z., Huang, Q., 2012. Integration of SWAP and MODFLOW-2000 for modeling groundwater dynamics in shallow water table areas. J. Hydrol. 412–413, 170–181. https://doi.org/10.1016/j.jhydrol.2011.07.002

Yang, Y., Watanabe, M., Zhang, X., Zhang, J., Wang, Q., Hayashi, S., 2006. Optimizing irrigation management for wheat to reduce groundwater depletion in the piedmont region of the Taihang Mountains in the North China Plain. Agric. Water Manag. 82, 25–44. https://doi.org/10.1016/j.agwat.2005.07.020

Zhang, Y., Gong, H., Gu, Z., Wang, R., Li, X., Zhao, W., 2014. Characterization of land subsidence induced by groundwater withdrawals in the plain of Beijing city, ChinaCaractérisation de la subsidence induite par les prélèvements d'eaux souterraines dans la plaine de Pékin, ChineCaracterización de la subsidencia del. Hydrogeol. J. 22, 397–409. https://doi.org/10.1007/s10040-013-1069-x

CHAPTER 3 – USING DSSAT-MODFLOW TO DETERMINE THE CONTROLS OF GROUNDWATER STORAGE AND CROP YIELD IN GROUNGWATER-BASED IRRIGATED REGIONS[2]

3.1 INTRODUCTION

Groundwater resources are declining rapidly (Aeschbach-Hertig and Gleeson, 2012; Castle et al., 2014b; Famiglietti, 2014; Haacker et al., 2016; Konikow, 2011; Konikow and Kendy, 2005; McGuire et al., 2003; Virginia L McGuire, 2014; Wada, 2016; Wada et al., 2010) notably in arid and semi-arid regions due to overexploitation (Rodríguez-Estrella, 2012) and lack of other viable water sources for irrigation and drinking water (Steward and Allen, 2016). Anthropogenic influences on groundwater storage (Döll et al., 2012) include the route of water movement (e.g. allocation (Petts, 1996), canal (Kanooni and Monem, 2014), etc.), domestic use (Chávez García Silva et al., 2020), agricultural irrigation (Wada et al., 2012), and manufacturing and industry (Gracia-de-Rentería et al., 2020), with depletion problems becoming worse due to increasing population (Carter and Parker, 2009; Castle et al., 2014). According to an estimation by Konikow (2011), groundwater globally depleted by about 4,500 km^3 during 1900 – 2008, and, regionally, 1000 km^3 in the United States during 1900 – 2008 (Konikow, 2015); 170.3 km^3 in North China Plain during 1900 – 2008 (Feng et al., 2013); 91.3 km^3 in north-central Middle East during 2003 – 2009 (Voss et al., 2013); and 1.5 km^3 in the Nairobi aquifer, Kenya since 1950 (Oiro et al., 2020).

In view of groundwater sustainability, many studies have focused on conserving groundwater resources (Chang et al., 2017; Gates et al., 2011; Q. Huang et al., 2013; Mays, 2013; Sheng, 2005). Most studies use a water balance modeling approach to estimate historical

[2] This paper has been submitted to *Journal of Hydrology*

and current groundwater volumes and explore the effect of management strategies and future stresses (e.g. population growth, land use change, climate) (Batelaan et al., 2003; Candela et al., 2012a; Carter and Parker, 2009; Cuthbert et al., 2019; Deng and Bailey, 2017; Farhadi et al., 2016; Gorelick and Zheng, 2015; Holman et al., 2012; Huang et al., 2013b; Jha et al., 2007; Kløve et al., 2014; Kumar, 2012; Masciopinto and Liso, 2016; McCallum et al., 2010; Mishra, 2014; Sekhar et al., 2013). Other modeling approaches through the recognition that in many regions groundwater storage and associated fluxes are controlled by agricultural production through irrigation, link groundwater models to agronomic models, resulting in a hydro-agronomic modeling approach. These approaches include the Soil and Water Assessment Tool (SWAT) (Arnold et al., 1998), although the groundwater system is simulated in a simplistic, lumped basis; the linked system of MODFLOW and SWAP (Soil-Water-Atmosphere-Plant) (Xu et al., 2012); the linked system of MODFLOW and WEAP (Water Evaluation and Planning) (Hadded et al., 2013); a global Land Surface Model to simulate crop growth and associated groundwater depletion for regions worldwide (Pokhrel et al., 2015); the linked SWAT-MODFLOW system (Bailey et al., 2016), recently applied to assess impact of climate change on groundwater storage and crop yield in a large river basin in the western United States (Aliyari et al., 2021); and the linked DSSAT-MODFLOW system (Xiang et al., 2020), which links irrigation demand and groundwater pumping on an annual basis.

However, these modeling studies have been performed without a detailed assessment of the factors that control groundwater storage and crop yield in these linked hydro-agronomic systems. Such an understanding can provide valuable insights into 1) causes for groundwater depletion; 2) sustainable management strategies; and 3) possible future trends of groundwater depletion and crop yield in such systems. Quantifying these controls can be performed through

model sensitivity analysis (SA) schemes, which have been widely implemented to understand uncertainties of a system caused by model input factors (Mishra, 2009) for parameterization (Castaings et al., 2009; Dzotsi et al., 2013; Khatun et al., 2018), model understanding (Francos et al., 2003), model development (Pathak et al., 2007), model calibration (Foglia et al., 2009), model verification (Pfannerstill et al., 2015; Ratto et al., 2001), optimization (Yassin et al., 2017), model simplification (Brooks et al., 2001; Campolongo et al., 2007), uncertainty quantification (Vezzaro and Mikkelsen, 2012), management strategies (Roura-Pascual et al., 2010), and system design safety (Contini et al., 2000) in different fields of science and technology (Badra, 2007; Davis et al., 2011; Lamboni et al., 2009; Marino et al., 2008; Pianosi et al., 2016; Song et al., 2015; Tjiputra et al., 2007; Zhang et al., 2020). Prior research has proved the necessity of sensitivity analysis (Kisekka et al., 2013; Sin et al., 2009; Trucano et al., 2006). SA has been applied to groundwater systems (Allen et al., 2004; Bahremand and Smedt, 2008; Deng and Bailey, 2020; Henderson et al., 2010; Javadi et al., 2011; Sun and Yeh, 1990; Sykes et al., 1985) and agronomic systems (Confalonieri et al., 2010; Dzotsi et al., 2013; Lamboni et al., 2009; Richter et al., 2010; Ruget et al., 2002; Thorp et al., 2020; Wang et al., 2013, 2005). For example, to simplify the complexity of hydrological parameter dimension, Chen et al. (2017) used the Sobol' method, with Latin-Hypercube sampling, to identify influential input parameters for the process of calibration with the goal of reducing computation cost. Climate change increases uncertain factors on groundwater systems, McCallum et al. (2010) used SA to determine the most important parameters in controlling groundwater recharge, within the context of climate change. For agronomic systems, Makowski et al. (2006) applied two SA schemes (i.e., winding stairs and extended FAST) to the AZODYN crop model to assess the contributions of genetic parameters on model responses. Varella et al. (2010) improved the quality of estimation

of soil-related parameters using the Extended FAST method and the Bayes theory-based function of RMSE through the STICS-wheat crop model. Adejuwon (2005) applied SA to the EPIC crop model to determine the suitability of an agronomic model for assessing the impact of future climate on crop yield prediction. However, SA has not yet been applied to a coupled groundwater-agronomic system, which may provide insights into the system that could not be achieved by assessing either system independently.

The objective of this chapter is to present results of applying SA to the linked DSSAT-MODFLOW modeling system (Xiang et al., 2020) to determine the governing environmental and management factors that control groundwater storage and crop yield in an intensively irrigated groundwater basin. Methods are applied to the DSSAT-MODFLOW linkage system using the Morris screening method followed by the Sobol' variance-based method, using random sampling. In total, fifty-seven parameters are considered for this study, including 10 soil-related parameters, 3 hydrologic parameters, and 44 cultivar genetic parameters. The study region for the research is in Southwest Kansas, a portion of the High Plains Aquifer (HPA) experiencing overdraft due to appropriation of water for irrigation.

3.2 MATERIALS AND METHODS

This section provides details about the DSSAT-MODFLOW modeling system, its application to the study region in Southwest Kansas, and the implementation of SA to identify the system parameters that govern groundwater storage and crop yield. The study region will be presented first to provide context for the subsequent description of methods. The overall description of DSSAT-MODFLOW theory and linkage, and its initial application and testing to the study region, was detailed in Xiang et al. (2020).

3.2.1 STUDY REGION: FINNEY COUNTY, KANSAS

The High Plains Aquifer (HPA), also referred to as the Ogallala Aquifer, is one of the largest fresh groundwater sources in the world, with a total area of 450,000 km^2 (174,000 mi^2), partially covering eight Central States, including South Dakota, Wyoming, Nebraska, Colorado, Kansas, Oklahoma, New Mexico, and Texas (Fig.3-1A). The agricultural area of the aquifer

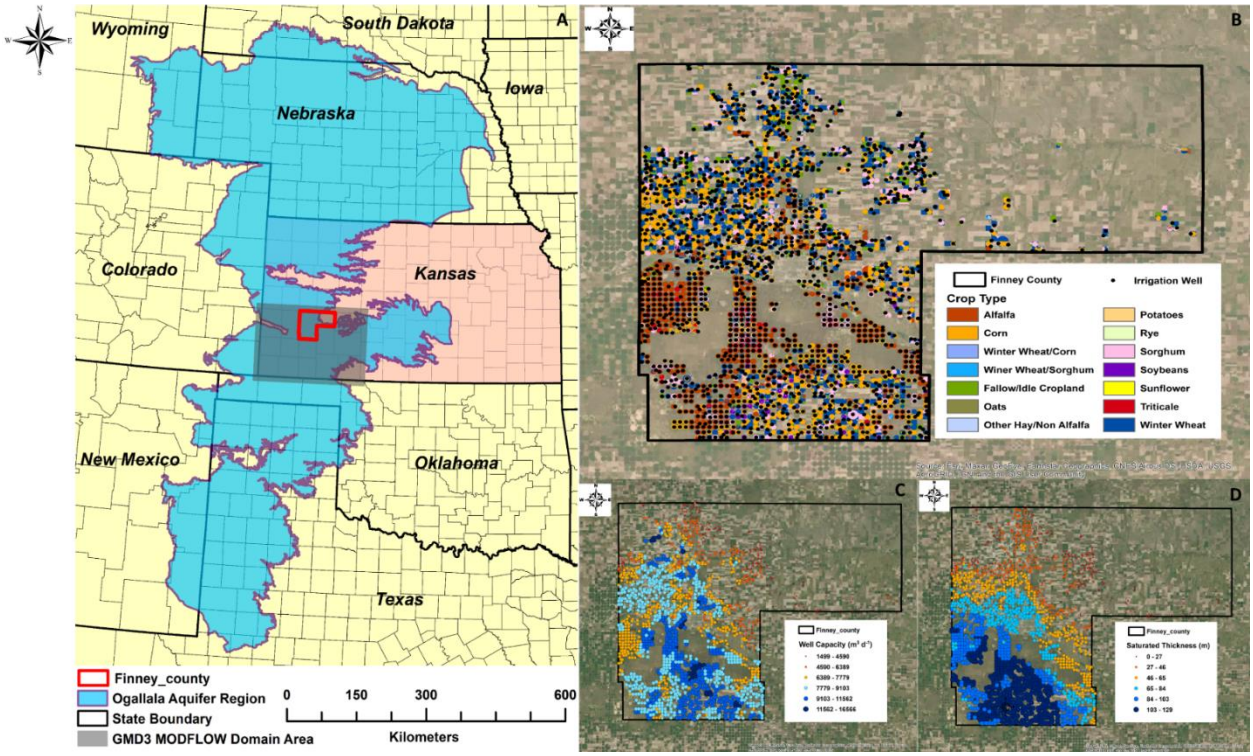

Fig. 3-1 Map of study region and related information. Fig.A shows map of study region of Finney County, southwest of Kansas, in the Ogallala Aquifer. The Finney County area is encompassed within the red contour line. The blue region enclosed with light purple line is the Ogallala Aquifer, and the states are divided with black lines; Fig.B shows map of irrigation well and crop types (Finney County mainly contains five crops, including corn, winter wheat, soybeans, sorghum, and triticale); Fig.C & D show initial well capacity during 1975-1978 and initial average saturated thickness during 1975-1978 in Finney County, respectively.

region provides 30% of total crop and animal production for the U.S.A. (Guru and Horne, 2001; Rosenberg et al., 1999) accounting for 41% (i.e., 20% irrigated cropland in the U.S.A.) of total land area with an annual production of over $35 billion (Basso et al., 2013). Of crops produced in the HPA, 86% is for row crops and small grains, and 14% is for pasture, alfalfa, and fallow lands ("USGS High Plains Aquifer WLMS: Physical/Cultural Setting," n.d.). Approximately 90% of water pumped from the HPA is used for agricultural irrigation, compared with 42% of

groundwater withdrawn for cropland in other regions of the U.S.A. (Gollehon and Winston, 2013; Scanlon et al., 2012). The composition of aquifer material in the HPA consists of poorly sorted clay, silt, sand, and gravel, and the composition of bedrock unit is siltstone, shale, loosely to moderately cemented clay and silt, chalk, limestone, dolomite, conglomerate, claystone, gypsum, anhydrite, and bedded salt. The range of the elevation of aquifer bedrock is from 366 m (1200ft) to 1829 m (6000ft) (Gutentag et al., 1984).

Due to excessive pumping for agricultural irrigation, the HPA has experienced severe depletion in the past few decades. Between 1960 and 2008, groundwater storage has decreased by 360 km^3, accounting for 36% of total groundwater depletion in U.S.A., while the change in water table elevation varies from a decline of 78 m (256 ft) to a rise of 26 m (85 ft), with an average of 5 m (16ft) in decline, accounting for 9% of the area-weighted average saturated thickness (McGuire, 2014). Declines have taken place mainly in Eastern Colorado, Southwest Kansas, the Panhandle of Oklahoma, and Northwest Texas. Increases have occurred in Central Nebraska due to higher precipitation rates, composition of soil layer (e.g., the sandy soils that allow more infiltration and percolation) and the presence of streams for surface water irrigation. Finney County (Fig. 3-1) (105,218 ha; 260,000 ac), located in Southwestern Kansas, was chosen as the study region for this research due to a strong dependence on groundwater pumping (1,629 wells) for irrigation resulting in water table elevation declines up to 15 m since 1950. Main crop types cultivated in this region are corn (maize), winter wheat, soybeans, sorghum, and triticale. Fig. 3-1 shows the location of Finney County within Southwest Kansas and the broader High Plains Aquifer (Fig. 3-1A), the crop type in 2006 and the location of pumping wells (Fig. 3-1B), the well capacity (i.e., available pumping rate) during 1975-178 (Fig. 3-1C), and the point-calculated saturated thickness of the aquifer at pumping well locations in 1975-1878 (Fig. 3-1D).

3.2.2 DSSAT-MODFLOW LINKED MODEL

The Decision Support System for Agrotechnology Transfer (DSSAT) (Jones et al., 2003) is a computer program that can used on over 40 crops to simulate growth, development, and yield on the basis of the dynamics among the soil-plant-atmosphere system. The DSSAT cropping modeling system model requires input information (e.g., weather, soil, crop management, cultivar genetic coefficient data, etc.) to perform agronomic simulations. The model is designed for single field applications. MODFLOW (Harbaugh, 2005) is a 3D groundwater flow model widely used to simulate groundwater head, groundwater storage, and groundwater flow rates in both confined and unconfined aquifers. The aquifer domain is discretized into grid cells horizontally and vertically, with each cell representing a volume of aquifer and provided values of hydraulic conductivity, specific yield, and specific storage, in addition to a suite of groundwater sources and sinks (e.g., recharge, pumping, groundwater discharge to streams, stream seepage to groundwater, groundwater ET). The finite difference method is used to solve for groundwater head for each grid cell, for each time step of a specified simulation period. The span of the simulation period is first divided into stress periods (i.e., a simulation time that groundwater stresses stay constant), and then into time steps.

The linked DSSAT-MODFLOW modeling system (shown in Fig. 3-2) was developed (Xiang et al., 2020) to exchange information between the groundwater system (i.e., water table elevation, saturated thickness, and well capacity) and the agronomic system (i.e., irrigation depth, and volume of drained water from the soil profile that recharges the aquifer) on an annual basis, so that each system can be impacted by the other. The data flow within the linked DSSAT-MODFLOW system is shown in Fig. 3-2. The simulation of the whole linked hydro-agronomic system contains four steps. Step 1 is an ensemble of DSSAT simulations, with a

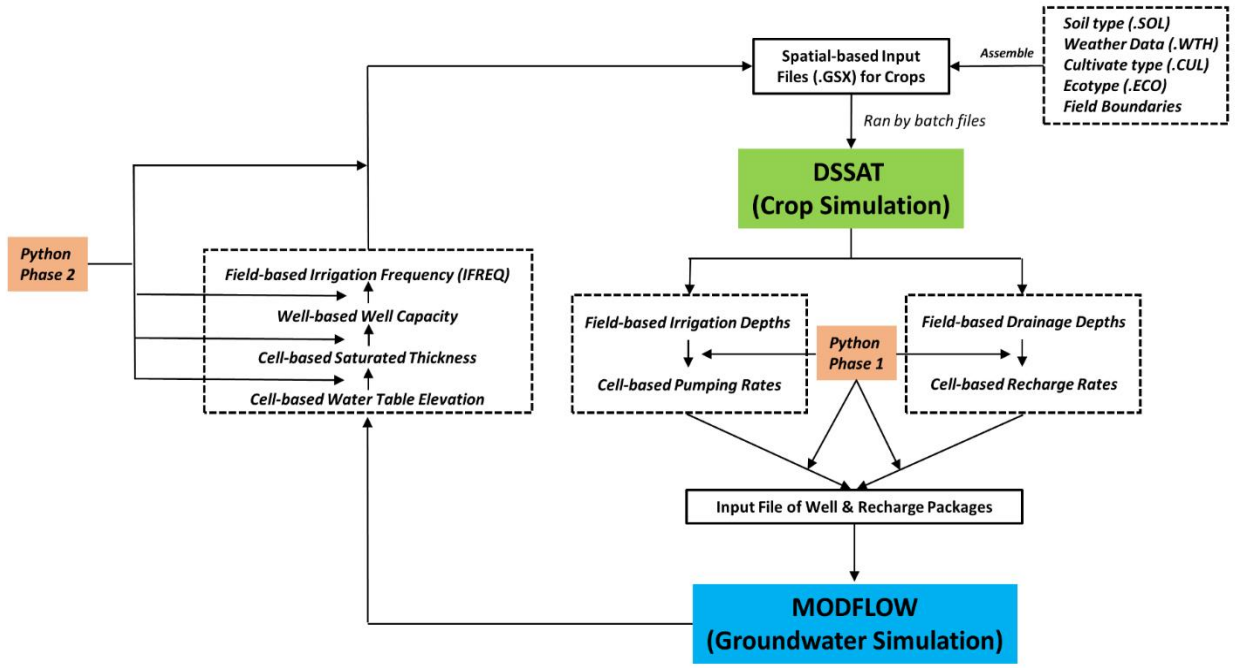

Fig. 3-2 The DSSAT-MODFLOW framework showing the linkage between DSSAT and MODFLOW simulations.

single DSSAT simulation for each cultivated field in the study region, with a spatial module mode through a batch file. Input information includes soil type, weather data, and cultivar genetic information in input files .SOL, .WTH., .CUL, respectively to trigger agronomic simulations through spatial-input files of .GSX for each crop type. Step 2 is the conversion of DSSAT outputs to inputs for MODFLOW. Python programming language is used as the linkage script (Python phase 1) to convert daily field-based irrigation depth and recharge depth simulated by DSSAT to daily grid cell-based pumping rates and recharge rates for MODFLOW simulations (Xiang et al., 2020). Python phase 1 is also used for preparing MODFLOW input files. Step 3 is the MODFLOW simulation. MODFLOW simulates groundwater hydraulic head (i.e., water table elevation for unconfined aquifers) for each gird cell, with daily stress periods to be consistent with daily outputs by DSSAT for daily pumping and recharge rates. The hydraulic head in the last day of year is saved as initial head for the subsequent year. Step 4 is to i) calculate well capacity for each irrigation well in terms of saturated thickness (i.e., water table

elevation – bedrock elevation); ii) update irrigation frequency (i.e., irrigation parameter for DSSAT simulation) based on well capacity in i); and iii) create input files for DSSAT simulations of the following year (i.e., .CUL, .ECO, and .GSX). All detailed information about MODFLOW, DSSAT, and the linkage procedure is demonstrated in Xiang et al. (2020).

3.2.3 DSSAT-MODFLOW APPLICATION TO FINNEY COUNTY, KANSAS

For Finney County, DSSAT was previously calibrated for corn, wheat, sorghum, and soybean (Araya et al., 2017). For application with the DSSAT-MODFLOW framework, each of the 1,332 cultivated fields are included 564, 484, 28, 206, and 50 fields for corn, winter wheat, soybean, sorghum, and triticale, respectively, Fig. 3-1B), with a single DSSAT simulation for each field. The MODFLOW model for Groundwater Management District No.3 (GMD3) (see gray shaded area Fig. 3-1A), developed by the Kansas Geological Survey (KGS) (Liu et al., 2011), was used to link with DSSAT. The MODFLOW model includes a steady-state simulation and transient simulation in the period of 1944 – 1946 and 1947 – 2007, respectively. The domain area of KGS model is 161 km by 241 km (100 miles by 150 miles shown in grey area in Fig. 3-1A), and each grid cell is 1.61 km by 1.61 km (1 mile by 1 mile). To be consistent with daily irrigation and recharge depths from DSSAT for daily pumping and recharge rates, the MODFLOW model was converted to daily stress periods, requiring files to be updated (e.g., Discretization file (.DIS), Recharge Package file (.RCH), and Time-Variant Specified-Head Package file (.CHD), and Stream Package file (.STR)). As described in Xiang et al. (2020), the DSSAT-MODFLOW model was run for the 2000-2007 time period and tested against measured groundwater levels and county-wide crop yield.

3.2.4 FRAMEWORK FOR SENSITIVITY ANALYSIS

Sensitivity analysis (SA) was applied to the DSSAT-MODFLOW model provided in Xiang et al. (2020) to qualitatively (Morris screening method) and quantitatively (Sobol' method) evaluate the factors governing groundwater storage and crop yield in Finney County, Kansas. In so doing, we attempt to provide general insights and conclusions for groundwater-irrigated regions that are experiencing groundwater overdraft. In total, 57 parameters were included in the SA.

Based on Saltelli et al. (2004), SA explores how variation in model input factors influence uncertainty related to the model outputs. Sensitivity analysis is generally classified into two groups: 1) local sensitivity analysis (LSA), and 2) global sensitivity analysis (GSA). LSA assesses the local impact of the variation in inputs on model response through evaluating the gradient or partial derivative of model outputs in vicinity of nominal values of the input factors, while GSA apportions the uncertainty of model outputs to the variation of each input parameter in their entire range of interest. LSA is implemented by altering one value of an input with other values of input factors remaining constant, whereas in GSA all input factors are changed simultaneously over the entire range of each input factor (Zhou and Lin, 2017). The limitations of LSA are: 1) not applicable for nonlinear models (Frey and Patil, 2002) and 2) interactions between parameters are not considered (Saltelli et al., 2008). Therefore, GSA was applied in this study to quantitatively evaluate factors governing the hydro-agronomic system.

3.2.4.1 MORRIS SCREENING METHOD

The Morris SA is a GSA method developed by Morris (1991) to reduce the model complexity through identifying the non-influential input factors using 'One at A Time' (OAT) design, with several incremental ratios called elementary effects (EE). The distribution of EE

that is related to each input parameter is acquired by randomly sampling the space of model input parameters. Two sensitivity measurements obtained by the Morris screening method are μ, measuring the primary effect of an input factor on model response and σ, describing interaction effects of a parameter with other parameters, with nonlinear effects. The potential results that can be determined by the Morris method are negligible, linear, nonlinear, or involved in interactions with other parameters in terms of μ and σ. To estimate two measurements, Morris (1991) suggested that the number of executions is determined by the following relationship (Equ. 3-1):

$$N = r \times (k + 1) \qquad (3 - 1)$$

where *N* is the number of executable model runs, *r* is the number of trajectories (usually 4 to 10), and *k* is the number of input factors of a model. *(see Fig. 3-S1 in Supplementary Information for one year example*)

3.2.4.3 SOBOL' VARIANCE-BASED METHOD

The Sobol' variance-based SA offers quantitative measurements (e.g., first-order, second-order, total-order sensitivity indices, etc.) to obtain the percentage of each input parameters' contribution to the distribution of uncertainty of model responses. Compared with the first-order index, the total-order index is a more relatively reliable measurement of the effect of an input factor on model output due to the consideration of interactions of a parameter with other parameters. To implement Sobol' sensitivity analysis for obtaining first-order and total-order indices, the number of simulation runs needed is determined by:

$$N = n \times (2k + 2) \qquad (3 - 2)$$

where *n* is the sample size for estimation of one individual effect and *k* is the number of input parameters.

3.2.4.3 OVERALL SENSITIVITY ANALYSIS FRAMEWORK

Since DSSAT integrates genotype, environmental, experimental data, and management data, it is considerably driven by cultivar genetic, climate-related, and soil-related parameters (Jones et al., 2015; Li et al., 2018; Mourice et al., 2014; Rezzoug et al., 2008). In addition, movement of groundwater in confined and unconfined aquifers exceptionally depends on property of geologic formations of soil, sand, and rock, with relation to hydrogeologic parameters of specific yield (Xiao et al., 2021) and hydraulic conductivity (Gómez-Hernández and Gorelick, 1989). Furthermore, to quantify interactions between groundwater and surface water, riverbed conductance (Wei and Bailey, 2019) is also another significant factor for the hydro-agronomic system. Therefore, 57 parameters (Tab. 3-1), including 44 cultivar parameters (DSSAT model), 10 soil parameters (DSSAT model), and 3 hydrogeologic parameters (MODFLOW model), are selected for the Morris screening method. Based on Equ. 3-1, 580 model simulations were run for the Morris method calculations. The Sobol' method was then applied only to the most influential parameters as identified by the Morris screening method, in addition to four climate-related parameters (i.e., maximum temperature, minimum temperature, solar radiation, and precipitation). The climate parameters were not screened by the Morris method due to their importance in the hydro-agronomic system (Jones et al., 2003; Kour et al., 2016). As described in Section 3.3, 24 parameters of the 57 initial parameters were identified in the Morris screening method as being influential. With the additional four climate parameters, and according to Equ. 3-2, the number of DSSAT-MODFLOW model simulations run in the Sobol' method was 14,848. Model results were processed using SimLab (*SIMLAB, Version 2.2 Simulation Environment for Uncertainty and Sensitivity Analysis*, 2004).

Tab. 3-1 Parameters from the hydro-agronomic system selected for the Morris screening method

Parameter Name	File Name	Definition	Unit	Range
Cultivar Genetic Parameters				
P1[a]	MZCER047.CUL	Thermal time from seedling emergence to the end of the juvenile phase (expressed in degree days above a base temperature of 8 deg. C) during which the plant is not responsive to changes in photoperiod	degree-day	100 - 450 (Kisekka et al., 2017)
P2[a]	MZCER047.CUL	Extent to which development (expressed as days) is delayed for each hour increase in photoperiod above the longest photoperiod at which development proceeds at a maximum rate (which is considered to be 12.5 hours).	day	0.01 - 2.0 (Kisekka et al., 2017)
P5[a]	MZCER047.CUL	Thermal time from silking to physiological maturity (expressed in degree days above a base temperature of 8 deg.C).	degree-day	600 - 1000 (Kisekka et al., 2017)
G2[a]	MZCER047.CUL	Maximum possible number of kernels per plant.	Kernel	440 - 1000 (Kisekka et al., 2017)
G3[a]	MZCER047.CUL	Kernel filling rate during the linear grain filling stage and under optimum conditions.	mg-day^{-1}	5- 16 (Kisekka et al., 2017)
PHINT[a]	MZCER047.CUL	Phylochron interval; the interval in thermal time (degree days) between successive leaf tip appearances.	degree-day	25 - 75 (DeJonge et al., 2012; Kisekka et al., 2017)
RUE[a]	MZCER047.ECO	Radiation use efficiency	g-MJ^{-1}	2 - 5 (DeJonge et al., 2012)
P1[b]	SGCER047.CUL	Thermal time from seedling emergence to the end of the juvenile phase (expressed in degree days above TBASE during which the plant is not responsive to changes in photoperiod	degree-day	150 - 500(Lamsal, 2017)
P2[b]	SGCER047.CUL	Thermal time from the end of the juvenile stage to tassel initiation under short days (degree days above TBASE)	degree-day	90 - 110 (Lamsal, 2017)
P2O[b]	SGCER047.CUL	Critical photoperiod or the longest day length (in hours) at which development occurs at a maximum rate. At values higher than P2O, the rate of development is reduced	hour	11 - 16 (Lamsal, 2017)
P2R[b]	SGCER047.CUL	Extent to which phasic development leading to panicle initiation (expressed in degree days) is delayed for each hour increase in photoperiod above P2O	degree-day	0 - 300 (Araya et al., 2017)
PANTH[b]	SGCER047.CUL	Thermal time from the end of tassel initiation to anthesis (degree days above TBASE)	degree-day	500 - 700 (Araya et al., 2017)
P3[b]	SGCER047.CUL	Thermal time from to end of flag leaf expansion to anthesis (degree days above TBASE)	degree-day	0 - 200 (Araya et al., 2017)
P4[b]	SGCER047.CUL	Thermal time from anthesis to beginning grain filling (degree days above TBASE)	degree-day	50 - 100 (Araya et al., 2017)
P5[b]	SGCER047.CUL	Thermal time from beginning of grain filling to physiological maturity (degree days above TBASE)	degree-day	400 - 700 (Lamsal, 2017)

PHINT[b]	SGCER047.CUL	Phylochron interval; the interval in thermal time between successive leaf tip appearances (degree days)	degree-day	30 - 90 (Lamsal, 2017)
G1[b]	SGCER047.CUL	Scaler for relative leaf size	-	0 - 30 (Lamsal, 2017)
G2[b]	SGCER047.CUL	Scaler for partitioning of assimilates to the panicle (head).	-	4 - 10 (Lamsal, 2017)
TBASE[b]	SGCER047.ECO	Base temperature	^{o}C	4 - 9 (Lamsal, 2017)
RUE[b]	SGCER047.ECO	Radiation use efficiency	$g\text{-}MJ^{-1}$	3 - 6 (Lamsal, 2017)
P1V[c]	WHCER047.CUL	Days, optimum vernalizing temperature, required for vernalization	day	25 - 100 (Li et al., 2018)
P1D[c]	WHCER047.CUL	Photoperiod response (% reduction in rate/10 h drop in pp)	%	35 - 200 (Li et al., 2018)
P5[c]	WHCER047.CUL	Grain filling (excluding lag) phase duration (oC.d)	degree-day	500 - 1000 (Li et al., 2018)
G1[c]	WHCER047.CUL	Kernel number per unit canopy weight at anthesis (#/g)	Number/gram	15 - 60 (Li et al., 2018)
G2[c]	WHCER047.CUL	Standard kernel size under optimum conditions (mg)	mg	20 - 90 (Li et al., 2018)
G3[c]	WHCER047.CUL	Standard,non-stressed mature tiller wt (incl grain) (g dwt)	g-dwt	0.5 - 10 (Li et al., 2018)
PHINT[c]	WHCER047.CUL	Interval between successive leaf tip appearances (oC.d)	deg.C-days	0 - 200 (Araya et al., 2017)
CSDL[d]	SBGRO047.CUL	Critical Short Day Length below which reproductive development progresses with no daylength effect (for short-day plants) (hour)	hour	11 - 15 (Boote et al., 2003)
PPSEN[d]	SBGRO047.CUL	Slope of the relative response of development to photoperiod with time (positive for shortday plants)	$hour^{-1}$	0.1 - 0.4 (Boote et al., 2003)
EM-FL[d]	SBGRO047.CUL	Time between plant emergence and flower appearance (R1) (photothermal days)	days	10 - 35 (Boote et al., 2003)
FL-SH[d]	SBGRO047.CUL	Time between first flower and first pod (R3) (photothermal days)	days	3 - 12 (Boote et al., 2003)
FL-SD[d]	SBGRO047.CUL	Time between first flower and first seed (R5) (photothermal days)	days	10 - 20 (Boote et al., 2003)
SD-PM[d]	SBGRO047.CUL	Time between first seed (R5) and physiological maturity (R7) (photothermal days)	days	25 - 40 (Boote et al., 2003)
FL-LF[d]	SBGRO047.CUL	Time between first flower (R1) and end of leaf expansion (photothermal days)	days	10 - 30 (Boote et al., 2003)
LFMAX[d]	SBGRO047.CUL	Maximum leaf photosynthesis rate at 30 C, 350 vpm CO2, and high light (mg CO2/m2-s)	$mg\text{-}CO^2/m^2\text{-}s$	0.9 - 1.3 (Boote et al., 2003)
SLAVR[d]	SBGRO047.CUL	Specific leaf area of cultivar under standard growth conditions (cm2/g)	cm^2/g	280 - 410 (Boote et al., 2003)
SIZLF[d]	SBGRO047.CUL	Maximum size of full leaf (three leaflets) (cm2)	cm^2	140 - 210 (Boote et al., 2003)
WTPSD[d]	SBGRO047.CUL	Maximum weight per seed (g)	g	0.15 - 0.22 (Boote et al., 2003)
SFDUR[d]	SBGRO047.CUL	Seed filling duration for pod cohort at standard growth conditions (photothermal days)	days	15 - 27 (Boote et al., 2003)

SDPDV[d]	SBGRO047.CUL	Average seed per pod under standard growing conditions (#/pod)	number/pod	1.5 - 2.5 (Boote et al., 2003)
PODUR[d]	SBGRO047.CUL	Time required for cultivar to reach final pod load under optimal conditions (photothermal days)	day	7 - 17 (Boote et al., 2003)
THRSH[d]	SBGRO047.CUL	Threshing percentage. The maximum ratio of (seed/(seed+shell)) at maturity. Causes seeds to stop growing as their dry weight increases until shells are filled in a cohort.	-	75 - 80 (Boote et al., 2003)
SDPRO[d]	SBGRO047.CUL	Fraction protein in seeds (g(protein)/g(seed))	-	0.37 - 0.43 (Boote et al., 2003)
SDLIP[d]	SBGRO047.CUL	Fraction oil in seeds (g(oil)/g(seed))	-	0.18 - 0.22 (Boote et al., 2003)
Hydrogeologic Parameters				
K	Kst6.DAT	Hydraulic Conductivity	$ft\text{-}day^{-1}$	0.9-1.1
Sy	Sys6.DAT	Specific Yield	-	0.7-1.3
Cond	.str	Riverbed/streambed hydraulic conductance	$ft^2\text{-}day^{-1}$	0.7-1.3
Soil-related Parameters				
SLPF	SOIL.SOL	Soil fertility factor/Photosynthesis factor	-	0.7 - 1.0 (Lamsal, 2017)
SLU1	SOIL.SOL	Evaporation limit	cm	3 - 12 (Lamsal, 2017; Corbeels et al., 2016)
SLDR	SOIL.SOL	Drainage rate	day^{-1}	0 - 1 (Lamsal, 2017)
SLRO	SOIL.SOL	Runoff curve number	-	60 - 95 (Lamsal, 2017)
SLLL	SOIL.SOL	Drained lower limit	$cm^3\ cm^{-3}$	0.02 - 0.25 (Lamsal, 2017; Corbeels et al., 2016)
SDUL	SOIL.SOL	Drained upper limit	$cm^3\ cm^{-3}$	0.25 - 0.42 (Lamsal, 2017)
SSAT	SOIL.SOL	Saturated water limit	$cm^3\ cm^{-3}$	0.3 - 0.6(Lamsal, 2017; Corbeels et al., 2016)
SSKS	SOIL.SOL	Saturated hydraulic conductivity	cmh^{-1}	0.2 - 2.5 (Lamsal, 2017)
SBDM	SOIL.SOL	Bulk density	gcm^3	1.1 - 1.6 (Lamsal, 2017)
SLOC	SOIL.SOL	Soil organic carbon	%	0.3 - 2.5 (Lamsal, 2017)

[a] Maize genetic parameter; [b] Sorghum genetic parameter; [c] Wheat genetic parameter; [d] Soybean genetic parameter.

The framework for implementing SA with the DSSAT-MODFLOW linked system is described in Fig. 3-3. The major task of prior-processing is to create sample files for the Morris screening and Sobol' sensitivity analysis, respectively, based on identified parameters, with prior distribution and range of parameters, using the random sampling method. Python phase 1 (see Fig. 3-3) is used to update input files (i.e., .CUL, .ECO, .SOL, and .WTH for DSSAT and

Kst.DAT, Sys.DAT, and .str for MODFLOW) for the hydro-agronomic modeling system in terms of values of parameters in the DSSAT experiments in the sample file. To reduce computation cost, parallel simulations through batch files are introduced for all model runs on computing servers. The post-processing procedure has two main tasks: 1) organize outputs of model responses fitting them to the format of input files for SimLab to obtain qualitative and quantitative measurements; and 2) visualize the evaluations of SA (Fig. 3-3).

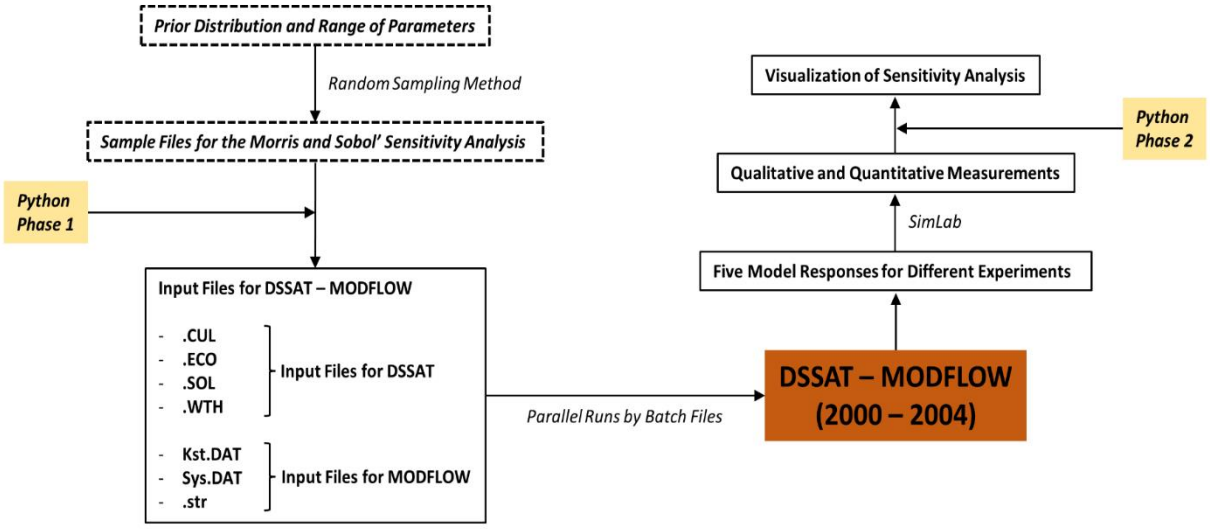

Fig. 3-3 Schematic showing the entire system of assemble with prior-processing, model simulation, and post-processing for sensitivity analysis of the linked DSSAT-MODFLOW system.

3.3 RESULTS AND DISCUSSION

3.3.1 SCREENING PARAMETER USING THE MORRIS METHOD

The results of qualitative measurements using the Morris screening sensitivity analysis are shown in Figs. 3-4A, B, C, D, and E for maize yield, soybean yield, wheat yield, sorghum yield, and water table elevation, respectively. As shown in Fig. 3-4A, most parameters are located within μ- σ plane below the 1:1 diagonal line, showing the parameters' primarily influence on maize yield, with little interactions with other parameters. The larger the value of μ is, the more the effect a parameter has on maize yield; therefore, RUE, G3, P5, P1, SLPF, and G2, with large μ, indicates maize yield is relatively more sensitive to these parameters (i.e., those

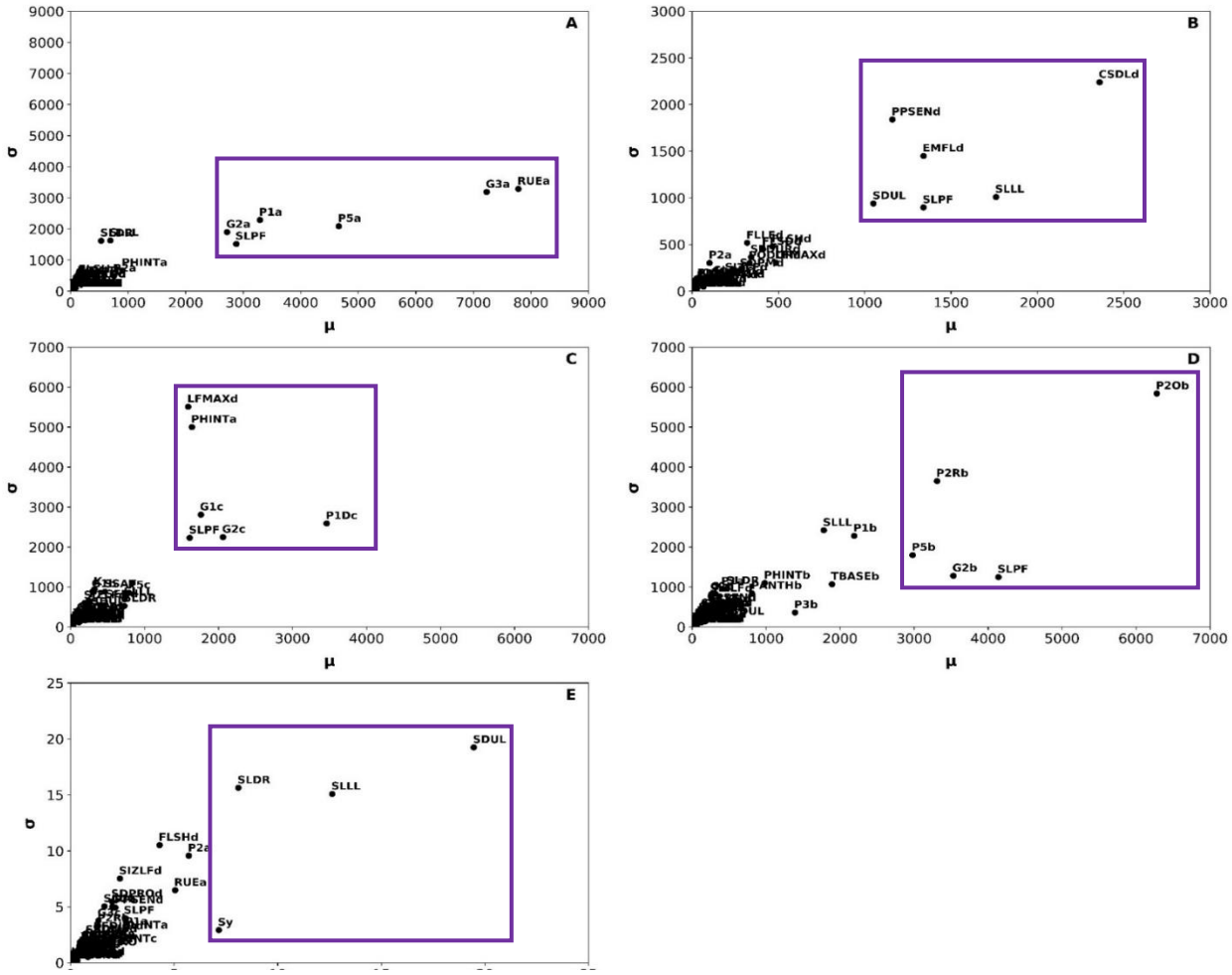

Fig. 3-4 Parameters (within the purple box) selected for the Sobol' sensitivity analysis after the Morris screening method (totally fifty-seven parameters for the Morris screening). The letter of a indicates maize genetic parameter; the letter of b indicates sorghum genetic parameters; the letter c indicates wheat genetic parameters; the letter d indicates soybean genetic parameters. A) Qualitative measurements of parameters for maize yield; B) Qualitative measurements of parameters for soybean yield; C) Qualitative measurements of parameters for wheat yield; D) Qualitative measurements of parameters for sorghum yield; E) Qualitative measurements of parameters for water table elevation.

parameters considerably affect uncertainty of maize yield). The parameters are further analyzed quantitatively using the Sobol' variance-based method. For soybean yield (shown in Fig. 3-4B), there are more interactions among soybean-related genetic and soil-related parameters, and the parameters with high μ and σ are selected for later quantitative analysis. In addition, since the entire hydro-agronomic system is focused on a system instead of a single hydrological, agronomic system or one crop type, parameters from the other system or crop model routines affect other model responses. PHINT is one of the maize-related genetic parameters, but it increases the uncertainty of wheat yield (Fig. 3-4C); in general, interactions with other

parameters are important in understanding the factors that govern the entire system. Results for sorghum yield are shown in Fig. 3-4D, indicating that the genetic parameters mainly influence the uncertainty in simulated sorghum yield, with strong interaction with other parameters. Water table elevation (Fig. 3-4E) is significantly driven by soil-related parameters, especially SDUL and SLLL, with relation to soil water capacity, soil specific yield, and overall drainage of soil water to the underlying aquifer. Overall, soil parameters have a strong influence on both crop yield and groundwater levels. The most influential twenty-four parameters (see Tab. 3-2) were selected to use in the Sobol' SA method.

Tab. 3-2 Parameters from the hydro-agronomic system selected for the Sobol' quantitative method after the Morris screening method

Parameter Name	File Name	Definition	Unit	Range
Cultivar Genetic Parameters				
P1[a]	MZCER047.CUL	Thermal time from seedling emergence to the end of the juvenile phase (expressed in degree days above a base temperature of 8 deg. C) during which the plant is not responsive to changes in photoperiod	degree-day	100 - 450 (Kisekka et al., 2017)
P5[a]	MZCER047.CUL	Thermal time from silking to physiological maturity (expressed in degree days above a base temperature of 8 deg.C).	degree-day	600 - 1000 (Kisekka et al., 2017)
G2[a]	MZCER047.CUL	Maximum possible number of kernels per plant.	Kernel	440 - 1000 (Kisekka et al., 2017)
G3[a]	MZCER047.CUL	Kernel filling rate during the linear grain filling stage and under optimum conditions.	mg-day^{-1}	5- 16 (Kisekka et al., 2017)
PHINT[a]	MZCER047.CUL	Phylochron interval; the interval in thermal time (degree days) between successive leaf tip appearances.	degree-day	25 - 75 (DeJonge et al., 2012; Kisekka et al., 2017)
RUE[a]	MZCER047.ECO	Radiation use efficiency	g-MJ^{-1}	2 - 5 (DeJonge et al., 2012)
P2O[b]	SGCER047.CUL	Critical photoperiod or the longest day length (in hours) at which development occurs at a maximum rate. At values higher than P2O, the rate of development is reduced	hour	11 - 16 (Lamsal, 2017)
P2R[b]	SGCER047.CUL	Extent to which phasic development leading to panicle initiation (expressed in degree days) is delayed for each hour increase in photoperiod above P2O	degree-day	0 - 300 (Araya et al., 2017)
P5[b]	SGCER047.CUL	Thermal time from beginning of grain filling to physiological maturity (degree days above TBASE)	degree-day	400 - 700 (Lamsal, 2017)
G2[b]	SGCER047.CUL	Scaler for partitioning of assimilates to the panicle (head).	-	4 - 10 (Lamsal, 2017)

P1D[c]	WHCER047.CUL	Photoperiod response (% reduction in rate/10 h drop in pp)	%	35 - 200 (Li et al., 2018)
G1[c]	WHCER047.CUL	Kernel number per unit canopy weight at anthesis (#/g)	Number/gram	15 - 60 (Li et al., 2018)
G2[c]	WHCER047.CUL	Standard kernel size under optimum conditions (mg)	mg	20 - 90 (Li et al., 2018)
CSDL[d]	SBGRO047.CUL	Critical Short Day Length below which reproductive development progresses with no daylength effect (for short-day plants) (hour)	hour	11 - 15 (Boote et al., 2003)
PPSEN[d]	SBGRO047.CUL	Slope of the relative response of development to photoperiod with time (positive for shortday plants)	$hour^{-1}$	0.1 - 0.4 (Boote et al., 2003)
EM-FL[d]	SBGRO047.CUL	Time between plant emergence and flower appearance (R1) (photothermal days)	days	10 - 35 (Boote et al., 2003)
LFMAX[d]	SBGRO047.CUL	Maximum leaf photosynthesis rate at 30 C, 350 vpm CO_2, and high light (mg CO_2/m^2-s)	mg-CO^2/m^2-s	0.9 - 1.3 (Boote et al., 2003)
Hydrogeologic Parameters				
K	Kst6.DAT	Hydraulic Conductivity	-	0.9-1.1
Sy	Sys6.DAT	Specific Yield	-	0.7-1.3
Cond	.str	Riverbed/streambed hydraulic conductance	-	0.7-1.3
Soil-related Parameters				
SLPF	SOIL.SOL	Soil fertility factor/Photosynthesis factor	-	0.7 - 1.0 (Lamsal, 2017)
SLDR	SOIL.SOL	Drainage rate	day^{-1}	0 - 1 (Lamsal, 2017)
SLLL	SOIL.SOL	Drained lower limit	cm^3 cm^{-3}	0.02 - 0.25 (Lamsal, 2017; Corbeels et al., 2016)
SDUL	SOIL.SOL	Drained upper limit	cm^3 cm^{-3}	0.25 - 0.42 (Lamsal, 2017)
Climate-related Parameters				
SRAD	.WTH	Solar radiation	MJ-m^{-2}-day^{-1}	0.6-1.4 (Tyagi et al., 2018)
TMAX	.WTH	Temperature Maximum	°C	0.6-1.4 (Tyagi et al., 2018)
TMIN	.WTH	Temperature Minimum	°C	0.6-1.4 (Tyagi et al., 2018)
RAIN	.WTH	Rainfall (including snow)	mm-day^{-1}	0.6-1.4 (Tyagi et al., 2018)

[a] Maize genetic parameter; [b] Sorghum genetic parameter; [c] Wheat genetic parameter; [d] Soybean genetic parameter.

3.3.2 QUANTITATIVE RANKING PARAMETERS USING THE SOBOL' METHOD

Results of the Sobol' method are shown in Figs. 3-5 and 3-6, and first- and total-order indices of 28 (24 identified from the Morris method + 4 climate parameters) parameters for both agronomic and hydrological responses are shown in Tabs. 3-3 and 3-4. Figure 3-5 summarizes

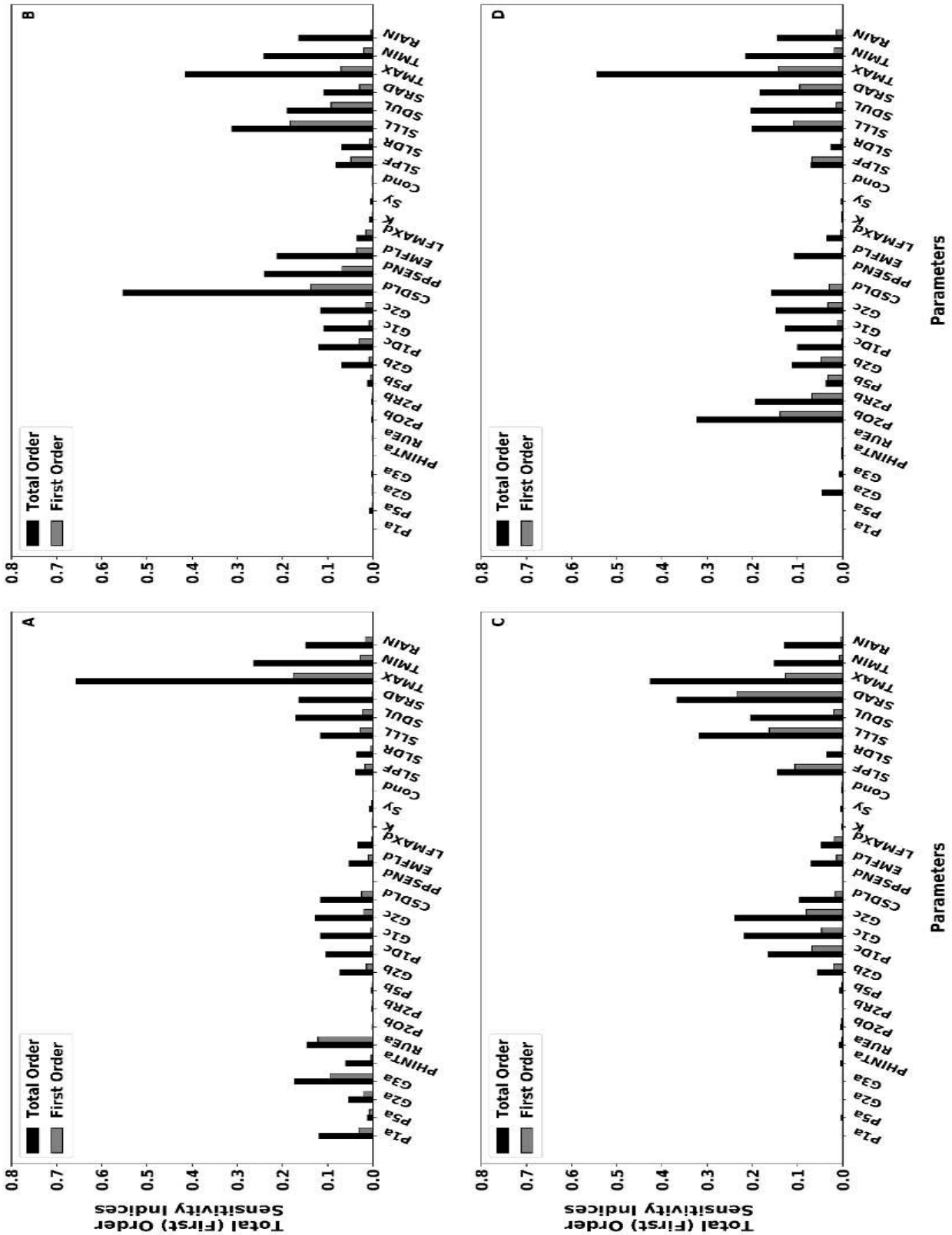

Fig. 3-5 Sobol' sensitivity indices of twenty-eight parameters from the DSSAT-MODFLOW framework system for agronomic responses (i.e., Fig. 3-5A maize yield; Fig. 3-5B soybean yield; Fig. 3-5C wheat yield; Fig. 3-5D sorghum yield) are shown above. First-order sensitivity indices (grey bar) and total-order sensitivity indices (black bar) are shown, respectively.

the sensitivity indices for crop yield, and Fig. 3-6 summarizes indices for hydrologic system responses (water table elevation, groundwater ET, recharge, irrigation pumping, river leakage, groundwater discharge). Based on results shown in Fig. 3-5, climate parameters contribute strongly to crop yield, and they also highly interact with other parameters in terms of the difference of first- and total-order indices. For quantitative measurements for maize yield shown in Fig. 3-5A, TMAX has the greatest control on model simulations due to its high first-order and total-order indices, and sorghum-related genetic and hydrological parameters are negligible due to low indices (close to 0). As shown in Fig. 3-5B, both soybean-related genetic, climate parameters, and soil parameters dominate the model response (i.e., soybean yield), and similarly, there is almost no impact of hydrological parameters on soybean yield, which is same for wheat and sorghum yields. Sorghum yield (Fig. 3-5D) is strongly influenced by climate-related parameters and sorghum genetic parameters, and by more parameters than those of winter wheat yield (Fig. 3-5C), indicating that uncertainty of sorghum yield is harder to control compared with winter wheat yield. Winter wheat is mainly driven by climate, soil-related parameters, and winter wheat genetic parameters (Fig. 3-5C). From a systems point of view, for those four major crop types, crop yields are not controlled by their own cultivar genetic parameters alone, but also by other cultivar genetic parameters. For example, besides maize genetic parameters, several winter wheat, and soybean cultivar genetic parameters are interactively sensitive to maize yield. Similarly, this situation occurs in other crop types; therefore, to have accurate simulations of crop yields, the different cultivar genetic parameters for the crops within the simulated system should be included in calibration.

Fig. 3-6 shows quantitative results of parameters for hydrologic responses (i.e., water table elevation, ET, recharge, irrigation pumping, river leakage, and aquifer seepage). As we can

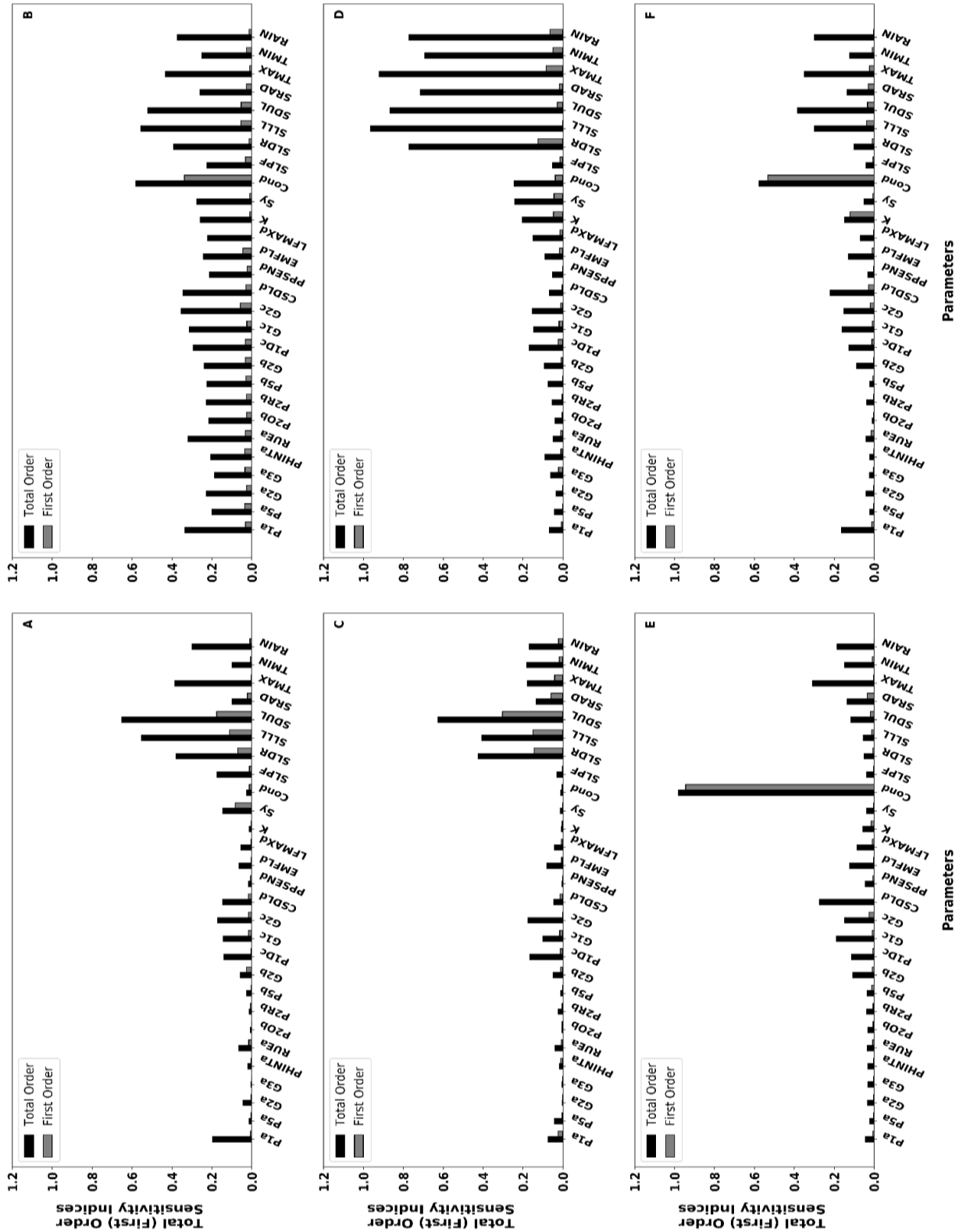

Fig. 3-6 Sobol' sensitivity indices of twenty-eight parameters from the DSSAT-MODFLOW framework system for hydrologic responses (i.e., Fig.6A water table elevation; Fig.6B ET; Fig.6C recharge; Fig.6D irrigation pumping; Fig.6E river leakage; Fig.6F groundwater discharge) are shown above. First-order sensitivity indices (grey bar) and total-order sensitivity indices (black bar) are shown, respectively.

see in Fig. 3-6A, few cultivar genetic parameters appreciably affect water table elevation, and specific yield, soil-related, and climate parameters contribute to the variation of water table elevation, especially soil parameters. In comparison with Fig. 3-6B, all parameters are related to the uncertainty of ET, and except for riverbed conductance, other parameters with very low first-order indices and high total-order indices indicate the system intensively interact among parameters, causing the high degree of uncertainty of ET. Compared with the uncertainty of water table elevation, the uncertainty of recharge (Fig. 3-6C) is caused by similar parameters, since recharge has a positive relationship with water table elevation. In Fig. 3-6D, soil-related and climate-related parameters influence the variability of irrigation pumping, because crop growth is driven by climate-related parameters, and then impact on water productivity; in addition, climate-related parameters can change water content in soil layer, which triggers irrigation. The interaction between river and groundwater (Fig. 3-6E and Fig. 3-6F) is principally controlled by riverbed conductance, and climate, sorghum and soybean genetic parameters are slightly sensitive to river leakage and aquifer discharge, respectively. These results indicate a complex system of interacting environmental factors. Of note is that, except for groundwater-surface water interactions (Fig. 3-6E, 3-6F), climate variables and soil properties have a stronger influence on hydrologic fluxes (recharge, ET, pumping) than hydrogeologic factors (*K* hydraulic conductivity, S_y specific yield). Climate impacts crop germination, growth, and irrigation needs, and therefore controls the overall response of crop yield and pumping in the region.

Tab. 3-3 First order and Total sensitivity indices of 28 parameters for agronomic responses.

S_i	Parameters	Sobol' value for maize yield	Sobol' value for soybean yield	Sobol' value for wheat yield	Sobol' value for sorghum yield	S_{Ti}	Parameters	Sobol' value for maize yield	Sobol' value for soybean yield	Sobol' value for wheat yield	Sobol' value for sorghum yield
1	P1[a]	0.02970	0.00000[e]	0.00034	0.00025	1	P1[a]	0.11826	0.00001	0.00057	0.00032
2	P5[a]	0.00779	0.00133	0.00054	0.00036	2	P5[a]	0.01170	0.00761	0.00409	0.00091
3	G2[a]	0.01936	0.00045	0.00049	0.00102	3	G2[a]	0.05416	0.00087	0.00083	0.04586

4	G3[a]	0.09471	0.00017	0.00000[e]	0.00021	4	G3[a]	0.17286	0.00255	0.00070	0.00784
5	PHINT[a]	0.00396	0.00000[e]	0.00071	0.00156	5	PHINT[a]	0.06033	0.00002	0.00542	0.00180
6	RUE[a]	0.12132	0.00012	0.00219	0.00083	6	RUE[a]	0.14555	0.00055	0.00773	0.00089
7	P2O[b]	0.00006	0.00129	0.00252	0.13837	7	P2O[b]	0.00059	0.00201	0.00463	0.32304
8	P2R[b]	0.00055	0.00133	0.00041	0.06774	8	P2R[b]	0.00183	0.00237	0.00087	0.19326
9	P5[b]	0.00067	0.00421	0.00211	0.03273	9	P5[b]	0.00331	0.01079	0.00578	0.03718
10	G2[b]	0.01450	0.00818	0.02010	0.04758	10	G2[b]	0.07263	0.06845	0.05648	0.11172
11	P1D[c]	0.00556	0.03000	0.06780	0.00224	11	P1D[c]	0.10316	0.12050	0.16472	0.09949
12	G1[c]	0.00447	0.00817	0.04653	0.01143	12	G1[c]	0.11517	0.108107	0.21783	0.12710
13	G2[c]	0.01930	0.01640	0.08067	0.03280	13	G2[c]	0.12812	0.11478	0.23919	0.14696
14	CSDL[d]	0.02494	0.13676	0.01620	0.03030	14	CSDL[d]	0.11494	0.55306	0.09503	0.15773
15	PPSEN[d]	0.00000[e]	0.06757	0.00075	0.00049	15	PPSEN[d]	0.00005	0.23995	0.00097	0.00027
16	EM-FL[d]	0.01050	0.03640	0.01367	0.00163	16	EM-FL[d]	0.05223	0.21110	0.06970	0.10673
17	LFMAX[d]	0.00308	0.01535	0.01860	0.00421	17	LFMAX[d]	0.03275	0.03498	0.04723	0.03532
18	K	0.00027	0.00119	0.00075	0.00145	18	K	0.00111	0.00639	0.00133	0.00191
19	Sy	0.00188	0.00109	0.00046	0.00103	19	Sy	0.00729	0.00598	0.00419	0.00315
20	Cond	0.00007	0.00051	0.00116	0.00012	20	Cond	0.00018	0.00081	0.00188	0.00059
21	SLPF	0.01756	0.04909	0.10584	0.06805	21	SLPF	0.03854	0.08031	0.14438	0.06987
22	SLDR	0.00447	0.00761	0.00111	0.00379	22	SLDR	0.03617	0.06922	0.03534	0.02664
23	SLLL	0.02804	0.18279	0.16301	0.10945	23	SLLL	0.11528	0.31228	0.31770	0.20096
24	SDUL	0.02240	0.09291	0.01940	0.01461	24	SDUL	0.17009	0.19009	0.20318	0.20303
25	SRAD	0.00126	0.02920	0.23446	0.09498	25	SRAD	0.16316	0.10774	0.36615	0.18345
26	TMAX	0.17644	0.07029	0.12633	0.14219	26	TMAX	0.65724	0.41471	0.42629	0.54271
27	TMIN	0.02741	0.01989	0.00778	0.01907	27	TMIN	0.26287	0.24095	0.15070	0.21435
28	RAIN	0.01640	0.00343	0.00388	0.01396	28	RAIN	0.14798	0.16435	0.12799	0.14571
	SUM	0.65659	0.78574	0.93780	0.84244		SUM	2.78755	3.07141	2.70090	2.98877

[a] Maize genetic parameter; [b] Sorghum genetic parameter; [c] Wheat genetic parameter; [d] Soybean genetic parameter; [e] The value of S_i for 4 parameters were slightly smaller than 0, due to numerical integration, and then the values were set to be 0.

Tab. 3-4 First order and Total sensitivity indices of 28 parameters for hydrologic responses.

S_i	**Parameters**	**Sobol' value for Water Table Elevation**	**Sobol' value for ET**	**Sobol' value for Recharge**	**Sobol' value for Irrigation Pumping**	**Sobol' value for River Leakage**	**Sobol' value for Aquifer Seepage**
1	P1[a]	0.00712	0.03150	0.02382	0.00859	0.00543	0.01212
2	P5[a]	0.00446	0.03590	0.00460	0.00034	0.00211	0.00122
3	G2[a]	0.00334	0.02510	0.00173	0.00202	0.00354	0.00247
4	G3[a]	0.00142	0.03420	0.00086	0.02210	0.00142	0.00394
5	PHINT[a]	0.00286	0.03560	0.01105	0.00990	0.00223	0.00101
6	RUE[a]	0.01508	0.03250	0.00844	0.01055	0.00717	0.01476
7	P2O[b]	0.00138	0.02490	0.00349	0.00488	0.00444	0.00224
8	P2R[b]	0.00648	0.02540	0.00470	0.00583	0.00417	0.00207
9	P5[b]	0.00243	0.02840	0.00223	0.00080	0.01223	0.00578
10	G2[b]	0.02647	0.03180	0.01230	0.00913	0.00888	0.00137
11	P1D[c]	0.00303	0.03182	0.01275	0.02398	0.00562	0.01120
12	G1[c]	0.01650	0.02440	0.01598	0.01921	0.00891	0.00797
13	G2[c]	0.01653	0.05680	0.00133	0.01072	0.02458	0.01951
14	CSDL[d]	0.01764	0.02860	0.01504	0.00406	0.00035	0.02712
15	PPSEN[d]	0.00682	0.02290	0.00135	0.00093	0.00532	0.00212
16	EM-FL[d]	0.00199	0.04440	0.00706	0.01780	0.00341	0.00990
17	LFMAX[d]	0.00372	0.00058	0.00830	0.01547	0.00841	0.00289
18	K	0.00205	0.00920	0.00514	0.04750	0.01472	0.12060
19	Sy	0.08279	0.01100	0.00126	0.04450	0.00279	0.00632
20	Cond	0.01240	0.33739	0.00479	0.03850	0.94473	0.53243
21	SLPF	0.01180	0.03130	0.00305	0.01530	0.00251	0.00498
22	SLDR	0.06984	0.01280	0.14486	0.12418	0.00587	0.00957
23	SLLL	0.11154	0.05400	0.15053	0.00126	0.01194	0.03665
24	SDUL	0.17573	0.05330	0.30284	0.02813	0.01880	0.03274
25	SRAD	0.02190	0.02720	0.05960	0.01810	0.03447	0.02910
26	TMAX	0.00238	0.01041	0.04100	0.08462	0.00231	0.02288
27	TMIN	0.00636	0.02570	0.01856	0.05012	0.00930	0.00906
28	RAIN	0.00883	0.01281	0.02228	0.06465	0.00057	0.00297
	SUM	0.64289	1.09991	0.88894	0.68317	1.15623	0.93499
S_{Ti}	**Parameters**	**Sobol' value for Water Table Elevation**	**Sobol' value for ET**	**Sobol' value for Recharge**	**Sobol' value for Irrigation Pumping**	**Sobol' value for River Leakage**	**Sobol' value for Aquifer Seepage**

1	P1[a]	0.19557	0.33438	0.07428	0.06795	0.04225	0.16258
2	P5[a]	0.01417	0.19827	0.04099	0.04256	0.02245	0.02055
3	G2[a]	0.04331	0.22789	0.00301	0.03448	0.03228	0.03906
4	G3[a]	0.00445	0.18589	0.00468	0.06048	0.03058	0.02277
5	PHINT[a]	0.01858	0.20483	0.01731	0.09080	0.03202	0.02261
6	RUE[a]	0.06531	0.31828	0.04018	0.04923	0.03501	0.04075
7	P2O[b]	0.00624	0.21469	0.00589	0.03930	0.03061	0.01025
8	P2R[b]	0.01175	0.22895	0.02282	0.05348	0.03621	0.03605
9	P5[b]	0.02570	0.22508	0.00978	0.07449	0.03523	0.02207
10	G2[b]	0.05776	0.23874	0.04783	0.09432	0.10714	0.08644
11	P1D[c]	0.13903	0.29249	0.16550	0.16757	0.11354	0.12679
12	G1[c]	0.14398	0.31210	0.10071	0.14546	0.18961	0.15944
13	G2[c]	0.17098	0.35393	0.17455	0.15411	0.14667	0.15205
14	CSDL[d]	0.14540	0.34475	0.04536	0.06718	0.27358	0.21894
15	PPSEN[d]	0.01546	0.21213	0.00396	0.05118	0.04487	0.03177
16	EM-FL[d]	0.06457	0.24193	0.08136	0.08886	0.12172	0.12729
17	LFMAX[d]	0.05378	0.22009	0.04187	0.14849	0.08603	0.06834
18	K	0.01157	0.25759	0.00813	0.20400	0.05592	0.14741
19	Sy	0.14408	0.27624	0.01246	0.24200	0.03809	0.05090
20	Cond	0.02520	0.57992	0.01173	0.24500	0.98057	0.57723
21	SLPF	0.17447	0.22519	0.03079	0.05200	0.03834	0.04010
22	SLDR	0.38021	0.39229	0.42547	0.77019	0.05021	0.10043
23	SLLL	0.55292	0.55542	0.40689	0.96535	0.05428	0.30001
24	SDUL	0.65232	0.52115	0.62618	0.86728	0.11475	0.38296
25	SRAD	0.09775	0.25840	0.13483	0.71359	0.13514	0.13494
26	TMAX	0.38574	0.43237	0.17710	0.92156	0.30957	0.35008
27	TMIN	0.09876	0.24876	0.18147	0.69244	0.14758	0.12203
28	RAIN	0.29872	0.37421	0.16863	0.77064	0.18430	0.29862
	SUM	3.99778	8.47596	3.06376	7.87399	3.48855	3.85246

[a] Maize genetic parameter; [b] Sorghum genetic parameter; [c] Wheat genetic parameter; [d] Soybean genetic parameter; [e] The value of S_i for 4 parameters were slightly smaller than 0, due to numerical integration, and then the values were set to be 0.

3.3.3 PARAMETERS QUANTITIVELY CONTRIBUTING TO UNCERTAINITY OF MODEL RESPONSE

The contribution of each model parameter to model output (crop yield, hydrologic fluxes) is quantified further using frequency distribution plots and pie charts, shown in Fig. 3-7 (crop yield) and Fig. 3-8 (hydrologic fluxes). The left side of each subplot in Fig. 3-7 and Fig. 3-8 shows the distribution of uncertainty of model responses. Compared with uncertainties of hydrological responses (Fig. 3-8), uncertainties of agronomic response (Fig. 3-7) generally have wider dispersions. For maize yield (Fig. 3-7A), over 55% of the uncertainty is due to climate-related (44.2%) and soil-related (13.5%) parameters. Climate and soil parameters account for 34%, 73%, and 50% of yield uncertainty for soybeans (Fig. 3-7B), wheat (Fig. 3-7C), and sorghum (Fig. 3-7D).

Hydrological responses have less uncertainty in terms of shape and range of distributions, with narrow and peaked distributions. Results are summarized in Fig. 3-8. Note that the scales of

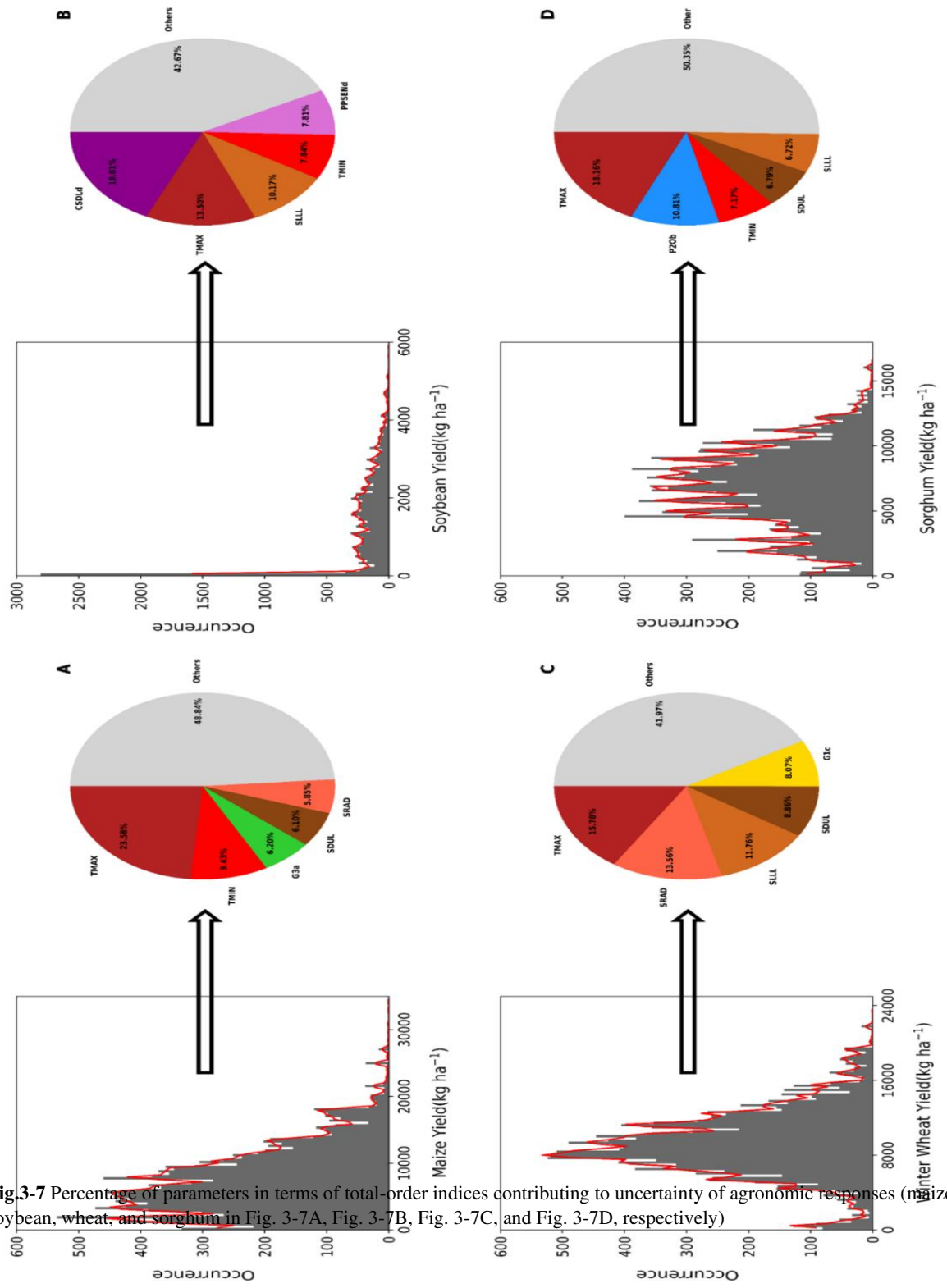

Fig.3-7 Percentage of parameters in terms of total-order indices contributing to uncertainty of agronomic responses (maize yield, soybean, wheat, and sorghum in Fig. 3-7A, Fig. 3-7B, Fig. 3-7C, and Fig. 3-7D, respectively)

hydrologic fluxes on the x axis of each chart in Fig. 3-8 vary in magnitude, to provide more accurate visualization. Recharge (Fig. 3-8C) and pumping (Fig. 3-8D) have much larger

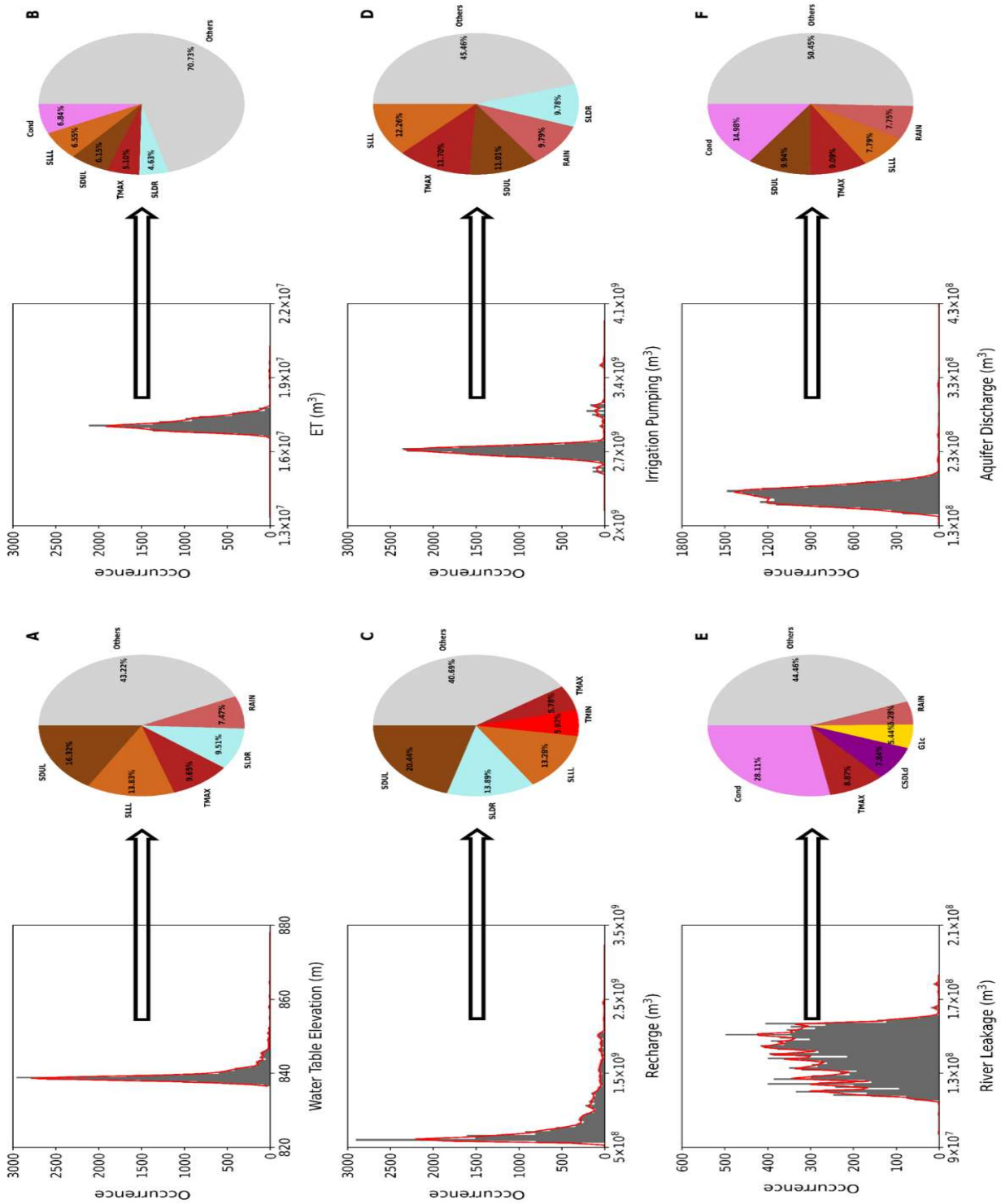

Fig.3-8 Percentage of parameters in terms of total-order indices contributing to uncertainty of hydrological responses (water table elevation, ET, recharge, irrigation pumping, river leakage, and aquifer discharge in Fig.8A, Fig.8B, Fig.8C, Fig.8D, Fig.8E, and Fig.8F, respectively)

magnitudes than ET (Fig. 3-8B), stream seepage (Fig. 3-8E), and groundwater discharge (Fig. 3-8F). Soil-related parameters considerably affect water table elevation (44% of uncertainty) and recharge (53% of uncertainty), with relation to interaction between soil properties and the amount of water that passes from the soil profile to the water table (Fig. 3-8A, C). As shown in Fig. 3-8B, uncertainty of ET is caused by all parameters, with almost even uncertainty in input factors to ET. Over 80% of uncertainty in irrigation pumping can be attributed to soil-related, climate-related, and hydrogeological parameters (Fig. 3-8D) mainly due to the control of these parameters on rainfall and crop growth, which triggers irrigation events and associated pumping. Stream seepage to the aquifer (Fig. 3-8E) and groundwater discharge to streams (Fig. 3-8F) are controlled by riverbed conductance, climate parameters, and, to a lesser degree, crop genetic parameters.

3.3.4 COMPARISON OF MODEL RESPONSES UNDER EXTREME CONDITIONS

To quantitatively identify the influence of sensitive parameters on model responses, the most sensitive parameter for each model response is selected to implement a case study. Fig. 3-9 shows comparisons of model responses under scenarios with minimum and maximum values of the corresponding most sensitive parameters. The most influential parameters for each model response are shown in Figs. 3-6 and 3-7. For example, TMAX is the most influential parameter for maize yield (Fig. 3-6A), CDSLd is the most influential parameter for soybean yield (Fig. 3-6B), and SDUL is the most influential parameter for water table elevation (Fig. 3-7A). ET, with riverbed conductance as the most influential parameter (see Figure 3-6B), is increased only by 3% (Fig. 3-9A), demonstrating that although parameters may have a relatively high sensitivity index for a given system response, the magnitude of response change can be quite minimal. Similar to groundwater ET, river leakage (lkg) and groundwater discharge (spg) are

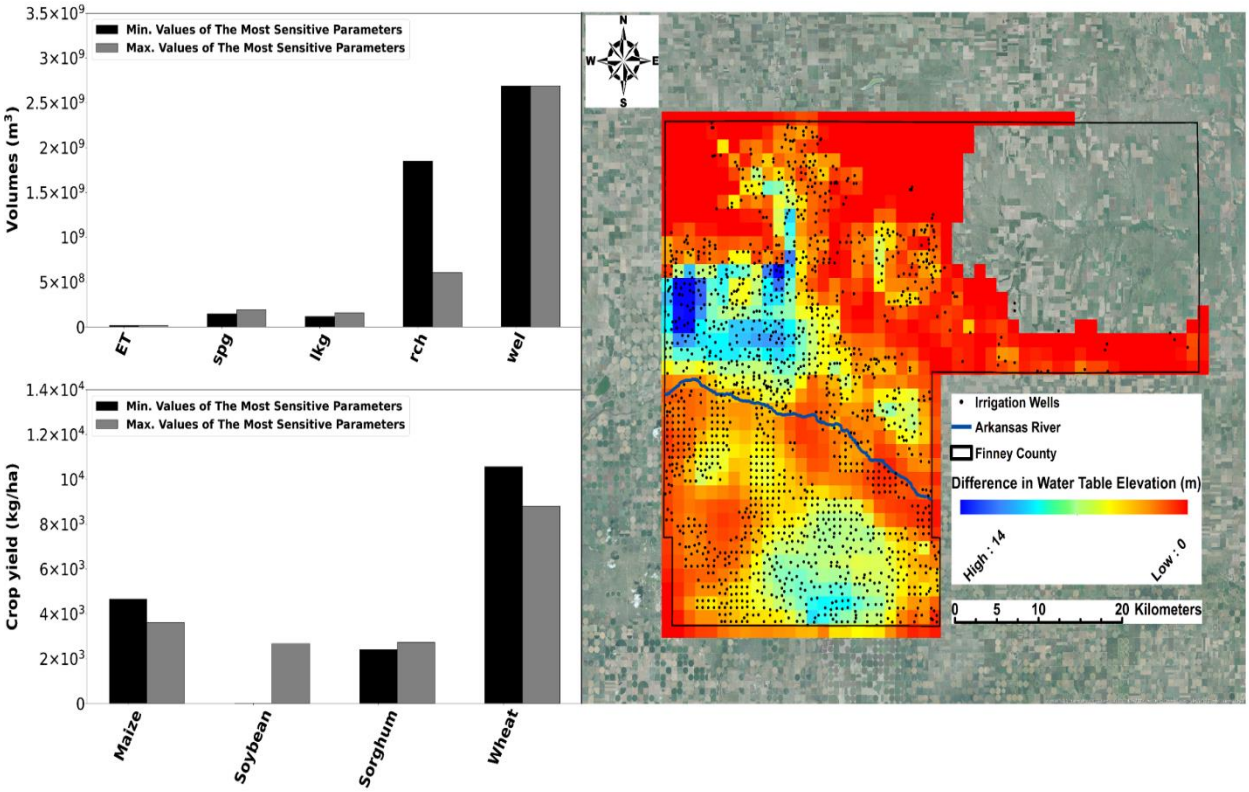

Fig. 3-9 Comparison of responses of the hydro-agronomic system under scenarios with minimum and maximum values of the corresponding most sensitive parameters. Fig.9A shows the influence of the most sensitive parameter on each hydrological model response; Fig.9B shows the influence of the most sensitive parameter on each agronomic model response; Fig.9C shows the spatial influence of the most sensitive parameter on water table elevation.

increased by 38% and 29% when applying the values of their respective influential parameters. However, the overall volume of water attributed to these two fluxes is very small compared to the change in recharge and groundwater pumping. For example, the volume of pumping is 18 times than that of the volume of groundwater discharge. This is due to the small spatial area in which the Arkansas River is in connection with the aquifer, as compared to the area over which recharge and pumping occur. Regardless, the flux values shown in Figure 3-9A are important regarding the overall influence of system parameters on the hydrologic balance in the system. With comparison to original volumes of the baseline simulation (i.e., 16,313,840 m^3 for ET, 159,131,449 m^3 for groundwater discharge, 72,440,221 m^3 for river leakage, 877,641,153 m^3 for recharge, and 2,651,042,093 m^3 for groundwater pumping), the relative percentage change in

hydrologic fluxes are 4% to 7%, -8% to 20%, 60% to 120%, -31% to 111%, and 13% to 15% for ET, groundwater discharge, river leakage, recharge, and groundwater pumping, respectively, under scenarios with minimum and maximum values of the corresponding most sensitive parameters. The large change in groundwater pumping volume is demonstrated by the change in water table elevation, shown in Figure 3-9C for each MODFLOW grid cell in the Finney County area. Some locations have a difference of up to 14 m, which is severe compared to observed decadal changes in the region. The largest changes in water table elevation occur in areas of maize (compared with crop type distribution in Fig. 3-1B).

Similarly, Figure 3-9B shows the change in crop yield when the values of the respective influential parameters are implemented in the simulations. Maximum temperature is the most sensitive parameter for maize, sorghum, and wheat yield, but higher maximum temperature for maize and wheat has negatively impact on crop yields, indicating maximum temperature should be in a reasonable range (Kassie et al., 2016). The soybean yield is mostly driven by a cultivar genetic parameter of CSDL, and the difference between the two scenarios is 2670 kg/ha. For each crop, the yield values shown in Fig. 9B represent a change of 29%, 2,567%, 13%, and 20%, respectively, for maize, soybean, sorghum, and wheat. Compared to crop yields of the baseline simulation (i.e., 12,356 kg/ha for maize, 2,436 kg/ha for soybean, 11,244 kg/ha for sorghum, and 10,561 kg/ha for wheat), the relative percentage change in crop yields is -71% to -62%, -96% to 10%, -79% to -76%, and -32% to -18% for maize, soybean, sorghum, and wheat, respectively, under scenarios with minimum and maximum values of the corresponding most sensitive parameters.

3.4 SUMMARY AND CONCLUSION

Two sensitivity analyses (i.e., Morris screening method and Sobol' variance-based method) were applied to a groundwater-irrigated hydro-agronomic system to assess the governing system factors on crop yield and groundwater storage. The DSSAT-MODFLOW linked modeling system was used as the simulator. A combination of Python scripts and SimLab pre- and post-processing were used to generate parameter values, update model files for DSSAT and MODFLOW, run the model simulations, and calculate sensitivity indices for both the Morris method and the Sobol' method. Fifty-seven parameters were reduced to 24 parameters after the Morris screening method, and the sensitivity of 28 parameters (including 4 climate-related parameters) were analyzed on 10 model responses (i.e., maize yield, soybean yield, winter wheat yield, sorghum yield, water table elevation, ET, recharge, irrigation pumping, river leakage, and aquifer seepage) using Sobol' variance-based sensitivity analysis.

From the results we conclude that climate-related parameters significantly affect crop yields, especially for maize and sorghum, and soybean and winter wheat yields are sensitive to a combination of cultivar genetic parameters, soil-related parameters, and climate-related parameters. Climatic parameters account for 44%, 29%, 40%, and 36% variation in yield of maize, soybean, winter wheat, and sorghum. Hydrogeologic parameters (aquifer hydraulic conductivity, aquifer specific yield, and riverbed conductance) have a relatively low influence on crop yields. Hydrological responses show variations in influential parameters. Water table elevation, recharge, and irrigation pumping are considerably sensitive to soil- and climate-related parameters, while ET, river leakage, and aquifer seepage are highly influenced by hydrogeological parameter (e.g., riverbed conductance, and specific yield) (shown in Fig. 6). Soil

parameters accounted for 44%, 20%, 50%, and 34% variation in water table elevation, ET, recharge, and irrigation pumping.

These results point to the general importance of soil water management and climatic patterns in groundwater-irrigated regions. They can be helpful from the perspective of understanding what might increase crop yield and conserve groundwater, and also what parameters should receive more attention in field sampling and monitoring. Although the study area is in a region with sparse rainfall and hence the need for ongoing pumping, climate plays an important role in crop yield, principally through maximum daily temperature and solar radiation. Therefore, future climate change will have an ever-increasing impact on crop production and associated groundwater conservation, even without accounting for future changing rainfall patterns. Climate cannot be controlled by local water managers and growers; however, they should be made aware of the implications of increasing temperatures on crop yields and hydrologic fluxes in these systems. For hydrologic fluxes, climate and soil parameters have approximately the same influence, pointing to the need for advanced irrigation systems that increase irrigation efficiency. Also, since the influence of maximum temperature on crop growth is exacerbated by water deficits (Hatfield and Prueger, 2015), a minimum level of soil water content should be maintained throughout the growing season. These general results are applicable to other regions within the High Plains Aquifer and similar groundwater-irrigated systems, and the methods presented herein can serve as a guide for identifying controlling factors in other hydro-agronomic systems.

REFERENCES

Adejuwon, J., 2005. Application of the EPIC Crop Model, West Africa. Singapore Journal of Tropical Geography 26, 44–60.

Aeschbach-Hertig, W., Gleeson, T., 2012. Regional strategies for the accelerating global problem of groundwater depletion. Nature Geoscience 5, 853–861. https://doi.org/10.1038/ngeo1617

Aliyari, F., Bailey, R.T., Arabi, M., 2021. Appraising climate change impacts on future water resources and agricultural productivity in agro-urban river basins. Science of the Total Environment 788. https://doi.org/10.1016/j.scitotenv.2021.147717

Allen, D.M., Mackie, D.C., Wei, M., 2004. Groundwater and climate change: A sensitivity analysis for the Grand Forks aquifer, southern British Columbia, Canada. Hydrogeology Journal 12, 270–290. https://doi.org/10.1007/s10040-003-0261-9

Araya, A., Kisekka, I., Gowda, P.H., Prasad, P.V.V., 2017. Evaluation of water-limited cropping systems in a semi-arid climate using DSSAT-CSM. Agricultural Systems 150, 86–98. https://doi.org/10.1016/j.agsy.2016.10.007

Arnold, J.G., Srinivasan, R., Muttiah, R.S., Williams2, J.R., 1998. LARGE AREA HYDROLOGIC MODELING AND ASSESSMENT PART I: MODEL DEVELOPMENT. JOURNAL OF THE AMERICAN WATER RESOURCES ASSOCIATION 34, 73–89.

Badra, N.M., 2007. Sensitivity Analysis of Transportation Problems. Journal of Applied Sciences Research 3, 668–675.

Bahremand, A., Smedt, F., 2008. Distributed hydrological modeling and sensitivity analysis in Torysa Watershed, Slovakia. Water Resources Management 22, 393–408. https://doi.org/10.1007/s11269-007-9168-x

Bailey, R.T., Wible, T.C., Arabi, M., Records, R.M., Ditty, J., 2016. Assessing regional-scale spatio-temporal patterns of groundwater–surface water interactions using a coupled SWAT-MODFLOW model. Hydrological Processes 30, 4420–4433. https://doi.org/10.1002/hyp.10933

Basso, B., Kendall, A.D., Hyndman, D.W., 2013. The future of agriculture over the Ogallala Aquifer: Solutions to grow crops more efficiently with limited water. Earth's Future 1, 39–41. https://doi.org/10.1002/2013ef000107

Batelaan, O., de Smedt, F., Triest, L., 2003. Regional groundwater discharge: Phreatophyte mapping, groundwater modelling and impact analysis of land-use change. Journal of Hydrology 275, 86–108. https://doi.org/10.1016/S0022-1694(03)00018-0

Brooks, R.J., Semenov, M.A., Jamieson, P.D., 2001. Simplifying Sirius: sensitivity analysis and development of a meta-model for wheat yield prediction. European Journal of Agronomy 14, 43–60.

Campolongo, F., Cariboni, J., Saltelli, A., 2007. An effective screening design for sensitivity analysis of large models. Environmental Modelling and Software 22, 1509–1518. https://doi.org/10.1016/j.envsoft.2006.10.004

Candela, L., Elorza, F.J., Jiménez-Martínez, J., von Igel, W., 2012. Global change and agricultural management options for groundwater sustainability. Computers and Electronics in Agriculture 86, 120–130. https://doi.org/10.1016/j.compag.2011.12.012

Carter, R.C., Parker, A., 2009. Climate change, population trends and groundwater in Africa. Hydrological Sciences Journal 54, 676–689. https://doi.org/10.1623/hysj.54.4.676

Castaings, W., Dartus, D., le Dimet, F.-X., Saulnier, G.-M., 2009. Hydrology and Earth System Sciences Sensitivity analysis and parameter estimation for distributed hydrological modeling: potential of variational methods. Hydrol. Earth Syst. Sci 13, 503–517.

Castle, S.L., Thomas, B.F., Reager, J.T., Rodell, M., Swenson, S.C., Famiglietti, J.S., 2014. Groundwater depletion during drought threatens future water security of the Colorado River Basin. Geophysical Research Letters 41, 5904–5911. https://doi.org/10.1002/2014GL061055

Chang, F.J., Huang, C.W., Cheng, S.T., Chang, L.C., 2017. Conservation of groundwater from over-exploitation—Scientific analyses for groundwater resources management. Science of the Total Environment 598, 828–838. https://doi.org/10.1016/j.scitotenv.2017.04.142

Chávez García Silva, R., Grönwall, J., van der Kwast, J., Danert, K., Foppen, J.W., 2020. Estimating domestic self-supply groundwater use in urban continental Africa. Environmental Research Letters 15. https://doi.org/10.1088/1748-9326/ab9af9

Chen, M., Izady, A., Abdalla, O.A., 2017. An efficient surrogate-based simulation-optimization method for calibrating a regional MODFLOW model. Journal of Hydrology 544, 591–603. https://doi.org/10.1016/j.jhydrol.2016.12.011

Confalonieri, R., Bellocchi, G., Tarantola, S., Acutis, M., Donatelli, M., Genovese, G., 2010. Sensitivity analysis of the rice model WARM in Europe: Exploring the effects of different locations, climates and methods of analysis on model sensitivity to crop parameters. Environmental Modelling and Software 25, 479–488. https://doi.org/10.1016/j.envsoft.2009.10.005

Contini, S., Scheer, S., Wilikens, M., 2000. Sensitivity Analysis for System Design Improvement, in: Proceedings of the 2000 International Conference on Dependable Systems and Networks. New York, pp. 243–248.

Cuthbert, M.O., Gleeson, T., Moosdorf, N., Befus, K.M., Schneider, A., Hartmann, J., Lehner, B., 2019. Global patterns and dynamics of climate–groundwater interactions. Nature Climate Change 9, 137–141. https://doi.org/10.1038/s41558-018-0386-4

Davis, M.J., Skodje, R.T., Tomlin, A.S., 2011. Global sensitivity analysis of chemical-kinetic reaction mechanisms: Construction and deconstruction of the probability density function. Journal of Physical Chemistry A 115, 1556–1578. https://doi.org/10.1021/jp108017t

Deng, C., Bailey, R.T., 2020. Assessing causes and identifying solutions for high groundwater levels in a highly managed irrigated region. Agricultural Water Management 240. https://doi.org/10.1016/j.agwat.2020.106329

Deng, C., Bailey, R.T., 2017. Assessing groundwater availability of the Maldives under future climate conditions. Hydrological Processes 31, 3334–3349. https://doi.org/10.1002/hyp.11246

Döll, P., Hoffmann-Dobrev, H., Portmann, F.T., Siebert, S., Eicker, A., Rodell, M., Strassberg, G., Scanlon, B.R., 2012. Impact of water withdrawals from groundwater and surface water on continental water storage variations. Journal of Geodynamics 59–60, 143–156. https://doi.org/10.1016/j.jog.2011.05.001

Dzotsi, K.A., Basso, B., Jones, J.W., 2013. Development, uncertainty and sensitivity analysis of the simple SALUS crop model in DSSAT. Ecological Modelling 260, 62–76. https://doi.org/10.1016/j.ecolmodel.2013.03.017

Famiglietti, J.S., 2014. The global groundwater crisis. Nature Climate Change 4, 945–948. https://doi.org/10.1038/nclimate2425

Farhadi, S., Nikoo, M.R., Rakhshandehroo, G.R., Akhbari, M., Alizadeh, M.R., 2016. An agent-based-nash modeling framework for sustainable groundwater management: A case study. Agricultural Water Management 177, 348–358. https://doi.org/10.1016/j.agwat.2016.08.018

Feng, W., Zhong, M., Lemoine, J.M., Biancale, R., Hsu, H.T., Xia, J., 2013. Evaluation of groundwater depletion in North China using the Gravity Recovery and Climate Experiment (GRACE) data and ground-based measurements. Water Resources Research 49, 2110–2118. https://doi.org/10.1002/wrcr.20192

Foglia, L., Hill, M.C., Mehl, S.W., Burlando, P., 2009. Sensitivity analysis, calibration, and testing of a distributed hydrological model using error-based weighting and one objective function. Water Resources Research 45. https://doi.org/10.1029/2008WR007255

Francos, A., Elorza, F.J., Bouraoui, F., Bidoglio, G., Galbiati, L., 2003. Sensitivity analysis of distributed environmental simulation models: understanding the model behaviour in hydrological studies at the catchment scale. Reliability Engineering & System Safety 79, 205–218.

Frey, H.C., Patil, S.R., 2002. Identification and Review of Sensitivity Analysis Methods. Risk Analysis 22, 553–578.

Gates, J.B., Scanlon, B.R., Mu, X., Zhang, L., 2011. Impacts of soil conservation on groundwater recharge in the semi-arid Loess Plateau, China. Hydrogeology Journal 19, 865–875. https://doi.org/10.1007/s10040-011-0716-3

Gollehon, N., Winston, B., 2013. Groundwater Irrigation and Water Withdrawals: The Ogallala Aquifer Initiative 15. https://doi.org/10.1787/261513543751

Gómez-Hernández, J.J., Gorelick, S.M., 1989. Effective Groundwater Model Parameter Values' Influence of Spatial Variability of Hydraulic Conductivity, Leakance, and Recharge. WATER RESOURCES RESEARCH 25.

Gorelick, S.M., Zheng, C., 2015. Global change and the groundwater management challenge. Water Resources Research 3031–3051. https://doi.org/10.1002/2014WR016825

Gracia-de-Rentería, P., Barberán, R., Mur, J., 2020. The groundwater demand for industrial uses in areas with access to drinking publicly-supplied water: A microdata analysis. Water (Switzerland) 12. https://doi.org/10.3390/w12010198

Guru, M., Horne, J., 2001. The Ogallala Aquifer. Progress in Water Resources 48, 321–328.

Gutentag, E.D., Heimes, F.J., Krothe, N.C., Luckey, R.R., Weeks, J.B., 1984. GEOHYDROLOGY OF THE HIGH PLAINS AQUIFER IN PARTS OF COLORADO, KANSAS, NEBRASKA, NEW MEXICO, OKLAHOMA, SOUTH DAKOTA, k. TEXAS, AND WYOMING.

Haacker, E.M.K., Kendall, A.D., Hyndman, D.W., 2016. Water Level Declines in the High Plains Aquifer: Predevelopment to Resource Senescence. Groundwater 54, 231–242. https://doi.org/10.1111/gwat.12350

Hadded, R., Nouiri, I., Alshihabi, O., Maßmann, J., Huber, M., Laghouane, A., Yahiaoui, H., Tarhouni, J., 2013. A Decision Support System to Manage the Groundwater of the Zeuss Koutine Aquifer Using the WEAP-MODFLOW Framework. Water Resources Management 27, 1981–2000. https://doi.org/10.1007/s11269-013-0266-7

Harbaugh, A.W., 2005. MODFLOW-2005, the US Geological Survey modular ground-water model: the ground-water flow process. US Department of the Interior, US Geological Survey Reston, VA.

Hatfield, J.L., Prueger, J.H., 2015. Temperature extremes: Effect on plant growth and development. Weather and Climate Extremes 10, 4–10. https://doi.org/10.1016/j.wace.2015.08.001

Henderson, R.D., Day-Lewis, F.D., Abarca, E., Harvey, C.F., Karam, H.N., Liu, L., Lane, J.W., 2010. Magerie de la résistivité électrique de sorties d'eaux souterraines en milieu marin: Analyse de sensibilité et mise en œuvre dans la baie de Waquoit, Massachusetts, Etats-Unis d'Amérique. Hydrogeology Journal 18, 173–185. https://doi.org/10.1007/s10040-009-0498-z

Holman, I.P., Allen, D.M., Cuthbert, M.O., Goderniaux, P., 2012. Towards best practice for assessing the impacts of climate change on groundwater. Hydrogeology Journal 20, 1–4. https://doi.org/10.1007/s10040-011-0805-3

Huang, Q., Wang, J., Rozelle, S., Polasky, S., Liu, Y., 2013. The effects of well management and the nature of the aquifer on groundwater resources. American Journal of Agricultural Economics 95, 94–116. https://doi.org/10.1093/ajae/aas076

Huang, T., Pang, Z., Edmunds, W.M., 2013. Soil profile evolution following land-use change: Implications for groundwater quantity and quality. Hydrological Processes 27, 1238–1252. https://doi.org/10.1002/hyp.9302

Javadi, S., Kavehkar, N., Mohammadi, K., Khodadadi, A., Kahawita, R., 2011. Calibrating DRASTIC using field measurements, sensitivity analysis and statistical methods to assess groundwater vulnerability. Water International 36, 719–732. https://doi.org/10.1080/02508060.2011.610921

Jha, M.K., Chowdhury, A., Chowdary, V.M., Peiffer, S., 2007. Groundwater management and development by integrated remote sensing and geographic information systems: Prospects and constraints. Water Resources Management 21, 427–467. https://doi.org/10.1007/s11269-006-9024-4

Jones, J.W., He, J., Boote, K.J., Wilkens, P., Porter, C.H., Hu, Z., 2015. Estimating DSSAT Cropping System Cultivar-Specific Parameters Using Bayesian Techniques. pp. 365–393. https://doi.org/10.2134/advagricsystmodel2.c13

Jones, J.W., Hoogenboom, G., Porter, C.H., Boote, K.J., Batchelor, W.D., Hunt, L.A., Wilkens, P.W., Singh, U., Gijsman, A.J., Ritchie, J.T., 2003. The DSSAT cropping system model.

Kanooni, A., Monem, M.J., 2014. Integrated stepwise approach for optimal water allocation in irrigation canals. Irrigation and Drainage 63, 12–21. https://doi.org/10.1002/ird.1798

Kassie, B.T., Asseng, S., Porter, C.H., Royce, F.S., 2016. Performance of DSSAT-Nwheat across a wide range of current and future growing conditions. European Journal of Agronomy 81, 27–36. https://doi.org/10.1016/j.eja.2016.08.012

Khatun, S., Sahana, M., Jain, S.K., Jain, N., 2018. Simulation of surface runoff using semi distributed hydrological model for a part of Satluj Basin: parameterization and global sensitivity analysis using SWAT CUP. Modeling Earth Systems and Environment 4, 1111–1124. https://doi.org/10.1007/s40808-018-0474-5

Kisekka, I., Migliaccio, K.W., Muñoz-Carpena, R., Khare, Y., Boyer, T.H., 2013. SENSITIVITY ANALYSIS AND PARAMETER ESTIMATION FOR AN APPROXIMATE ANALYTICAL MODEL OF CANAL-AQUIFER INTERACTION APPLIED IN THE C-111 BASIN. Transactions of the ASABE 56, 977–992.

Kløve, B., Ala-Aho, P., Bertrand, G., Gurdak, J.J., Kupfersberger, H., Kværner, J., Muotka, T., Mykrä, H., Preda, E., Rossi, P., Uvo, C.B., Velasco, E., Pulido-Velazquez, M., 2014.

Climate change impacts on groundwater and dependent ecosystems. Journal of Hydrology 518, 250–266. https://doi.org/10.1016/j.jhydrol.2013.06.037

Konikow, L.F., 2015. Long-Term Groundwater Depletion in the United States. Groundwater 53, 2–9. https://doi.org/10.1111/gwat.12306

Konikow, L.F., 2011. Contribution of global groundwater depletion since 1900 to sea-level rise. Geophysical Research Letters 38. https://doi.org/10.1029/2011GL048604

Konikow, L.F., Kendy, E., 2005. Groundwater depletion: A global problem. Hydrogeology Journal 13, 317–320. https://doi.org/10.1007/s10040-004-0411-8

Kour, R., Patel, N., Krishna, A.P., 2016. Climate and hydrological models to assess the impact of climate change on hydrological regime: a review. Arabian Journal of Geosciences 9. https://doi.org/10.1007/s12517-016-2561-0

Kumar, C.P., 2012. Climate Change and Its Impact on Groundwater Resources. RESEARCH INVENTY: International Journal of Engineering and Science 1, 43–60.

Lamboni, M., Makowski, D., Lehuger, S., Gabrielle, B., Monod, H., 2009. Multivariate global sensitivity analysis for dynamic crop models. Field Crops Research 113, 312–320. https://doi.org/10.1016/j.fcr.2009.06.007

Li, Zhenhai, He, J., Xu, X., Jin, X., Huang, W., Clark, B., Yang, G., Li, Zhenhong, 2018. Estimating genetic parameters of DSSAT-CERES model with the GLUE method for winter wheat (Triticum aestivum L.) production. Computers and Electronics in Agriculture 154, 213–221. https://doi.org/10.1016/j.compag.2018.09.009

Liu, G., Wilson, B., Whittemore, D., Jin, W., Butler, J., 2011. Ground-Water Model for Southwest Kansas Groundwater Management District No. 3.

Makowski, D., Naud, C., Jeuffroy, M.H., Barbottin, A., Monod, H., 2006. Global sensitivity analysis for calculating the contribution of genetic parameters to the variance of crop model prediction. Reliability Engineering and System Safety 91, 1142–1147. https://doi.org/10.1016/j.ress.2005.11.015

Marino, S., Hogue, I.B., Ray, C.J., Kirschner, D.E., 2008. A methodology for performing global uncertainty and sensitivity analysis in systems biology. Journal of Theoretical Biology 254, 178–196. https://doi.org/10.1016/j.jtbi.2008.04.011

Masciopinto, C., Liso, I.S., 2016. Assessment of the impact of sea-level rise due to climate change on coastal groundwater discharge. Science of the Total Environment 569–570, 672–680. https://doi.org/10.1016/j.scitotenv.2016.06.183

Mays, L.W., 2013. Groundwater Resources Sustainability: Past, Present, and Future. Water Resources Management 27, 4409–4424. https://doi.org/10.1007/s11269-013-0436-7

McCallum, J.L., Crosbie, R.S., Walker, G.R., Dawes, W.R., 2010. Impacts of climate change on groundwater in Australia: A sensitivity analysis of recharge. Hydrogeology Journal 18, 1625–1638. https://doi.org/10.1007/s10040-010-0624-y

McGuire, V.L., 2014. Water-level changes and change in water in storage in the High Plains aquifer, predevelopment to 2013 and 2011-13, Scientific Investigations Report. Reston, VA. https://doi.org/10.3133/sir20145218

McGuire, V.L., Johnson, M.R., Schieffer, R.L., Stanton, J.S., Sebree, S.K., Verstraeten, I.M., 2003. Water in storage and approaches to ground-water management, High Plains Aquifer, 2000. US Geological Survey Circular 1–51.

Mishra, N., 2014. Impact of Land Use Change on Groundwater-A Review.

Mishra, S., 2009. Uncertainty and sensitivity analysis techniques for hydrologic modeling. Journal of Hydroinformatics 11, 282–296. https://doi.org/10.2166/hydro.2009.048

Morris, M.D., 1991. Factorial Sampling Plans for Preliminary Computational Experiments. Technometrics 33, 161–174.

Mourice, S.K., Rweyemamu, C.L., Tumbo, S.D., Amuri, N., 2014. Maize Cultivar Specific Parameters for Decision Support System for Agrotechnology Transfer (DSSAT) Application in Tanzania. American Journal of Plant Sciences 05, 821–833. https://doi.org/10.4236/ajps.2014.56096

Oiro, S., Comte, J.C., Soulsby, C., MacDonald, A., Mwakamba, C., 2020. Depletion of groundwater resources under rapid urbanisation in Africa: recent and future trends in the Nairobi Aquifer System, Kenya. Hydrogeology Journal 28, 2635–2656. https://doi.org/10.1007/s10040-020-02236-5

Pathak, T.B., Fraisse, C W, Jones, J W, Messina, C D, Hoogenboom, G., Jones, James W, Fellow, A., Messina, Carlos D, Fraisse, Clyde W, Hall, F.R., 2007. USE OF GLOBAL SENSITIVITY ANALYSIS FOR CROPGRO COTTON MODEL DEVELOPMENT. Transactions of the ASABE 50, 2295–2302.

Petts, G.E., 1996. WATER ALLOCATION TO PROTECT RIVER ECOSYSTEMS 12, 353–365.

Pfannerstill, M., Guse, B., Reusser, D., Fohrer, N., 2015. Process verification of a hydrological model using a temporal parameter sensitivity analysis. Hydrology and Earth System Sciences 19, 4365–4376. https://doi.org/10.5194/hess-19-4365-2015

Pianosi, F., Beven, K., Freer, J., Hall, J.W., Rougier, J., Stephenson, D.B., Wagener, T., 2016. Sensitivity analysis of environmental models: A systematic review with practical workflow. Environmental Modelling and Software 79, 214–232. https://doi.org/10.1016/j.envsoft.2016.02.008

Pokhrel, Y.N., Koirala, S., Yeh, P.J.F., Hanasaki, N., Longuevergne, L., Kanae, S., Oki, T., 2015. Incorporation of groundwater pumping in a global Land Surface Model with the

representation of human impacts. Water Resources Research 51, 78–96. https://doi.org/10.1002/2014WR015602

Ratto, M., Tarantola, S., Saltelli, A., 2001. Sensitivity analysis in model calibration: GSA-GLUE approach. Computer Physics Communications 136, 212–224.

Rezzoug, W., Gabrielle, B., Suleiman, A., Benabdeli, K., 2008. Application and evaluation of the DSSAT-wheat in the Tiaret region of Algeria. African Journal of Agricultural Research, Academic Journals 3, 284–296.

Richter, G.M., Acutis, M., Trevisiol, P., Latiri, K., Confalonieri, R., 2010. Sensitivity analysis for a complex crop model applied to Durum wheat in the Mediterranean. European Journal of Agronomy 32, 127–136. https://doi.org/10.1016/j.eja.2009.09.002

Rodríguez-Estrella, T., 2012. The problems of overexploitation of aquifers in semi-arid areas: the Murcia Region and the Segura Basin (South-east Spain) case. Hydrology and Earth System Sciences Discussions 9, 5729–5756. https://doi.org/10.5194/hessd-9-5729-2012

Rosenberg, N.J., Epstein, D.J., Wang, D., Vail, L., Srinivasan, R., Arnold, J.G., Northwest, P., 1999. POSSIBLE IMPACTS OF GLOBAL WARMING ON THE HYDROLOGY OF THE OGALLALA AQUIFER REGION 1 . Introduction The Ogallala or High Plains aquifer underlies about 450 , 000 km 2 of the states of South Dakota , Wyoming , Colorado , Nebraska , Kansas , Oklahoma , Texa. Source 677–692.

Roura-Pascual, N., Krug, R.M., Richardson, D.M., Hui, C., 2010. Spatially-explicit sensitivity analysis for conservation management: Exploring the influence of decisions in invasive alien plant management. Diversity and Distributions 16, 426–438. https://doi.org/10.1111/j.1472-4642.2010.00659.x

Ruget, F., Brisson, N., Delécolle, R., Faivre, R., 2002. Sensitivity analysis of a crop simulation model, STICS, in order to choose the main parameters to be estimated. Agronomie 22, 133–158. https://doi.org/10.1051/agro:2002009

Saltelli, A., Ratto, M., Andres, T., Campolongo, F., Cariboni, J., Gatelli, D., Saisana, M., Tarantola, S., 2008. Global Sensitivity Analysis. The Primer.

Saltelli, A., Tarantola, S., Campolongo, F., Ratto, M., 2004. Sensitivity Analysis in Practice: a Guide to Assessing Scientific Models. John Wiley & Sons.

Scanlon, B.R., Faunt, C.C., Longuevergne, L., Reedy, R.C., Alley, W.M., McGuire, V.L., McMahon, P.B., 2012. Groundwater depletion and sustainability of irrigation in the US High Plains and Central Valley. Proceedings of the National Academy of Sciences of the United States of America 109, 9320–9325. https://doi.org/10.1073/pnas.1200311109

Sekhar, M., Shindekar, M., Tomer, S.K., Goswami, P., 2013. Modeling the vulnerability of an urban groundwater system due to the combined impacts of climate change and management scenarios. Earth Interactions 17. https://doi.org/10.1175/2012EI000499.1

Sheng, Z., 2005. An aquifer storage and recovery system with reclaimed wastewater to preserve native groundwater resources in El Paso, Texas. Journal of Environmental Management 75, 367–377. https://doi.org/10.1016/j.jenvman.2004.10.007

SIMLAB, Version 2.2 Simulation Environment for Uncertainty and Sensitivity Analysis, 2004.

Sin, G., Gernaey, K. v., Lantz, A.E., 2009. Good Modeling Practice for PAT Applications: Propagation of Input Uncertainty and Sensitivity Analysis. American Institute of Chemical Engineers Biotechnol. Prog 25, 1043–1053. https://doi.org/10.1021/bp.166

Song, X., Zhang, J., Zhan, C., Xuan, Y., Ye, M., Xu, C., 2015. Global sensitivity analysis in hydrological modeling: Review of concepts, methods, theoretical framework, and applications. Journal of Hydrology 523, 739–757. https://doi.org/10.1016/j.jhydrol.2015.02.013

Steward, D.R., Allen, A.J., 2016. Peak groundwater depletion in the High Plains Aquifer, projections from 1930 to 2110. Agricultural Water Management 170, 36–48. https://doi.org/10.1016/j.agwat.2015.10.003

Sun, N.-Z., Yeh, W.W.-G., 1990. Coupled Inverse Problems in Groundwater Modeling 1. Sensitivity Analysis and Parameter Identification. WATER RESOURCES RESEARCH 26, 2507–2525.

Sykes, J.F., Wilson, J.L., Andrews, R.W., 1985. Sensitivity Analysis for Steady State Groundwater Flow Using Adjoint Operators. WATER RESOURCES RESEARCH 21, 359–371.

Thorp, K.R., DeJonge, K.C., Marek, G.W., Evett, S.R., 2020. Comparison of evapotranspiration methods in the DSSAT Cropping System Model: I. Global sensitivity analysis. Computers and Electronics in Agriculture 177. https://doi.org/10.1016/j.compag.2020.105658

Tjiputra, J.F., Polzin, D., Winguth, A.M.E., 2007. Assimilation of seasonal chlorophyll and nutrient data into an adjoint three-dimensional ocean carbon cycle model: Sensitivity analysis and ecosystem parameter optimization. Global Biogeochemical Cycles 21. https://doi.org/10.1029/2006GB002745

Trucano, T.G., Swiler, L.P., Igusa, T., Oberkampf, W.L., Pilch, M., 2006. Calibration, validation, and sensitivity analysis: What's what. Reliability Engineering and System Safety 91, 1331–1357. https://doi.org/10.1016/j.ress.2005.11.031

USGS High Plains Aquifer WLMS: Physical/Cultural Setting [WWW Document], n.d. URL https://ne.water.usgs.gov/ogw/hpwlms/physsett.html (accessed 8.28.19).

Varella, H., Guérif, M., Buis, S., 2010. Global sensitivity analysis measures the quality of parameter estimation: The case of soil parameters and a crop model. Environmental Modelling and Software 25, 310–319. https://doi.org/10.1016/j.envsoft.2009.09.012

Vezzaro, L., Mikkelsen, P.S., 2012. Application of global sensitivity analysis and uncertainty quantification indynamic modelling of micropollutants in stormwater runoff. Environmental Modelling and Software 27–28, 40–51. https://doi.org/10.1016/j.envsoft.2011.09.012

Voss, K.A., Famiglietti, J.S., Lo, M., de Linage, C., Rodell, M., Swenson, S.C., 2013. Groundwater depletion in the Middle East from GRACE with implications for transboundary water management in the Tigris-Euphrates-Western Iran region. Water Resources Research 49, 904–914. https://doi.org/10.1002/wrcr.20078

Wada, Y., 2016. Modeling Groundwater Depletion at Regional and Global Scales: Present State and Future Prospects. Surveys in Geophysics. https://doi.org/10.1007/s10712-015-9347-x

Wada, Y., van Beek, L.P.H., Bierkens, M.F.P., 2012. Nonsustainable groundwater sustaining irrigation: A global assessment. Water Resources Research 48. https://doi.org/10.1029/2011WR010562

Wada, Y., van Beek, L.P.H., van Kempen, C.M., Reckman, J.W.T.M., Vasak, S., Bierkens, M.F.P., 2010. Global depletion of groundwater resources. Geophysical Research Letters 37. https://doi.org/10.1029/2010GL044571

Wang, J., Li, X., Lu, L., Fang, F., 2013. Parameter sensitivity analysis of crop growth models based on the extended Fourier Amplitude Sensitivity Test method. Environmental Modelling and Software 48, 171–182. https://doi.org/10.1016/j.envsoft.2013.06.007

Wang, X., He, X., Williams, J.R., Izaurralde, R.C., Atwood, J.D., 2005. SENSITIVITY AND UNCERTAINTY ANALYSES OF CROP YIELDS AND SOIL ORGANIC CARBON SIMULATED WITH EPIC. Transactions of the ASAE 48, 1041–1054.

Wei, X., Bailey, R.T., 2019. Assessment of system responses in intensively irrigated stream-aquifer systems using SWAT-MODFLOW. Water (Switzerland) 11. https://doi.org/10.3390/w11081576

Xiang, Z., Bailey, R.T., Nozari, S., Husain, Z., Kisekka, I., Sharda, V., Gowda, P., 2020. DSSAT-MODFLOW: A new modeling framework for exploring groundwater conservation strategies in irrigated areas. Agricultural Water Management 232. https://doi.org/10.1016/j.agwat.2020.106033

Xiao, X., Xu, X., Huang, G., 2021. Improved analytical expressions for transient specific yield in shallow groundwater drainage. Journal of Hydrology 597. https://doi.org/10.1016/j.jhydrol.2021.126186

Xu, X., Huang, G., Zhan, H., Qu, Z., Huang, Q., 2012. Integration of SWAP and MODFLOW-2000 for modeling groundwater dynamics in shallow water table areas. Journal of Hydrology 412–413, 170–181. https://doi.org/10.1016/j.jhydrol.2011.07.002

Yassin, F., Razavi, S., Wheater, H., Sapriza-Azuri, G., Davison, B., Pietroniro, A., 2017. Enhanced identification of a hydrologic model using streamflow and satellite water storage

data: A multicriteria sensitivity analysis and optimization approach. Hydrological Processes 31, 3320–3333. https://doi.org/10.1002/hyp.11267

Zhang, X., Lardizabal, A., Silverman, A.I., Vione, D., Kohn, T., Nguyen, T.H., Guest, J.S., 2020. Global Sensitivity Analysis of Environmental, Water Quality, Photoreactivity, and Engineering Design Parameters in Sunlight Inactivation of Viruses. Environmental Science and Technology 54, 8401–8410. https://doi.org/10.1021/acs.est.0c01214

Zhou, X., Lin, H., 2017. Global Sensitivity Analysis, in: Shekhar Shashi and Xiong, H. and Z.X. (Ed.), Encyclopedia of GIS. Springer International Publishing, Cham, p. 787. https://doi.org/10.1007/978-3-319-17885-1_538

CHAPTER 4 – QUANTIFYING THE IMPACT OF CLIMATE AND MANAGEMENT STRATEGIES ON GROUNDWATER CONSERVATION IN THE HIGH PLAINS AQUIFER[3]

4.1 INTRODUCTION

Groundwater is significant for domestic use, agricultural irrigation, industrial processes, etc. Groundwater provides 50% of all drinking water (Lall et al., 2020) for 35% of the world's population (Grönwall & Danert, 2020). Of the groundwater used globally, 43% (Siebert et al., 2010) is for crop irrigation and 33% is for industrial applications (Lall et al., 2020). In semi-arid and arid regions, agricultural irrigation is highly dependent on groundwater (Foster et al., 2014), which often leads to groundwater depletion in aquifer systems and associated impacts such as land subsidence, wetland degradation, lowering of well pumping capacity, increase in pumping costs, and reduction or cessation of groundwater discharge (i.e. baseflow) to streams (Konikow and Kendy, 2005; Motagh et al., 2008; Werner 2010; Varela-Ortega et al., 2011; Aeschbach-Hertig and Gleeson, 2012; Zhang et al., 2014). In the past century, global groundwater storage lost approximately 3,400 km^3 (Konikow, 2011), with depletion rates of 126 $km^3\ yr^{-1}$ in 1960 to 283 $km^3\ yr^{-1}$ in 2000 (Wada et al., 2010), while more than 1,100 km^3 was depleted merely in the first 8 years of the 21st century (Konikow, 2011), with an average deplete rate of 138 $km^3\ yr^{-1}$. Regionally, groundwater depletions are 1000 km^3 in the United States during the years of 1900 to 2008 (Konikow, 2015), with depletion rates of 12.5 $km^3\ yr^{-1}$ (27.6 mm yr^{-1}) and 3.1 $km^3\ yr^{-1}$ (20.4 mm yr^{-1}) for the High Plains and California's Central Valley (Famiglietti, 2014); 170.3 km^3 in North China Plain throughout 1900 to 2008 (Feng et al., 2013), with an 8.3 $km^3\ yr^{-1}$ (22 mm yr^{-1}) depletion rate (Famiglietti, 2014); and 91.3 km^3 in north-central Middle East from 2003 to

[3] This paper is ready to submit to *Water Resources Research*

2009 (Voss et al., 2013), with a rate of 13 km^3 yr^{-1} (17.3 mm yr^{-1}) (Famiglietti, 2014). These depletions are caused principally by over-extraction for crop irrigation. Future changes in rainfall patterns and temperature may also exacerbate the issue of depletion in certain regions. Without management of groundwater resources, many aquifer systems may experience a complete depletion of groundwater in the coming decades (Haacker et al., 2016).

To assist with groundwater management in irrigated regions, many modeling frameworks have been proposed and used to explore the impact of future climate conditions (McCallum et al., 2010; Holman et al., 2012; Masciopinto & Liso, 2016; Deng & Bailey, 2017; Cuthbert et al., 2019) and the impact of potential management strategies (Manghi et al., 2012; Singh, 2013; Foster et al., 2014; Klaas et al., 2020). These frameworks use single application or combinations of hydrologic, hydrogeologic, agronomic, and economic modeling tools. Some studies use only hydrologic models such as MODFLOW (Harbaugh, 2005) or the Soil and Water Assessment Tool (SWAT) (Arnold et al., 1998) to explore future groundwater resources under management scenarios (Jha et al., 2007; Carter & Parker, 2009; Candela et al., 2012; Kumar, 2012; Huang et al., 2013; Sekhar et al., 2013; Klove et al., 2014; Mishra et al., 2014; Gorelick and Zheng, 2015; Farhadi et al., 2016; Ni and Parajuli, 2018), whereas others use only agronomic models such as EPIC (Williams et al., 1989) or DSSAT (Jones et al., 2003) to explore future crop yield under management scenarios (Parry et al., 2004; Ewert et al., 2005; Wei et al., 2009; Audsley et al., 2006; Deryng et al., 2011; Ventrella et al., 2012; Kadiyala et al., 2015; Kihara et al., 2015; Christian et al., 2016; Grundy et al., 2016).

Several studies have used combinations of models such as MPM-WEAP (Varela-Ortega et al., 2011), MODFLOW-SWAP (Xu et al., 2012), MODFLOW-WEAP (Hadded et al., 2013), SWAT-MODFLOW (Bailey et al., 2016), AquaCrop-Economic model with SPIDERR (Foster et

al., 2017), or APSIM-Potato model with a simplistic lumped estimation of groundwater depletion (Tang et al., 2019). For example, Aliyari et al. (2021) used SWAT-MODFLOW to quantify the impact of climate change on groundwater storage and crop yield during the 21st century but did not include effects of management strategies. In general, studies have not yet assessed crop yield and groundwater storage conjunctively under scenarios of climate change and management practices in a physical based, spatially distributed manner. There is a need for a physically based modeling approach that can assist with identifying optimal conservation strategies (i.e., minimize groundwater depletion and maximize crop yield) for future climate patterns in groundwater-depleted regions.

The objective of this chapter is to quantify the impact of climate change and potential management strategies on hydro-agronomic state variables (groundwater storage, crop yield) in a semi-arid region that has experienced significant groundwater depletion in recent decades. The area of interest is southwest Kansas, a region of the High Plains Aquifer, USA, with the linked DSSAT-MODFLOW (Xiang et al., 2020) model applied to Finney County, Kansas (3,370 km^2) to simulate the interactions between the agronomic (soil-plan system) and groundwater systems. Interactions include recharge from the soil profile to the water table, and groundwater pumping from the aquifer to the land surface as irrigation. Irrigation is limited based on available groundwater storage in localized sections of the aquifer. Once the best set of model parameters is identified, the DSSAT-MODFLOW model is run for the years 2021-2050 under scenarios of climate patterns, irrigation systems, and planting levels. The result of the modeling scenarios is the identification of management strategies that provide the lowest groundwater depletion and the highest crop yield under varying future climate trends (wet, dry). As the conditions of

southwest Kansas are similar to other regions worldwide in patterns of crop production and groundwater irrigation, results from this study can be applied elsewhere.

4.2 MATERIALS AND METHODS

This section discusses the DSSAT-MODFLOW linked model and its application to the study region in Finney County, in southwest Kansas, USA to quantify the impact of future downscaled climate scenarios and management strategies on groundwater storage and crop yield during the 2021-2050 period. Characteristics of the study region will be presented first, followed by a method to identify the best set of model parameters for a historical period, and then the use of the calibrated model for the future climate and management scenarios.

4.2.1 STUDY REGION: FINNEY COUNTY, KANSAS, HIGH PLAINS AQUIFER

The study region is Finney County (38.0625° N latitude and 100.8903° W longitude), with a total area of 3,370 km^2 (1,302 mi^2), in southwest Kansas, within the High Plains Aquifer (HPA), also referred to as the Ogallala Aquifer. The HPA (Fig. 4-1) is one of the largest freshwater aquifers in the world and resides in portions of eight states: South Dakota, Wyoming, Nebraska, Colorado, Kansas, Oklahoma, New Mexico, and Texas, with a total area of 450,000 km^2 (174,000 mi^2). Approximately 88% of pumped groundwater from the HPA is used for irrigated croplands (41% of total land area) (Gollehon and Winston, 2013; Scanlon et al., 2012), accounting for 20% of irrigated croplands in the U.S. and 30% of total crop and animal production in the U.S. (Guru and Horne, 2001; Rosenberg et al., 1999), with an annual output value of over $35 billion (Basso et al., 2013). The agricultural area in the HPA contains 53% row crops, 33% small grains, and 14% pasture, etc. In addition, it provides 18% production of cattle and swine (USGS High Plain Aquifer WLMS: Physical/Cultural Setting, 2019). The composition of aquifer material and the bedrock unit are poorly sorted clay, silt, sand, gravel and siltstone,

shale, loosely to moderately cemented clay and silt, chalk, limestone, dolomite, conglomerate, claystone, gypsum, anhydrite, bedded salt, respectively.

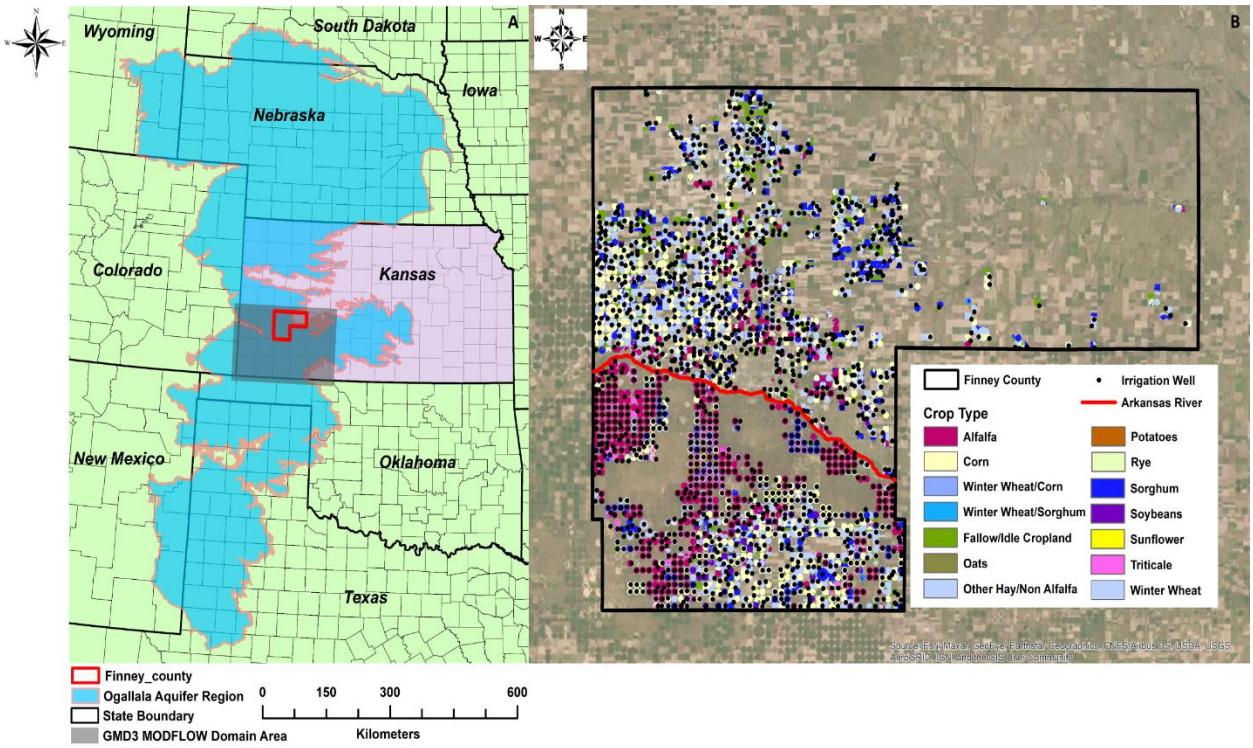

Fig. 4-1 Map of study region and related information. Fig. 4-1A shows map of study region of Finney County, southwest of Kansas, in the Ogallala Aquifer. The Finney County area is encompassed within the red contour line. The blue region enclosed with light brown line is the Ogallala Aquifer, and the states are divided with black lines; Fig.1B shows map of irrigation well and crop types (Finney County mainly contains five crops, including corn, winter wheat, soybeans, sorghum, and triticale).

Excessive pumping in the HPA since the 1950s has led to extensive groundwater depletion. For example, the rate of groundwater depletion increased by about 10 km^3 yr^{-1} on average throughout 2003 to 2013 compared with that during the 20th century (Famiglietti, 2014), and the quantity of groundwater storage decreased by approximately 400 km^3 during 1900 – 2008, which accounts for 40% of overall depletion in the U.S. However, the change of water table elevation varies spatially, with some areas (central Nebraska) experiencing an increase in groundwater storage due to higher precipitation rates and less dependence on groundwater for irrigation. In other areas, such as eastern Colorado, southwest Kansas, the panhandle of Oklahoma, and the panhandle of Texas, declines have been up to 78 m.

Finney County, in the southwest Kansas, is selected in this study to identify optimal management strategies under the effect of climate change, due to a high dependence on groundwater irrigation (over 95% pumped groundwater for crop irrigation) and an excessive drawdown of water table elevation (i.e., approximately 15 m (50 ft) decline in water head since 1950). There are approximately 1,630 irrigation wells in the county, providing water for a total cropland of 105,218 ha (260,000 ac). The main crops grown in Finney County include corn (corn), winter wheat, soybeans, and sorghum.

4.2.2 DSSAT-MODFLOW: DETAILS AND APPLICATION TO FINNEY COUNTY, KANSAS

This study uses the coupled DSSAT-MODFLOW model of Xiang et al. (2020). This model simulates jointly agronomic processes and state variables (crop yield, soil hydrologic and nutrient dynamics) and hydrogeologic processes and state variables (groundwater storage, groundwater head, groundwater pumping, groundwater-surface water interactions), with deep percolation (i.e. recharge) and applied irrigation (i.e. groundwater pumping volumes) passed from DSSAT to MODFLOW, and resulting simulated groundwater storage from MODFLOW providing a constraint on allowed irrigation application during the following growing season for DSSAT. A separate DSSAT model is prepared for each cultivated field.

DSSAT (Jones et al., 2003), Decision Support System for Agrotechnology Transfer, is an assembly of programming codes to simulate crop growth, development, and production in terms of dynamics among cycles of soil-plant-atmosphere for over 40 possible crop types in a one-dimensional soil profile setting. It is often applied for policy decision-making, management strategies and yield prediction under different scales (i.e., on-farm or regional assessment). DSSAT needs input information to make simulations, including weather data, soil profile, crop

management, cultivar genetic parameters, etc., and it contains multiple modules of simulations (i.e., seasonal, spatial, sequential simulations) specified by users.

MODFLOW (Harbaugh, 2005) is a 3D physically based groundwater flow model that simulates groundwater head, groundwater budget (e.g., groundwater storage, groundwater recharge and discharge, etc.), and groundwater flow rates using the finite difference method. MODFLOW requires aquifer properties (hydraulic conductivity, specific yield, and specific storage) be specified for each finite difference cell in the model domain. The simulation period is divided into stress period (i.e., a groundwater stress remains constant), and then into time steps.

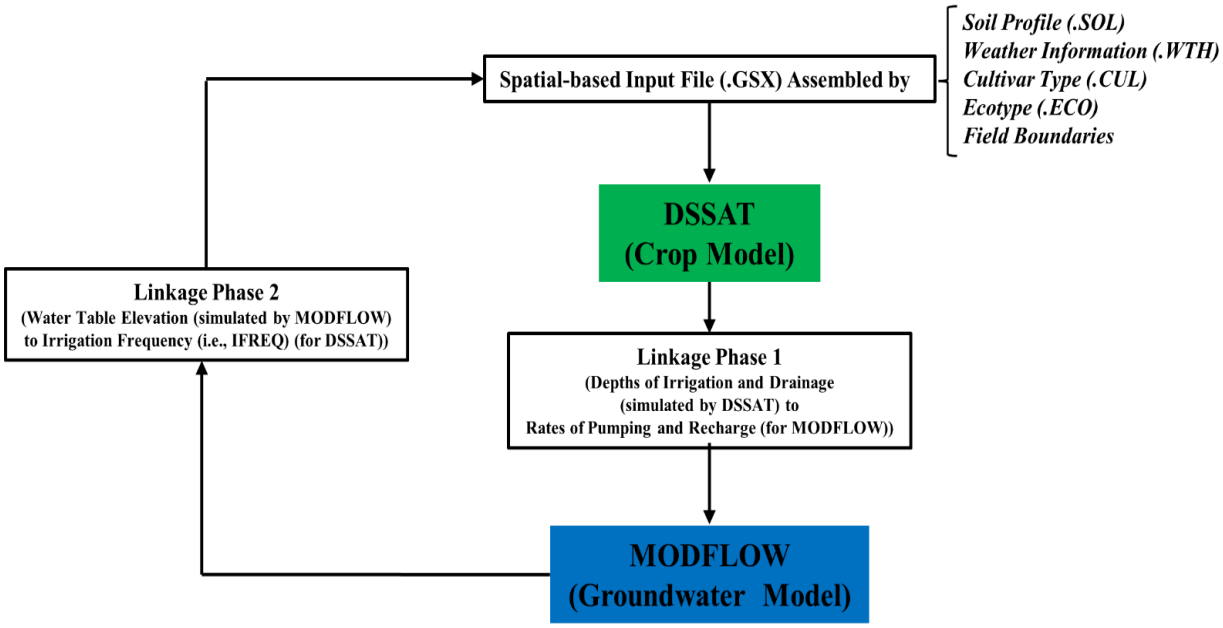

Fig. 4-2 The DSSAT-MODFLOW framework showing the linkage between DSSAT and MODFLOW simulation.

The linkage framework of DSSAT-MODFLOW is described in Fig. 4-2. The major task for the linked DSSAT-MODFLOW is to make a connection between the agronomic and hydrological systems through exchanging information (i.e., depths of irrigation and drainage for the agronomic system and water table elevation, saturated thickness, and well capacity for the hydrogeologic system). The overall linkage procedure, which occurs on an annual basis, is summarized by the following steps:

1. *Run ensemble of DSSAT simulations*. Since DSSAT is a 1D model, a separate DSSAT model must be set up and run for each cultivated field in the model domain. The ensemble is prepared using the spatial module mode through a batch file with all input information assembling into the .GSX input file. The ensemble of simulations is run for an entire growing season.

2. *Convert DSSAT outputs to MODFLOW inputs*. Daily depths of applied irrigation are converted to groundwater pumping volumes to be used in MODFLOW's Well package, and daily soil drainage depths are converted to recharge volumes to be used in MODFLOW's Recharge package. Python scripts are used to read DSSAT outputs and prepare MODFLOW input files.

3. *Run MODFLOW*. MODFLOW is run for the growing season, simulated daily groundwater head and groundwater storage for each finite difference cell. The groundwater head at the final day of the simulation period will be used as initial conditions for the following year.

4. *Prepare DSSAT inputs using MODFLOW outputs*. The final step in the linkage process prepares input variables for the ensemble of DSSAT simulations, to be run the following growing season. The DSSAT input variable IFREQ, which controls the irrigation frequency during the growing season, is constrained by the available groundwater storage in corresponding MODFLOW grid cells.

DSSAT and MODFLOW models for Finney County were constructed and calibrated separately by Araya et al. (2017) and Liu et al. (2011), respectively. The domain of DSSAT simulations contains corn, winter wheat, sorghum, soybean, and triticale (regarded same as winter wheat in our study), with a total of 1,332 cultivated fields: 564 for corn, 484 for winter

wheat, 28 for soybean, 206 for sorghum, and 50 for triticale. For each field, DSSAT simulates crop yield and water budgets (i.e., irrigation and drainage depths). The MODFLOW model has a simulation period of 1944 to 2007. The domain area of the MODFLOW model is 161 km by 241 km (100 miles by 150 miles, shown in grey area in Fig.1A), with each grid cell 1.61 km by 1.61 km (1 mile by 1 mile). The stress period of the MODFLOW model is changed to daily stress period to be consistent with daily outputs of DSSAT simulation (Xiang et al., 2020).

4.2.3 PARAMETER ESTIMATION FOR DSSAT-MODFLOW

Xiang et al. (2020) introduced the DSSAT-MODFLOW modeling framework. However, they used model parameters from the separate modeling studies in southwest Kansas of DSSAT (Araya et al., 2017) and MODFLOW (Liu et al., 2011) which, while providing good results for groundwater head in comparison to observed head at monitoring wells, provided poor results for yield of sorghum, winter wheat, and soybean. Therefore, before applying the model to investigate effects of future climate and management strategies on system variables, we estimate the values of major parameters of the coupled DSSAT-MODFLOW model. The years 2000-2003 are used as the calibration period, and the 2004-2007 years are used as the testing period.

The parameter estimation process is based on a sensitivity analysis of model parameters using the Sobol' method. This method was used by Xiang et al. (2022) in their study of hydro-agronomic controls on groundwater storage and crop yield in Finney County, and results from these simulations are used here. From the ensemble of simulations, the parameter values that provide the best fit between the simulated and observed state variables are selected. Model results are tested against annual-based measurements of crop yield (i.e., corn, soybean, sorghum, and winter wheat), derived from the NASS official website (https://quickstats.nass.usda.gov/), and groundwater head measurements from USGS monitoring wells. A description of the 28

parameters included in model parameter estimation are listed in Tab. 4-1. The method uses 14,848 simulations of DSSAT-MODFLOW for the 2000-2003 calibration period (Xiang. et al., 2022). From the results of these simulations, the top 1% of simulations with the highest Kling-Gupta Efficiency (KGE for hydrologic response) and Index of Agreement (*d* for agronomic response) based on fits between simulated and observed state variables (groundwater head, crop yield) are selected from which posterior distributions of model results are generated (Fig. 4-3). Due to a group of 28 parameters that can individually have effect on each of the 5 state variables (groundwater head, corn yield, soybean yield, winter wheat yield, sorghum yield), the best set of parameters for all state variables (the values in the 9th column summarized in Tab. 1) is estimated in terms of the best set of parameters for each of state variables (the mean value of each parameter's cumulative distribution function (CDF)) through weights of percentage of total Sobol' indices for each state variable.

Tab. 4-1. Best sets of estimation of parameters for individual model responses and the overall model responses with definitions and units of parameters.

Parameters	Description	Unit	Estimated parameters for water table elevation[1]	Estimated parameters for maize yield[2]	Estimated parameters for sorghum yield[2]	Estimated parameters for soybean yield[2]	Estimated parameters for winter wheat yield[2]	Estimated parameters for all model responses
P1[a]	Thermal time from seedling emergence to the end of the juvenile phase (expressed in degree days above a base temperature of 8 deg. C) during which the plant is not responsive to changes in photoperiod	degree-day	264.3 ± 52.3	286.6 ± 55.2	279.0 ± 31.4	292.2 ± 31.0	204.6 ± 43.3	274.5 ± 53.6
P5[a]	Thermal time from silking to physiological maturity (expressed in degree days above a base temperature of 8 deg.C).	degree-day	888.3 ± 68.1	785.2 ± 72.3	793.8 ± 46.3	818.3 ± 46.3	784.7 ± 41.6	822.5 ± 61.2

G2[a]	Maximum possible number of kernels per plant.	Kernel	679.5 ± 116.0	721.1 ± 90.9	792.2 ± 89.8	704.7 ± 75.1	707.3 ± 63.5	734.8 ± 96.1
G3[a]	Kernel filling rate during the linear grain filling stage and under optimum conditions.	mg-day^{-1}	10.36 ± 1.87	10.28 ± 1.58	11.23 ± 1.49	10.97 ± 0.85	10.17 ± 1.20	10.33 ± 1.57
PHINT[a]	Phylochron interval; the interval in thermal time (degree days) between successive leaf tip appearances.	degree-day	64.12 ± 10.25	48.44 ± 5.89	42.51 ± 7.52	48.55 ± 3.58	47.00 ± 5.46	50.74 ± 6.59
RUE[a]	Radiation use efficiency	g-MJ^{-1}	3.0± 0.5	4.0 ± 0.5	3.2 ± 0.3	3.3 ± 0.2	3.3 ± 0.2	3.7 ± 0.5
P2O[b]	Critical photoperiod or the longest day length (in hours) at which development occurs at a maximum rate. At values higher than P2O, the rate of development is reduced	hour	14.98 ± 0.80	14.15 ± 0.54	13.03 ± 0.65	13.23 ± 0.54	13.42 ± 0.43	13.07 ± 0.65
P2R[b]	Extent to which phasic development leading to panicle initiation (expressed in degree days) is delayed for each hour increase in photoperiod above P2O	degree-day	220.3 ± 49.1	155.5 ± 47.3	175.5 ± 43.8	100.2± 44.2	141.2 ± 22.9	176.2 ± 44.0
P5[b]	Thermal time from beginning of grain filling to physiological maturity (degree days above TBASE)	degree-day	614.5 ± 48.8	596.7 ± 53.3	552.5 ± 33.3	549.4 ± 29.9	531.5 ± 25.5	567.9 ± 37.0
G2[b]	Scaler for partitioning of assimilates to the panicle (head).	-	7.9 ± 1.0	5.9 ± 0.9	7.4 ± 0.7	8.0 ± 0.7	7.0 ± 0.6	7.2 ± 0.8
P1D[c]	Photoperiod response (% reduction in	%	98 ± 33	123 ± 28	129 ± 15	106 ± 11	134 ± 31	120 ± 24

	rate/10 h drop in pp)							
G1[c]	Kernel number per unit canopy weight at anthesis (#/g)	NO./gram	32 ± 7	21 ± 6	31 ± 6	47 ± 6	38 ± 4	34 ± 5
G2[c]	Standard kernel size under optimum conditions (mg)	mg	59 ± 12	50 ± 9	60 ± 10	54 ± 7	56 ± 7	56 ± 9
CSDL[d]	Critical Short Day Length below which reproductive development progresses with no daylength effect (for short-day plants) (hour)	hour	13.44 ± 0.89	12.40 ± 0.49	13.25 ± 0.59	13.13 ± 0.54	13.53 ± 0.37	13.13 ± 0.56
PPSEN[d]	Slope of the relative response of development to photoperiod with time (positive for shortday plants)	$hour^{-1}$	0.255 ± 0.049	0.220 ± 0.046	0.174 ± 0.038	0.239 ± 0.034	0.201 ± 0.029	0.240 ± 0.035
EM-FL[d]	Time between plant emergence and flower appearance (R1) (photothermal days)	days	13.8 ± 3.7	21.6 ± 3.5	21.04 ± 3.55	23.22 ± 2.87	18.44 ± 1.38	20.90 ± 2.94
LFMAX[d]	Maximum leaf photosynthesis rate at 30 C, 350 vpm CO_2, and high light (mg CO_2/m^2-s)	mg-CO^2/m^2-s	1.117 ± 0.060	1.127 ± 0.029	1.163 ± 0.067	1.127 ± 0.049	1.078 ± 0.031	1.118 ± 0.046
K	Hydraulic Conductivity	$-^3$	1.011 ± 0.047	0.988 ± 0.021	0.992 ± 0.023	0.981 ± 0.021	1.003 ± 0.025	0.998 ± 0.033
Sy	Specific Yield	$-^3$	0.869 ± 0.106	0.974 ± 0.049	1.033 ± 0.078	1.004 ± 0.056	0.979 ± 0.047	0.889 ± 0.097
Cond	Riverbed/streambed hydraulic conductance	$-^3$	0.999 ± 0.118	0.948 ± 0.063	1.025 ± 0.079	0.988 ± 0.070	1.000 ± 0.045	0.999 ± 0.108
SLPF	Soil fertility factor/Photosynthesis factor	-	0.9 ± 0.1	0.9 ± 0.0	0.8 ± 0.1	0.8 ± 0.0	0.9 ± 0.0	0.9 ± 0.0
SLDR	Drainage rate	day^{-1}	0.7 ± 0.2	0.5 ± 0.1	0.5 ± 0.1	0.5 ± 0.1	0.6 ± 0.1	0.6 ± 0.2
SLLL	Drained lower limit	cm^3 cm^{-3}	0.153 ± 0.041	0.162 ± 0.011	0.111 ± 0.023	0.140 ± 0.030	0.147 ± 0.024	0.143 ± 0.029
SDUL	Drained upper limit	cm^3 cm^{-3}	0.358 ± 0.028	0.341 ± 0.029	0.338 ± 0.023	0.345 ± 0.029	0.340 ± 0.016	0.347 ± 0.025
SRAD	Solar radiation	$-^3$	1.077 ± 0.135	1.037 ± 0.062	1.040 ± 0.079	0.978 ± 0.053	1.035 ± 0.054	1.033 ± 0.067
TMAX	Temperature Maximum	$-^3$	1.110 ± 0.112	0.951 ± 0.103	1.003 ± 0.085	1.004 ± 0.053	0.999 ± 0.059	1.000 ± 0.083

TMIN	Temperature Minimum	-[3]	0.884 ± 0.086	1.030 ± 0.133	0.984 ± 0.065	1.037 ± 0.075	0.965 ± 0.044	0.999 ± 0.085
RAIN	Rainfall (including snow)	-[3]	1.019 ± 0.079	1.082 ± 0.065	0.945 ± 0.056	0.987 ± 0.060	0.969 ± 0.048	1.003 ± 0.063

[1] Model KGE (Kling-Gupta Efficiency) Threshold for water table elevation is from 0.999852 to 0.999894.

[2] Model d (Index of Agreement) Thresholds for yields of maize, sorghum, soybean, and winter wheat are 0.82 to 0.96, 0.69 to 0.88, 0.92 to 0.95, and 0.56 to 0.91, respectively.

[3] The sign of '-' does not indicate those parameters are dimensionless, and multiplier factors are used for those parameters. The units are L/T, %, L^2/T, MJ/m^2-day, ºC, ºC, and mm/day for hydraulic conductivity, specific yield, riverbed conductance, solar radiation, temperature maximum, temperature minimum, and rainfall, respectively.

Notation for genetic parameters: [a] for maize genetic parameter; [b] for sorghum genetic parameter; [c] for winter wheat genetic parameter; [d] for soybean genetic parameter.

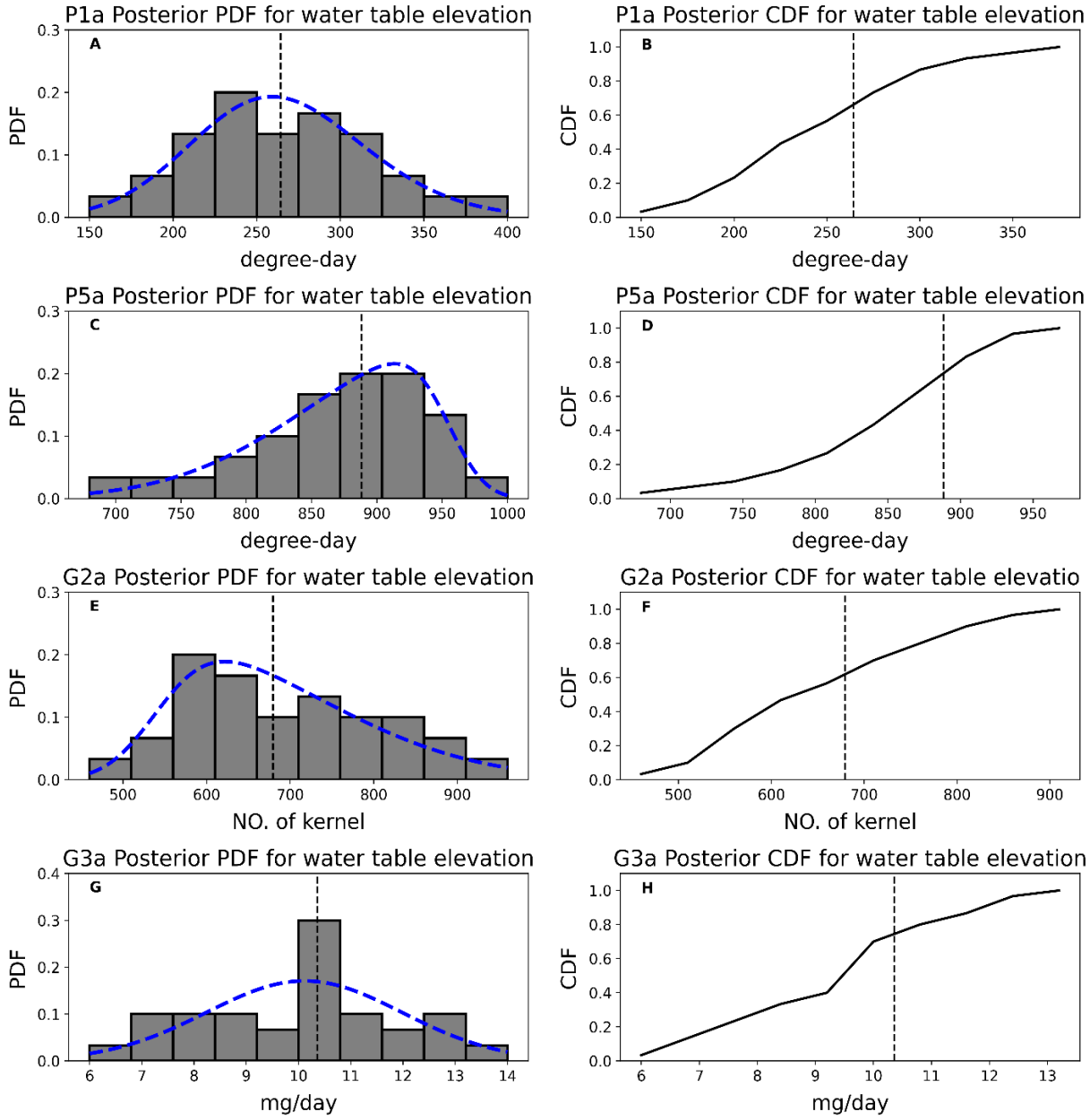

Fig. 4-3 Posterior distributions of PDFs and CDFs for 10 parameters, for the top 10% of the 14,848 simulations.

4.2.4 CLIMATE DATA FOR 2021 - 2050

Statistically downscaled global circulation model (GCM) data from the Coupled Model Intercomparison Project Phase 5 (CMIP5) (*see Figure 4-S1&S2 in Appendices)* is used for this study. Daily downscaled meteorological projection data is created at a 1/24-degree (~4km) resolution using the Multivariate Adapted Constructed Analogs (MACA) method (Abatzoglou and Brown, 2012; Abatzoglou, 2013). MACA uses bias correction and spatial patterns to achieve spatial and temporal downscaling, matching large-scale patterns (e.g., simulations of GCMs) to local, observed patterns. In this study we use available daily downscaled results (minimum and maximum temperature, precipitation, relative humidity, solar radiation) from 20 GCMs for Representative Concentration Pathways (RCP) 4.5 and 8.5. Due to the focus on identifying the most effective irrigation and crop management strategies under various possible future climates, we filter the 20 GCMs to three: one each that represents the wettest, driest, and average conditions. This is performed for both RCP 4.5 and RCP 8.5, resulting in 6 climate scenarios. The following three steps are used to identify these scenarios, which are used as input for the 2020-2050 DSSAT-MODFLOW scenario simulations:

1. GCMs are ranked according to average annual precipitation;
2. Based on the ranking from 1., climate scenarios are divided into four quartiles;
3. The temporal trend of annual precipitation during 2021-2050 is assessed using the Theil-Sen slope, i.e., the median value of all slopes between all pairs of points in the time series. It is due to its robustness to outliers. The most positive slope represents the wet climate trend in the first quartile, the most negative slope represents the dry climate trend in the fourth quartile, and the slope closest to 0 represents the average trends from the second and third quartiles.

Once the 6 climate scenarios are selected, the downscaled daily precipitation and temperature values are written into the DSSAT input files.

4.2.5 ASSESSMENT OF MANAGEMENT STRATEGIES UNDER A CHANGING CLIMATE

Effective irrigation and crop management strategies that limit groundwater use but maintain crop yield are now assessed for the various climate scenarios identified using the method described in Section 4.2.4. The following strategies are assessed:

- *Irrigation type*: surface irrigation (SI) with an irrigation efficiency of 60%; drip irrigation (DI) with an efficiency of 90%; sprinkler irrigation (SPI) with an efficiency of 80%; and center pivot (CP) irrigation with an efficiency of 85%.
- *Planting levels*: full field (level 1), half field (level 2), and quarter field (level 3).

Each of the 4 irrigation types and 3 planting levels are evaluated for each of the 6 future climate patterns, resulting in 72 scenarios. The MODFLOW model is extended to the year 2050, with all hydrogeologic parameters (aquifer hydraulic conductivity, aquifer specific storage, aquifer specific yield, riverbed conductance) held constant.

Results of each of the 72 scenarios are compared according to annual average total crop yield (kg) and average annual groundwater drawdown (m) (i.e., the difference between the initial and final groundwater head values during the year) in the study region. For scenarios that meet a threshold of crop production (based on historical annual average of yield and cultivated areas for each crop type), the ratio of crop yield (kg) to drawdown (m), termed *water use efficiency WUE (*kg/m*)*, is used to identify the most effective management strategies, with strategies being ranked highest for the highest value of W_e. Another term (i.e., *Water Use Profit* (*WUP*, U.S. dollar per m)) is introduced to identify the management strategies that provide the highest gross revenue of crop yield per unit of groundwater depletion.

4.3 RESULTS AND DISCUSSION

4.3.1 PARAMETER ESTIMATION AND MODEL TESTING

The PDFs and CDFs of the 28 targeted model parameters are shown in *Figs. 4-S3, S4, S5, S6, S7 in Appendices*. Graphical representation of only 4 parameters (i.e., P1a, P5a, G2a, and G3a) are shown here (Fig. 4-3) for water table elevation (i.e., one of the system responses), with distribution trendlines of parameters. The shape of each PDF indicates the degree of parameter uncertainty, for example the flat posterior distributions indicate greater uncertainty of parameters in comparison with those with peaked and shaped distributions. In addition, the shape of each CDF demonstrates the type of distribution. For instance, the linear shape of a CDF indicates the uniform distributions of probabilities of parameters. The best values of parameters are derived at the means of CDFs (i.e., when the value of a CDF is equal to 0.5), which are values along the x axis that intersects the CDF trendlines (see Fig. 4-3). The best values for each of the 28 parameters are summarized in Tab. 4-1, with standard deviations.

Fig. 4-4 shows the comparison between simulated and observed water table elevation (i.e., groundwater head) during the 2004-2007 period (Fig. 4-4A), and time-series plots of simulated water table elevation and observed measurements for two monitoring wells (Fig. 4-4B, C). The coefficient of Root Mean Square Deviation (RMSE), scaled RMSE, and Nash-Sutcliffe Efficiency Coefficient (NSCE) are 7.22 m, 0.07, and 0.83, respectively, for simulated and observed water table elevation for the calibrated DSSAT-MODFLOW model, compared to 12.1 m, 0.11, and 0.59, respectively, for the original model presented in Xiang et al. (2020), a reduction of 40% in RMSE and an increase of 41% in the NSCE.

Fig. 4-5 shows simulated crop yields for corn, soybean, winter wheat, and sorghum for 2004, 2005, 2006, and 2007. The model performs well for most crops and most years. For

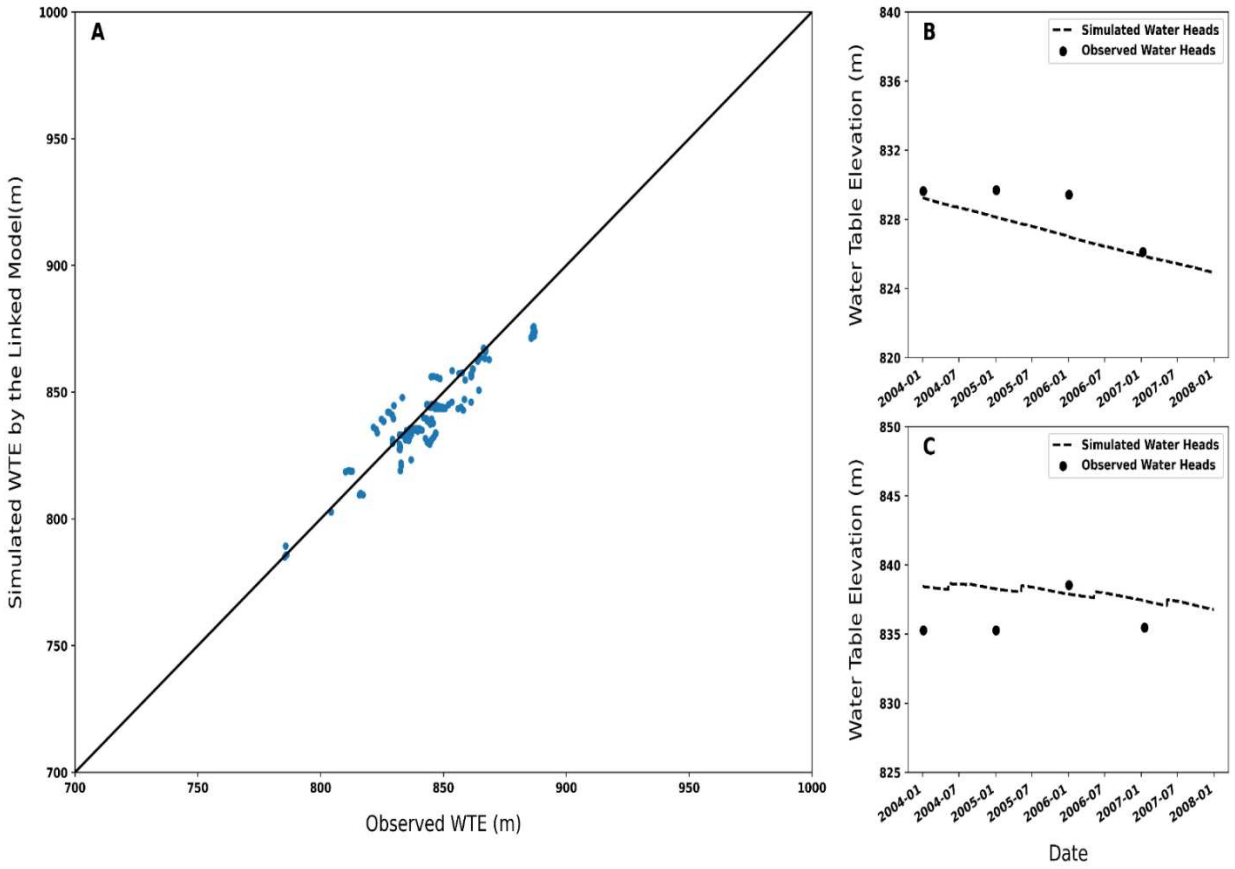

Fig. 4-4 Model validation. Fig.4A shows the comparison between observed water table elevation and simulated water table elevation. Fig.4B & C represent time series plots for simulated water table elevation, in comparison with measured values, in the locations of grid cell with row 17 and column 70 (Fig.4B) and gride cell with row 20 column 80 (Fig.4C).

example, reported crop yields are 13,983 kg/ha, 4,864 kg/ha, 3,195 kg/ha, and 3,121 kg/ha for corn, sorghum, winter wheat, and soybean, respectively, in 2007. Simulated crop yields for the same year using the initial parameter set of DSSAT-MODFLOW (Xiang et al., 2020) are 13,540 kg/ha for corn (3% difference with reported), 10,863 kg/ha for sorghum (123% difference), 10,830 kg/ha for winter wheat (239% difference), and 4,084 kg/ha for soybean (31% difference). Simulated crop yields using the calibrated parameter values in this study are 13,613 kg/ha for corn (3% difference), 5,316 kg/ha for sorghum (9% difference), 3,464 kg/ha for winter wheat (8% difference), and 2,881 kg/ha for soybean (8% difference). Results are similar for years 2004, 2005, and 2006, with the main deviations in simulated values from reported values occurring for corn (Fig. 4-5A), soybean (Fig. 4-5B), winter wheat (Fig. 4-5C), and sorghum (Fig. 4-5D).

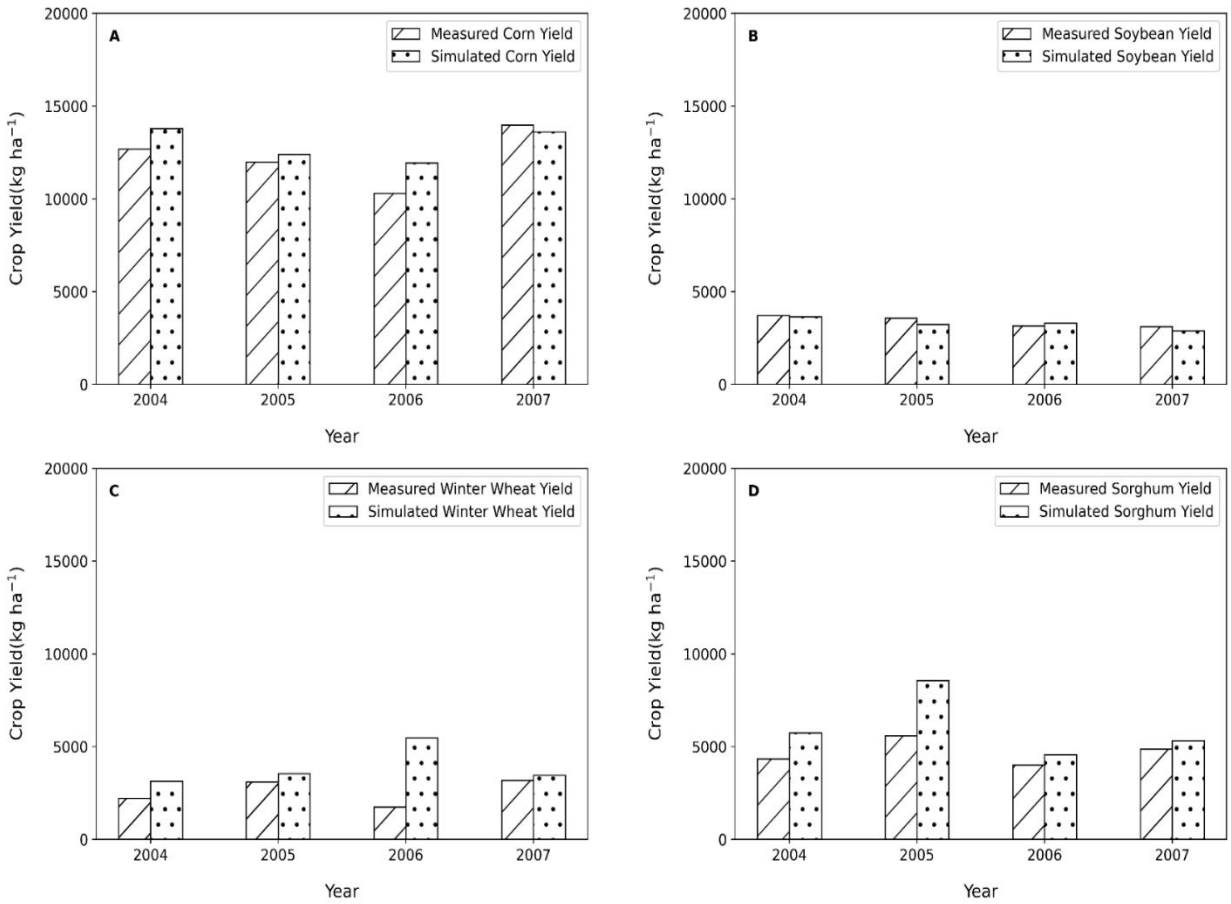

Fig. 4-5 Comparison of simulated crop yields and measured crop yields during 2004 to 2007. Fig.5A, 5B, 5C, and 5D show the simulated yields of corn, soybean, winter wheat, and sorghum, respectively, compared to measured crop yields in 2004, 2005, 2006, and 2007.

With these results for both groundwater head and crop yield, we conclude that the model can be used to estimate the impact of climate scenarios and irrigation strategies on groundwater storage, water table elevation, groundwater drawdown, and crop yield during the years 2020-2050.

4.3.2 MODEL RESPONSE DRIVEN BY CLIMATE PATTERNS

The impact of climate without management strategies is presented first to provide context for the management strategy results shown in Section 4.3.3. Fig. 4-6 shows annual average water table elevation and crop yield (corn, soybean, winter wheat, sorghum) for the 2021-2050 period, for each of the 40 climate scenarios. From these results we conclude that climate has a

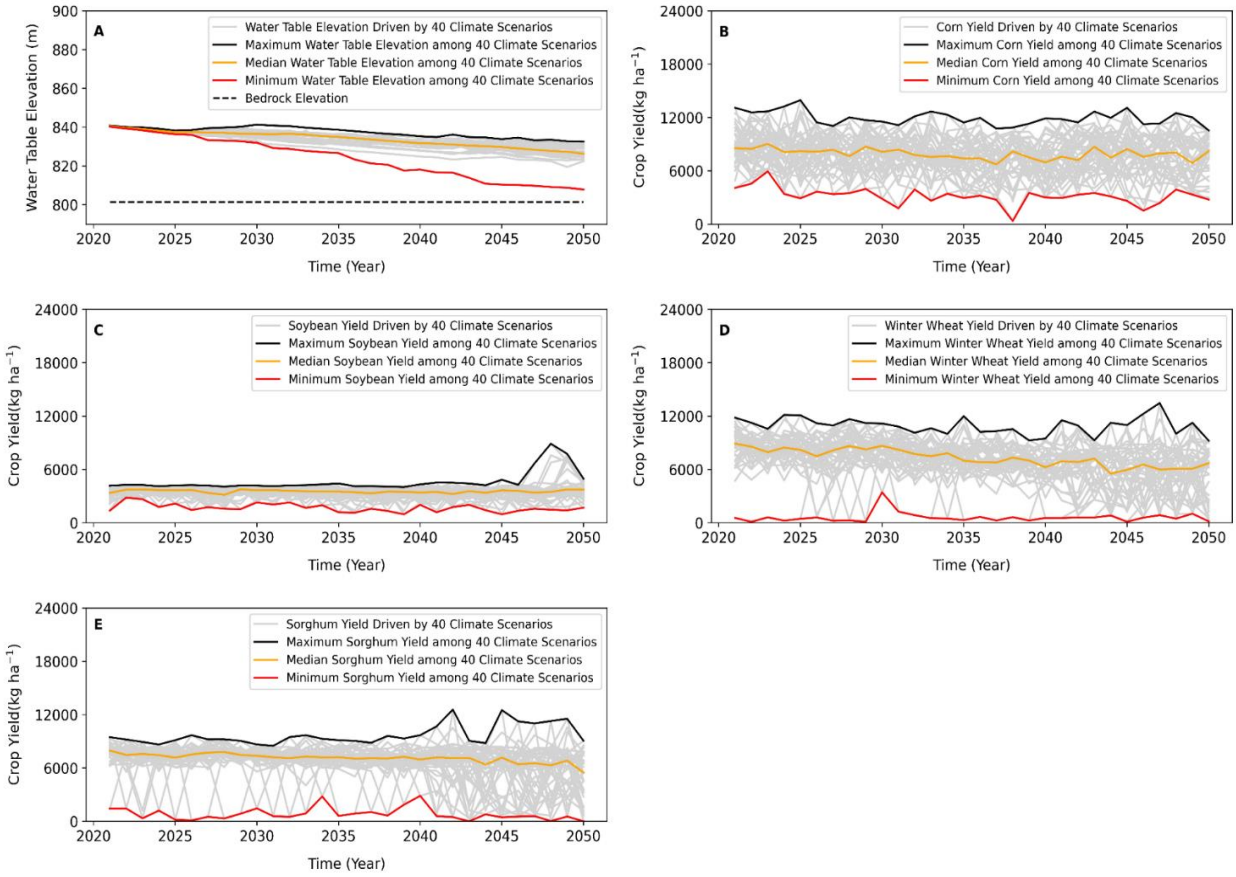

Fig. 4-6 Model responses (i.e., water table elevation in Fig. 4-6A, yields of corn in Fig. 4-6B, soybean in Fig. 4-6C, winter wheat in Fig. 4-6D, and sorghum in Fig. 4-6E) driven by long-term downscaled climate patterns.

significant effect on groundwater storage and crop yield in the study region. The water table elevation (Fig. 4-6A) decreases 8 m over 30 years (0.3 m/yr) under the best (wettest) scenario of climate patterns but decreases 32 m (1.1 m/yr) under the worst (driest) scenario. As seen in Fig. 4-6A, which shows the elevation of the bedrock (dashed black line; 800 m), by 2050 the water table elevation in the driest climate condition is within a few meters of the bedrock, indicating near depletion of all groundwater in the region. However, for most climate scenarios (gray lines), groundwater storage does not decline nearly as much, but still 20% to 50% of the original saturated thickness. In addition, crop yields are greatly influenced by future climate patterns. The average difference in corn yield over 30 years with the best and worst climate conditions is 8,779 kg/ha; similarly, the average differences in yields of soybean, winter wheat, and sorghum are 2,953 kg/ha, 10,323 kg/ha, and 8,902kg/ha, respectively.

4.3.3 IDENTIFYING EFFECTIVE MANAGEMENT STRATEGIES

The relationships between annual crop yield (kg/yr), annual gross revenue (dollars/yr), and annual average groundwater drawdown (m) are shown for the 24 management scenarios under wet climate conditions (Fig. 4-7), average climate conditions (Fig. 4-8), and dry climate conditions (Fig. 4-9), for Finney County. Annual gross revenue is based on data from https://www.nass.usda.gov/Charts_and_Maps/Agricultural_Prices/. Results are shown for maize, soybean, winter wheat, and sorghum. Each point in the plots represents a different climate-management combination. The color represents the management practices, whereas the symbol (dot, cross) represents the RCP level (4.5 vs. 8.5). Each figure plot shows a black dashed line that indicates the minimum allowed total crop yield, based on historical production. Therefore, each scenario that plots above this line represents a combination of climate and management that maintains adequate crop yield into future decades.

Based on results shown in Fig. 4-7, management scenarios under the RCP8.5 wet period for maize are rejected, while management scenarios under the RCP4.5 wet period for maize are accepted for the applications of *WUE* and *WUP*, with most gross revenue of 9.834×10^7 U.S. Dollars under the combination of drip irrigation system and quarter plant level (Fig. 4-7A). This indicates that if future climate conditions are wet but conform to the assumptions of the RCP8.5 carbon emission scenario, then likely no viable management practice will be able to maintain adequate maize yield. The situation is not so dire for the other three crop types (Fig. 4-7B, C, D), with management scenarios in both the RCP4.5 and RCP8.5 conditions providing many acceptable crop yields, although soybean has the fewest (Fig. 4-7B), with only four scenarios under RCP8.5 wet condition recognized as acceptable. For each crop type, the crop yield for the RCP8.5 conditions are always lower than for the RCP4.5 conditions. For winter wheat and

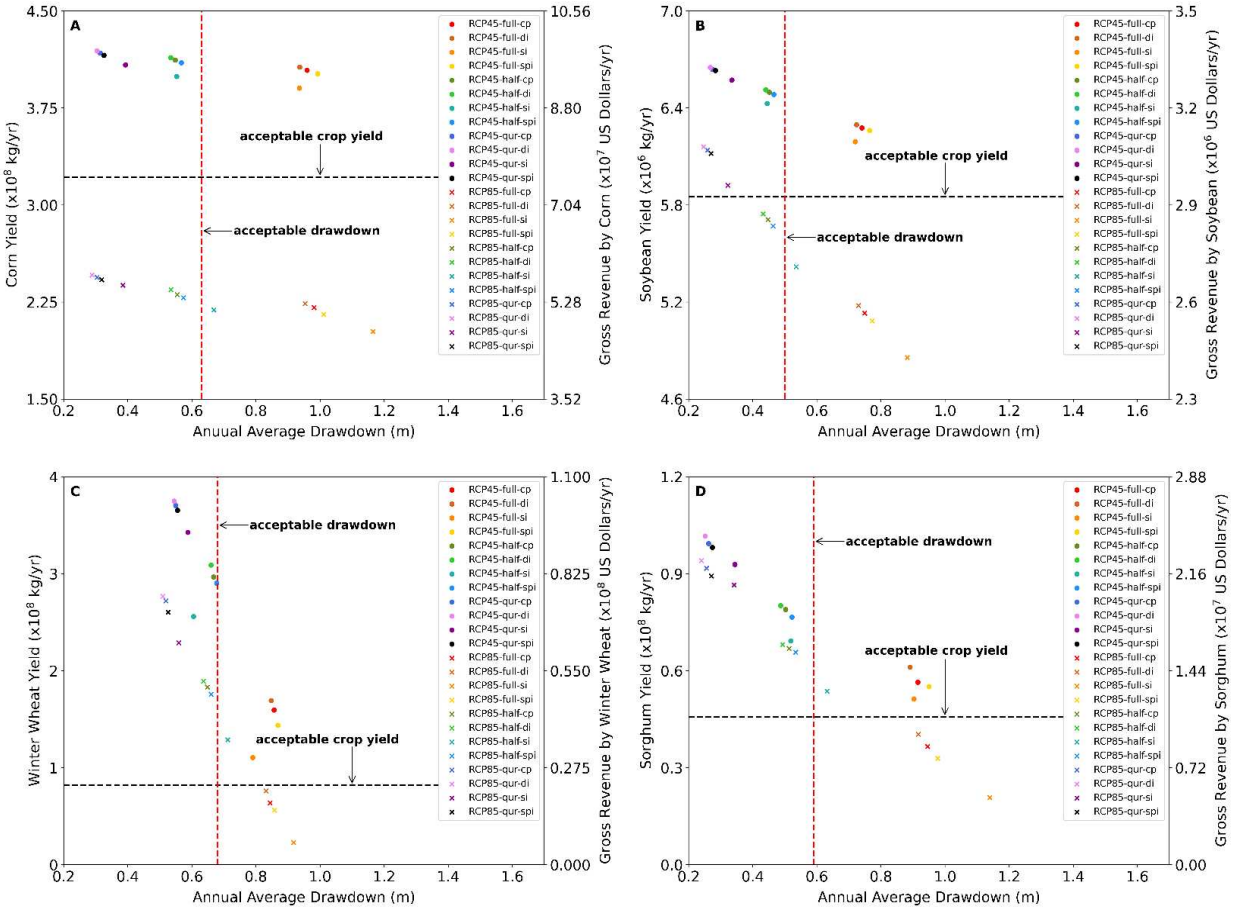

Fig. 4-7 Screening of the alternatives of BMPs under the wet climate condition (for both RCP4.5 and RCP8.5). Fig.7A, B, C, and D show annual average total crop yields vs. annual average drawdown for corn, soybean, winter wheat, and sorghum, respectively, during 2021 – 2050 in Finney County. Irrigation systems include center pivot irrigation (cp), drip irrigation (di), surface irrigation (si) and sprinkler irrigation (spi). Plant levels include full field (full), half field (half), and quarter field (qur).

sorghum, only four management scenarios under RCP8.5 wet condition are rejected; the eliminated management scenarios are involved in plant level 1 (full field planting), which use the most groundwater. If groundwater conservation is a constraint, and an annual drawdown of less than acceptable drawdown (i.e., the average of 24 management practice-based annual average drawdowns for crops in 3 climate conditions) is desired (see vertical red dashed line in Fig. 4-7), then only a few scenarios will yield adequate crop yield. See upper-left region in each plot in Fig. 4-7. The average gross revenue for maize, soybean, winter wheat, and sorghum that meet both acceptable drawdown and crop yield are 9.67×10^7 U.S. Dollars-yr^{-1}, 3.13×10^6 U.S. Dollars-yr^{-1}, 0.76×10^8 U.S. Dollars-yr^{-1}, and 2.02×10^7 U.S. Dollars-yr^{-1}, respectively.

Tab. 4-2. Water Use Efficiency (WUE) (x10^9 kg of crop yield per m of groundwater drawdown) for maize, soybean, winter wheat, and sorghum under future wet climate conditions.

Crop Type and Climate Conditions	Water Use Efficiency for 12 combinations of management scenarios (x***10^9 kg/m***)											
	1	2	3	4	5	6	7	8	9	10	11	12
Corn_wet_RCP4.5	0.4172	0.7227	1.0397	0.4044	0.7229	1.275	0.4213	0.7512	1.3291	0.434	0.7749	1.3764
Corn_wet_RCP8.5	0.1736	0.3276	0.6183	0.213	0.3975	0.7612	0.225	0.4163	0.8026	0.2347	0.4384	0.8526
Soybean_wet_RCP4.5	0.0086	0.0144	0.0196	0.0082	0.0139	0.0234	0.0085	0.0144	0.0242	0.0087	0.0148	0.0249
Soybean_wet_RCP8.5	0.0055	0.0101	0.0184	0.0066	0.0122	0.0227	0.0068	0.0127	0.0237	0.0071	0.0133	0.025
Winter Wheat_wet_RCP4.5	0.1399	0.4229	0.583	0.1655	0.4285	0.6582	0.1863	0.4443	0.6737	0.1997	0.4681	0.6878
Winter Wheat_wet_RCP8.5	0.025	0.181	0.4089	0.0656	0.2663	0.4949	0.0756	0.2823	0.5242	0.0917	0.2972	0.5434
Sorghum_wet_RCP4.5	0.0568	0.1335	0.2697	0.058	0.1467	0.3575	0.0617	0.157	0.3792	0.0686	0.1645	0.4039
Sorghum_wet_RCP8.5	0.0182	0.0849	0.2532	0.0337	0.1231	0.3298	0.0387	0.1304	0.3583	0.0441	0.138	0.3919

1- surface, full; 2 – surface, half; 3 – surface, quarter; 4 – sprinkler, full; 5 – sprinkler, half; 6 – sprinkler, quarter; 7 – center pivot, full; 8 – center pivot, half; 9 – center pivot, quarter; 10 – drip, full; 11 – drip, half; 12 – drip, quarter. Light blue means only acceptable for crop yield; light red means only acceptable for groundwater drawdown; light purple means acceptable for both.

The *WUE* and *WUP* for each of the scenarios shown in Fig. 4-7 is summarized in Tab. 2 and Tab. 4-S1 (*in the Appendices*), respectively. Higher values indicate more crop yield and gross revenue per groundwater used, which correspond to symbols in the upper-left regions of Fig. 4-7 plots. *WUE* and *WUP* values for scenarios that provide crop yield above the minimum threshold are colored in light blue, while values that limit drawdown to less than acceptable drawdown are colored in light red. Scenarios that meet both crop yield and groundwater constraints are colored in light purple. As expected, higher *WUE* values correspond to scenarios with higher irrigation efficiency and smaller plant level. For example, for corn under the wet climate condition with RCP4.5, drip irrigation for quarter plots (#12) has a *WUE* of 1.3764 x 10^9kg/m, with an increase of 2 times compared to drip irrigation for full plots (#10), which has as *WUE* of 0.434 x 10^9kg/m. Similar results occur for the other three crop types, and for the other irrigation types (surface, sprinkler, center pivot). The drip-quarter plot scenario (#12) is

represented by the pink dot in Fig. 4-7A, which is the farthest left on the plot. Only several scenarios (light purple color) meet both criteria. These are: #2, #3, #5, #6, #8, #9, #11, #12 for maize under the wet climate condition.

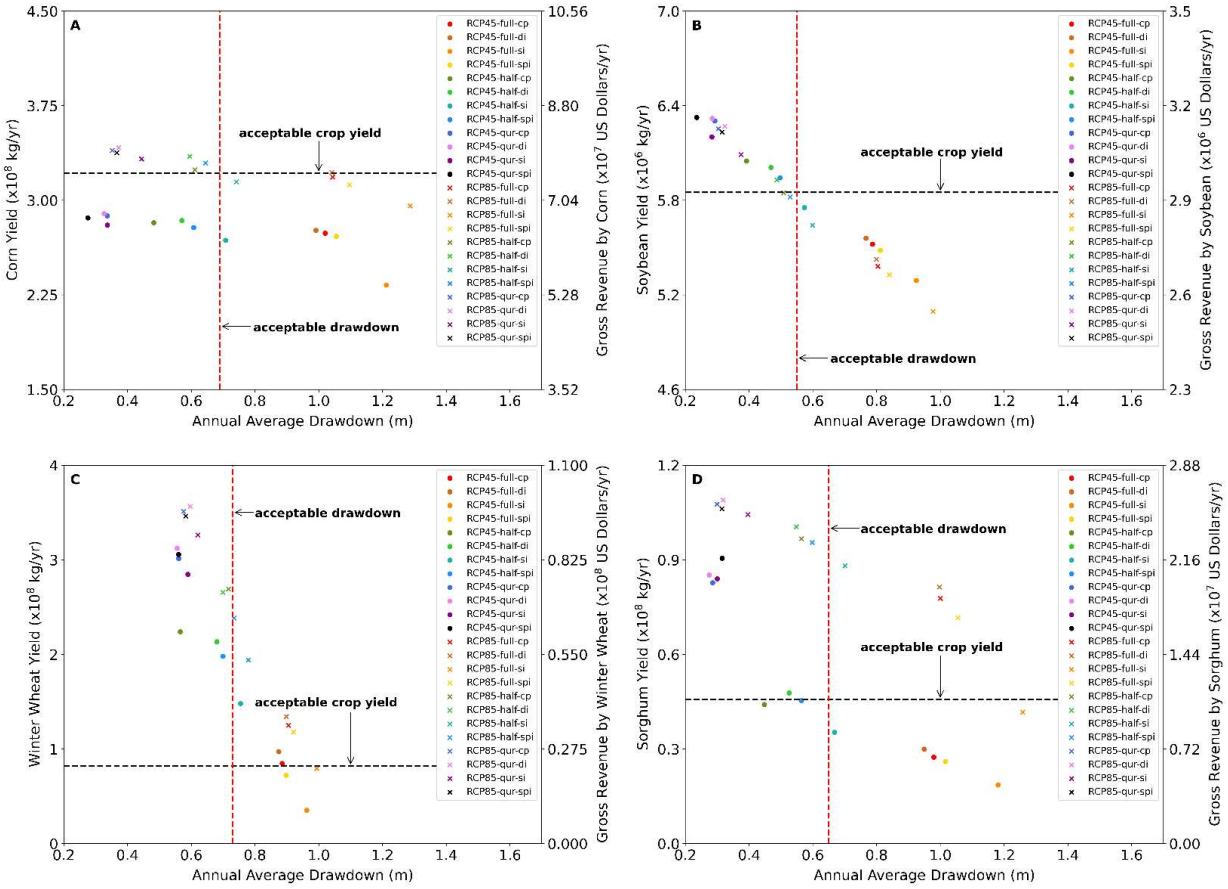

Fig. 4-8 Screening of the alternatives of BMPs under the average climate condition (for both RCP4.5 and RCP8.5). Fig.8A, B, C, and D show annual average total crop yields vs. annual average drawdown for corn, soybean, winter wheat, and sorghum, respectively, during 2021 – 2050 in Finney County. Irrigation systems include center pivot irrigation (cp), drip irrigation (di), surface irrigation (si) and sprinkler irrigation (spi). Plant levels include full field (full), half field (half), and quarter field (qur).

Similar patterns occur for average (Fig. 4-8) and dry (Fig. 4-9) climate conditions. None of the management strategies under the dry RCP8.5 climate scenario will provide adequate crop yield (Fig. 4-9A); similarly, only a few management strategies under average RCP8.5 climate condition are conducive to maize growth (Fig. 4-8A), but there are multiple strategies under the RCP8.5 scenario that will be sufficient for soybean (Figs. 4-8 & 9B), winter wheat (Figs. 4-8 & 9C), and sorghum (Figs. 4-8 & 9D). For soybean under an average climate, 5 and 7 management scenarios under the average climate conditions of RCP8.5 and RCP4.5, respectively, provide

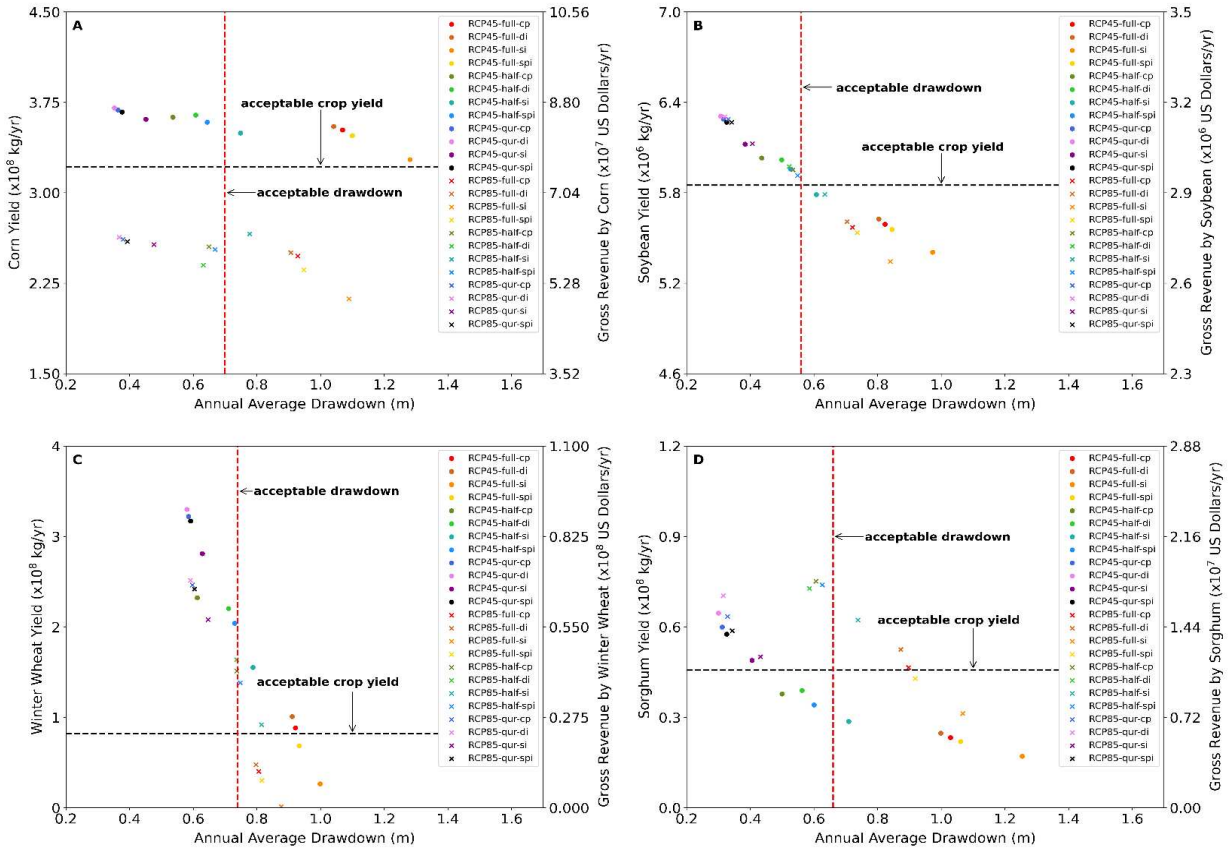

Fig. 4-9 Screening of the alternatives of BMPs under the dry climate condition (for both RCP4.5 and RCP8.5). Fig.9A, B, C, and D show annual average total crop yields vs. annual average drawdown for corn, soybean, winter wheat, and sorghum, respectively, during 2021 – 2050 in Finney County. Irrigation systems include center pivot irrigation (cp), drip irrigation (di), surface irrigation (si) and sprinkler irrigation (spi). Plant levels include full field (full), half field (half), and quarter field (qur).

adequate crop yield, with an average gross revenue of 2.99x10^6 U.S. Dollars-yr^{-1}. For winter wheat and sorghum under average climate conditions, only several management scenarios provide inadequate crop yield, with average gross revenues of 0.64 x10^8 U.S. Dollars-yr^{-1} and 2.15 x10^7 U.S. Dollars-$yr^{-1}$for winter wheat and sorghum, respectively, for providing adequate crop yield. The same trend occurs for the dry conditions (Fig. 4-9), although there are several more scenarios under the dry condition that do not provide adequate yield of winter wheat (Fig. 4-9C) and sorghum (Fig. 4-9D), with dry conditions overall providing lower crop yield. If groundwater conservation is considered, and an annual drawdown of acceptable drawdown is defined as the maximum allowed amount, then only 7, 12, 14, and 12 scenarios are adequate for

yield of maize (Fig. 4-8A), soybean (Fig. 4-8B), winter wheat (Fig. 4-8C), and sorghum (Fig. 4-8D), respectively, under the average climate conditions.. Similar results occur for dry conditions (Fig. 4-9).

Tab. 4-3. Water Use Efficiency (WUE) (x10^9 kg of crop yield per m of groundwater drawdown) for maize, soybean, winter wheat, and sorghum under future average climate conditions.

Crop Type and Climate Conditions	Water Use Efficiency for 12 combinations of management scenarios (x10^9 kg/m)											
	1	2	3	4	5	6	7	8	9	10	11	12
Corn_avg_RCP4.5	0.1921	0.3791	0.832	0.2572	0.4582	1.037	0.2684	0.5846	0.8545	0.2786	0.4976	0.8866
Corn_avg_RCP8.5	0.2297	0.4239	0.7498	0.2848	0.511	0.9214	0.3051	0.53	0.9649	0.3094	0.5626	0.9179
Soybean_avg_RCP4.5	0.0057	0.01	0.0219	0.0068	0.012	0.0269	0.007	0.0154	0.0216	0.0073	0.0128	0.0222
Soybean_avg_RCP8.5	0.0052	0.0094	0.0163	0.0063	0.011	0.0198	0.0067	0.0115	0.0206	0.0068	0.0122	0.0194
Winter Wheat_avg_RCP4.5	0.0366	0.1961	0.4829	0.0805	0.2832	0.5456	0.0957	0.3959	0.5374	0.1112	0.3138	0.5619
Winter Wheat_avg_RCP8.5	0.0799	0.2491	0.5254	0.1282	0.3247	0.5939	0.1382	0.3751	0.5977	0.1495	0.3798	0.61
Sorghum_avg_RCP4.5	0.0157	0.0528	0.2799	0.0256	0.0804	0.2869	0.028	0.0984	0.2894	0.0316	0.0909	0.3096
Sorghum_avg_RCP8.5	0.0331	0.1257	0.2633	0.0679	0.1597	0.3377	0.0777	0.1713	0.3596	0.0816	0.1833	0.342

1- surface, full; 2 – surface, half; 3 – surface, quarter; 4 – sprinkler, full; 5 – sprinkler, half; 6 – sprinkler, quarter; 7 – center pivot, full; 8 – center pivot, half; 9 – center pivot, quarter; 10 – drip, full; 11 – drip, half; 12 – drip, quarter. Light blue means only acceptable for crop yield; light red means only acceptable for groundwater drawdown; light purple means acceptable for both.

The results for the average and dry conditions are summarized in Tab. 3 and Tab. 4-S2 (*see in the Appendices*), and Tab. 4 and Tab. 4-S3 (*see in the Appendices*), respectively. Similar to the wet conditions, much higher *WUE* and *WUP* values occur for higher irrigation efficiency practices and less land irrigated. For average conditions, 57 scenarios satisfy the crop yield requirement, 56 scenarios satisfy the groundwater drawdown requirement, and only 45 scenarios satisfy both conditions. These scenarios are: #3, #5, #6, #8, #9, #11, #12 under RCP8.5 for maize; #3. #5, #6, #8, #9, #11, #12 under RCP4.5 and #3, #6, #9, #11, #12 under RCP8.5 for soybean; #3, #5, #6, #8, #9, #11, #12 under RCP4.5 and #3, #5, #6, #8, #9, #11, #12 under

RCP8.5 for winter wheat; #3, #6, #9, #11, #12 under RCP4.5 and #3, #5, #6, #8, #9, #11, #12 under RCP8.5 for sorghum. For dry conditions, 58 scenarios satisfy the crop yield requirement, 53 scenarios satisfy the groundwater drawdown requirement, and only 43 scenarios satisfy both conditions. These scenarios are: #3, #5, #6, #8, #9, #11, #12 under RCP4.5 for maize; #3, #5, #6, #8, #9, #11, #12 under both RCP4.5 and RCP8.5 for soybean; #3, #5, #6, #8, #9, #11, #12 under RCP4.5 and #3, #6, #9, #12 under RCP8.5 for winter wheat; #3, #6, #9, #12 under RCP4.5 and #3, #5, #6, #8, #9, #11, #12 under RCP8.5 for sorghum.

Tab. 4-4. Water Use Efficiency (WUE) (x10^9 kg of crop yield per m of groundwater drawdown) for maize, soybean, winter wheat, and sorghum under future dry climate conditions.

Crop Type And Climate Conditions	Water Use Efficiency for 12 combinations of management scenarios (x10^9 kg/m)											
	1	2	3	4	5	6	7	8	9	10	11	12
Corn_dry_RCP4.5	0.2557	0.4671	0.7998	0.3159	0.5569	0.975	0.3293	0.6764	1.0147	0.3411	0.5997	1.0522
Corn_dry_RCP8.5	0.1948	0.3422	0.5391	0.2492	0.3784	0.6603	0.2667	0.3929	0.6885	0.2763	0.3798	0.7173
Soybean_dry_RCP4.5	0.0056	0.0095	0.016	0.0066	0.0113	0.0192	0.0068	0.0138	0.0199	0.007	0.0121	0.0206
Soybean_dry_RCP8.5	0.0064	0.0091	0.0151	0.0075	0.0108	0.0184	0.0077	0.0111	0.019	0.008	0.0114	0.0197
Winter Wheat_dry_RCP4.5	0.0265	0.1972	0.447	0.0735	0.2795	0.536	0.0961	0.379	0.5505	0.1108	0.3098	0.5687
Winter Wheat_dry_RCP8.5	0.0017	0.1066	0.322	0.0372	0.1851	0.4005	0.0501	0.2052	0.4125	0.0598	0.2223	0.4257
Sorghum_dry_RCP4.5	0.0137	0.0404	0.1207	0.0207	0.0569	0.1769	0.0226	0.0756	0.1923	0.0248	0.0692	0.2154
Sorghum_dry_RCP8.5	0.0293	0.0843	0.116	0.0467	0.1181	0.1712	0.0518	0.124	0.1931	0.0602	0.1243	0.2234

1- surface, full; 2 – surface, half; 3 – surface, quarter; 4 – sprinkler, full; 5 – sprinkler, half; 6 – sprinkler, quarter; 7 – center pivot, full; 8 – center pivot, half; 9 – center pivot, quarter; 10 – drip, full; 11 – drip, half; 12 – drip, quarter. Light blue means only acceptable for crop yield; light red means only acceptable for groundwater drawdown; light purple means acceptable for both.

4.3.4 FIELD-BASED ANALYSIS OF EFFECTIVE MANAGEMENT STRATEGIES

Fig. 4-10, 11, &12 show field-scale results of average maize yield (kg/ha) and average annual drawdown (m) during 2021 - 2050 in different locations within the Finney County (maize is selected for case study). 4 spots/fields are selected for this study, including the field of NO.199

(top-middle related to results shown in Fig. 4-10A, 11A, &12A) with low saturated thickness and no surface-water interaction, the field of NO. 766 (bottom-middle related to results shown in Fig.4-10B, 11B, &12B) with high saturated thickness and no surface-water interaction, the field of NO.2142 (middle-left related to results shown in Fig. 4-10C, 11C, &12C) with high saturated thickness and surface-water interaction, and the field of NO. 4663 (middle-right related to results

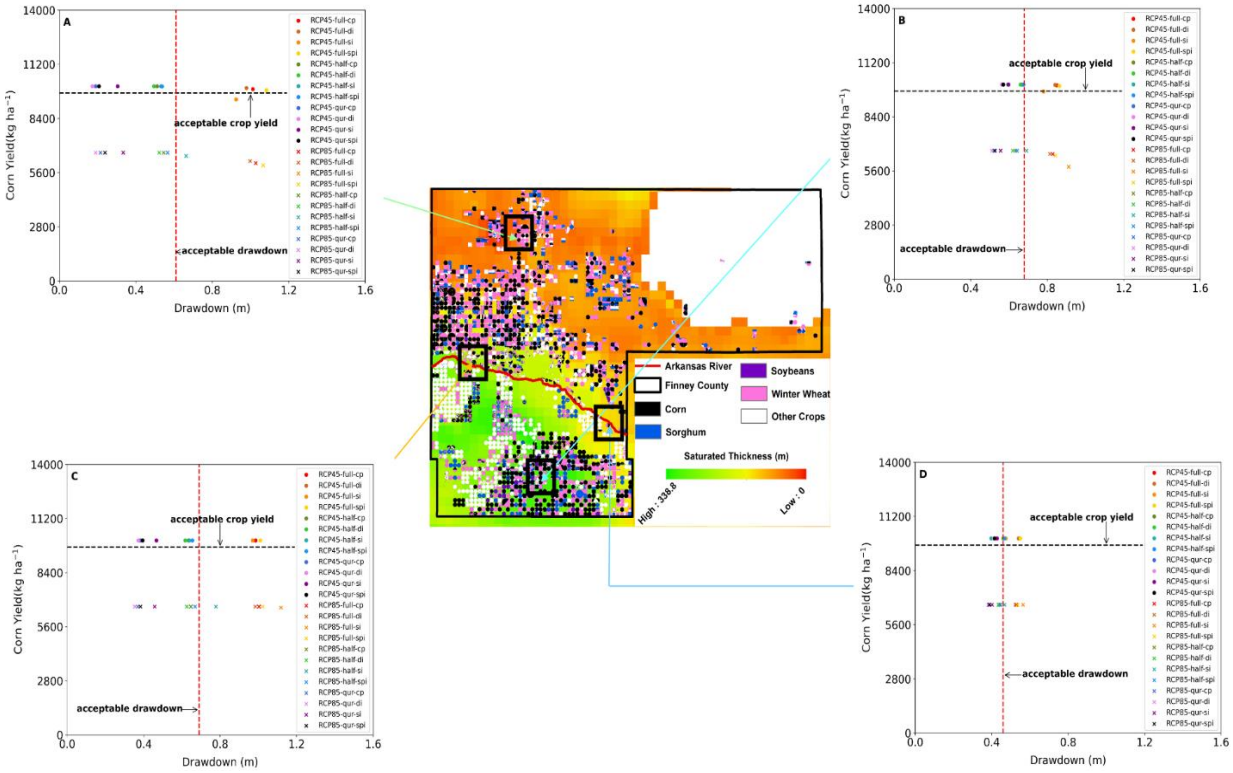

Fig. 4-10 Field-based analysis of the relationship between maize yield (kg/ha) and average annual drawdown (m) in different locations (Fig.10A, B, C, D in the field of NO.199, NO. 766, NO. 2142, NO. 4663 shown in the central map) with 24 BMPs under the wet climate condition (for both RCP4.5 and RCP8.5) during 2021 – 2050 in Finney County. Irrigation systems include center pivot irrigation (cp), drip irrigation (di), surface irrigation (si) and sprinkler irrigation (spi). Plant levels include full field (full), half field (half), and quarter field (qur).

Based on plots in Fig. 4-10, 11, &12, the management strategies do not significantly affect maize yield (see values of maize yield around a horizontal line under different climate conditions with RCP4.5 and RCP.8.5); however, they considerably have influence on groundwater depletion, which indicates the reasonable application of management strategies is conducive to local groundwater conservation. The yield of maize is mainly controlled by climate

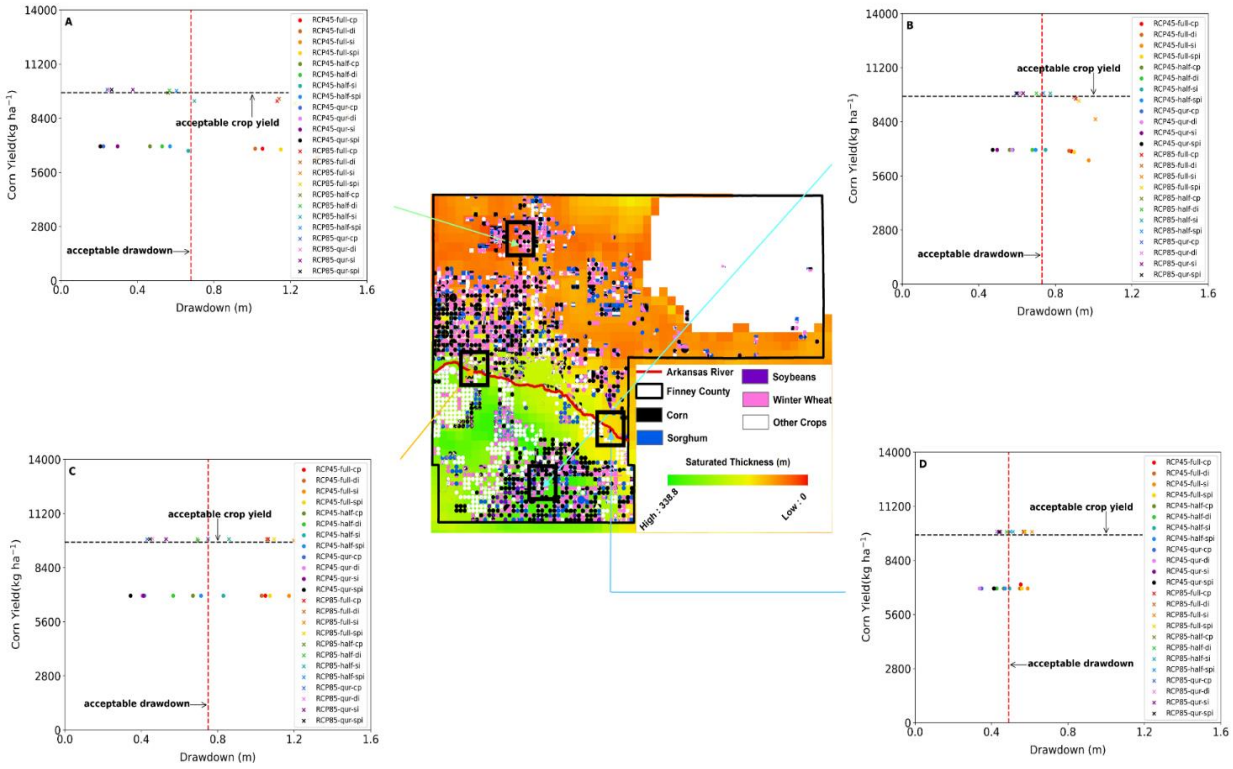

Fig. 4-11 Field-based analysis of the relationship between maize yield (kg/ha) and average annual drawdown (m) in different locations (Fig.10A, B, C, D in the field of NO.199, NO. 766, NO. 2142, NO. 4663 shown in the central map) with 24 BMPs under the average climate condition (for both RCP4.5 and RCP8.5) during 2021 – 2050 in Finney County. Irrigation systems include center pivot irrigation (cp), drip irrigation (di), surface irrigation (si) and sprinkler irrigation (spi). Plant levels include full field (full), half field (half), and quarter field (qur).

conditions (i.e., wet, average, dry) RCP emission conditions. Groundwater drawdown is greatly affected by management strategies applied in the field with low saturated thickness under 3 climate conditions (see changes in drawdown by management strategies in Fig. 4-10A, 11A, 12A), while it is less impacted by management strategies in the field with high saturated thickness (Fig.4-10B, 11B, 12B); in other words, the field in the areas with low groundwater availability requires more management strategies to conserve groundwater. Management strategies do not extremely influence groundwater depletion with areas of low saturated thickness when areas have interactions with surface-water (Fig. 4-10D); however, these areas could have less drawdowns due to recharge of surface-water into groundwater. The field interacting with groundwater, but with high saturated thickness, has a wide range of changes in

groundwater drawdown by management strategies; however, more groundwater depletion occurs to the field, with comparison with the field with both surface-water interaction and low saturated thickness, due to discharge from groundwater to surface-water in terms of high saturated thickness (Fig. 4-10C).

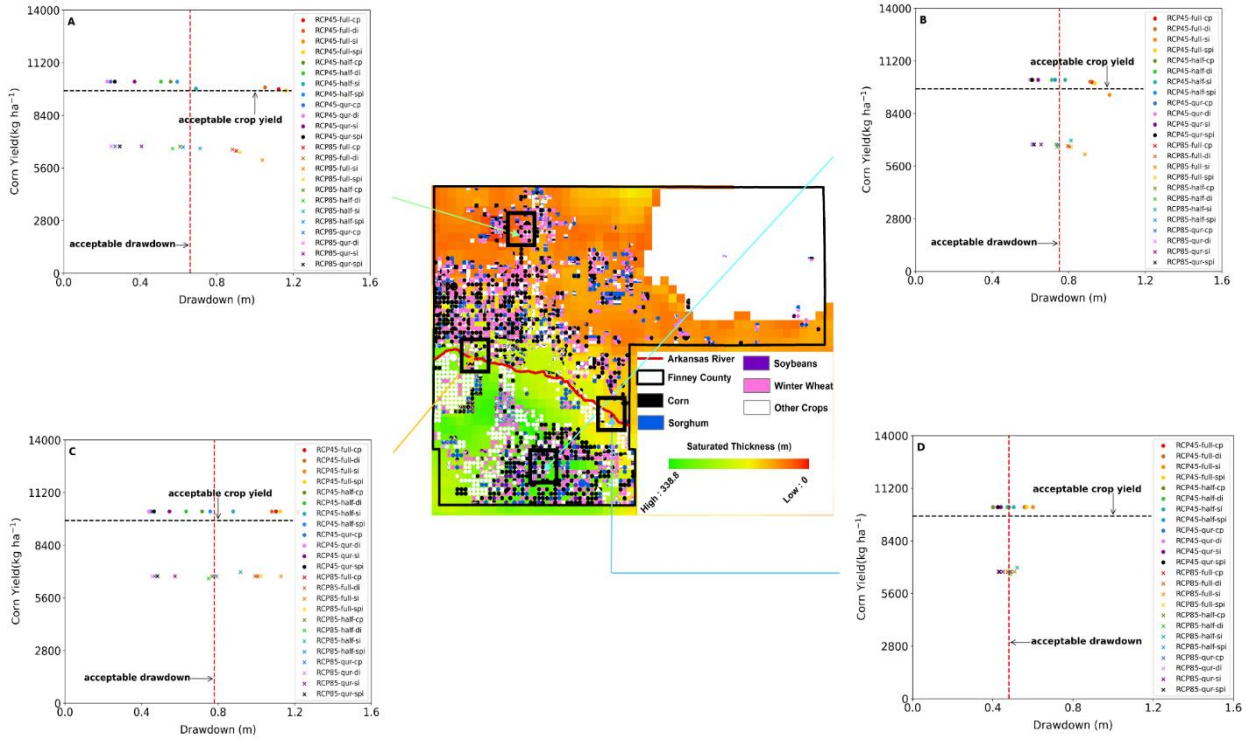

Fig. 4-12 Field-based analysis of the relationship between maize yield (kg/ha) and average annual drawdown (m) in different locations (Fig.10A, B, C, D in the field of NO.199, NO. 766, NO. 2142, NO. 4663 shown in the central map) with 24 BMPs under the dry climate condition (for both RCP4.5 and RCP8.5) during 2021 – 2050 in Finney County. Irrigation systems include center pivot irrigation (cp), drip irrigation (di), surface irrigation (si) and sprinkler irrigation (spi). Plant levels include full field (full), half field (half), and quarter field (qur).

4.3.5 EFFECT OF BEST MANAGEMENT STRATEGIES THROUGH TIME

The management strategies identified in Section 4.3.3 as providing the highest crop yield for the lowest groundwater drawdown (i.e., best strategies) are now shown in terms of annual water table elevation and crop yield. The strategies providing the lowest crop yield for the high groundwater drawdown (i.e., worst strategies) are shown alongside for comparison. The four scenarios therefore are 1) best strategy during dry conditions (BSD), 2) worst strategy during dry

conditions (WSD), 3) best strategy during wet conditions (BSW), and 4) worst strategy during wet conditions (WSW). Results of water table elevation are averaged according to the crop type associated with the groundwater, e.g., all MODFLOW grid cells that underly corn-cultivated

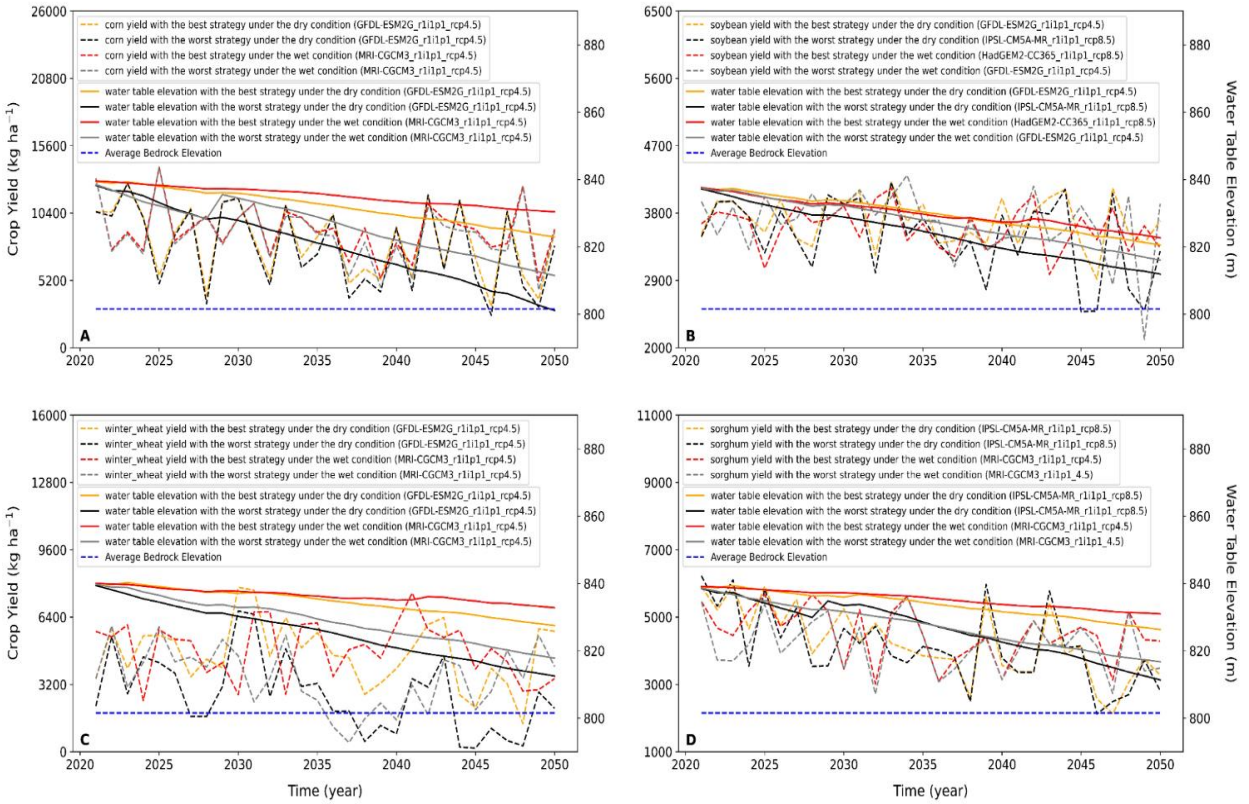

Fig. 4-13 Comparison of model responses under BMPs in the temporal mode. Fig.13A, B, C, and D represent corn-related, soybean-related, winter wheat-relate, and sorghum-related responses, respectively, under BMPs during years of 2021 to 2050.

Fig. 4-13 shows changes of water table elevation and crop yield over 30 years (i.e., years of 2021 to 2050) under the 4 management scenarios of BSD, WSD, BSW, and WSW. For corn (shown in Fig. 4-13A), management strategies can be conducive to corn production and groundwater conservation under both dry and wet climate conditions. For example, the best strategy can produce 449 kg/ha yield more on average under the dry condition than the corn yield produced by the worst strategy, and the best strategy causes an extra yield of 319 kg/ha for corn compared to corn yield with the worst strategy under the wet condition. In addition, the best management strategy saves 11.8 m (38.7 ft) in depth of groundwater on average over 30 years in

comparison with the water table elevation applied by the worst management strategy under the dry climate condition, with a maximum difference of 21.9 m (71.9 ft) in depletion in 2050, while the water table elevation has an extra depletion of 9.3 m (30.5 ft) caused by the worst management strategy compared to it with the best management strategy under the wet climate condition, with a maximum difference of 18.9 m (62 ft) in depletion in 2050. Climate conditions (i.e., dry and wet condition) also influence on crop yield and water table elevation when management strategies are applied. For example, corn yield increases by 871 kg/ha due to the wet condition under the best management practice applied, and the corn yield of 1,000 kg/ha under the wet condition can be produced more than the yield under the dry condition when the worst management practice is conducted. Also, the water table depletes 3.1 m (10.2 ft) more under the dry condition than that under the wet condition, with the best management strategy; the water table can be saved 5.6 m (18.4) in depth more under the wet condition than it is under the dry condition, when the worst management strategy is applied. It is worth noting that the water table has extra depletions of 14.9 m (48.9 ft) on average over 30 years and 29.3 m (96.1 ft) in 2050 under the dry condition with the worst strategy in comparison with those under the wet condition with the best strategy. After 30-year pumping, there is no available groundwater resources can be used for irrigation on condition that the worst management scenario is applied under the dry climate condition.

For soybean and soybean-related water table elevation shown in Fig. 4-13B, the temporal changes of crop yield and water table elevation are affected by both management strategies and climate conditions. Soybean yield increases by 217 kg/ha with the best strategy compared to soybean cultivated with the worst strategy in the dry condition, while the yield of soybean has 62 kg/ha for the best management strategy more than that planted through the worst

management strategy under the wet climate condition. In addition, soybean-related water table elevation depletes 2.4 m (7.9 ft) on average over 30 years for the best strategy more than that for the worst strategy in the dry condition, with a range of difference from 0.2 m (0.7 ft) to 4.5 m (14.8 ft), and a 6.1 m (20 ft) of groundwater in depth can be saved due to the best strategy during 30 years in comparison to the water table due to the application of the worst strategy under the wet condition, with a range of difference from 0.4 m (1.3 ft) to 10.8 m (35.4 ft). Furthermore, climate conditions also have significant impacts on soybean yield and water table elevation. For example, the best management strategy gives rise to a difference of 91.6 kg/ha on average for soybean yield between the dry and wet climate conditions, while the worst management strategy can make a difference of 187.7 kg/ha between the dry and wet conditions. An extra depletion of 0.3 m (1 ft) takes place in water table elevation on average over 30 years for the dry condition in comparison to water table elevation for the wet condition under the best management strategy, with a range of difference from -1.2 m (3.9 ft) to 2.4 m (7.9 ft). For the worst management strategy, the wet climate condition is conducive to save 3.4 m (11.2 ft) of groundwater resources in depth on average during 30 years more than water table elevation under the dry climate condition, with a range of difference from 0.2 m (0.7 ft) to 4.6 m (15.1 ft).

For winter wheat (Fig. 4-13C), the best management strategy produces 1,954 kg/ha more in yield of and consumes 5.8 m (19 ft) of groundwater less on average over 30 years than by the worst management strategy under the dry climate condition, while under the wet climate condition, the best strategy produces 1358 kg/ha more and avoids extra groundwater depletion of 11.1 m (36.4 ft) on average during the 30 years. 207 kg/ha more is produced for winter wheat under the wet condition than under the dry condition with the application of the best strategy; similarly, an average extra groundwater depletion of 1.8 m (5.9 ft) is taken place under the dry

climate condition in comparison with the water level under the wet climate condition, under the best management strategy. Under the application of the worst management strategies, the wet climate condition provides 804 kg/ha more and 3.6 m less in groundwater decline compared to those under the dry climate condition. Similar patterns occur for Sorghum (Fig. 4-13D). The best management strategy, as compared to the worst strategy, produces 114 kg/ha more for the dry climate condition and 323 kg/ha for the wet climate condition, and 7.1 m and 8.0 m less in groundwater decline.

4.4 SUMMARY AND CONCLUSIONS

This chapter uses a calibrated linked DSSAT-MODFLOW hydro-agronomic model to identify effective management strategies under future climate conditions in Finney County, Kansas, a semi-arid, groundwater-irrigated region of the High Plains Aquifer, USA. The DSSAT-MODFLOW model simulates crop growth, soil dynamics, and groundwater processes, with targeted state variables of crop yield (corn, soybean, winter wheat, sorghum) and groundwater drawdown. Strategies include irrigation type (surface, drip, sprinkler, center pivot) and planting level (full field, half field, quarter field). Climate conditions include wet, average, and dry trends, filtered from a set of 20 GCMs temporally downscaled to daily precipitation and temperature using the MACA dataset for both RCP 4.5 and RCP 8.5. Effective management strategies maximize crop yield while minimizing groundwater drawdown.

Conclusions from this chapter are:

- If current ("as-is") management strategies are used in future decades (i.e., years of 2021 to 2050), climate impacts include: i) the wettest predicted future climate results in a water table drawdown of 8 m over 30 years (0.3 m/yr), equal to approximately 20% of the current groundwater storage in the regional aquifer, whereas the driest climate results

in drawdowns of 32 m (1.1 m/yr), equal to approximately 80% of the current groundwater storage. Average conditions results in saturated thickness declines of 20% to 50% over the 30-year period. ii) average crop yields are maintained to near current production, but with a high degree of uncertainty.

- To maintain adequate crop yields (i.e., current production), groundwater levels will decline no matter the type of irrigation system (sprinkler, drip, center pivot) and no matter the cultivation level (quarter-plot, half-plot, full-plot).
- If future climate conditions are wet but conform to the assumptions of the RCP8.5 carbon emission scenario, then likely there are no viable management practices that can maintain adequate corn yield. However, there are multiple irrigation/planting combinations that will suffice for soybean, sorghum, and winter wheat. Therefore, under a future of high carbon emissions, corn cultivation may transfer to other crop types.
- For both dry and wet future climates, the best strategy is a combination of drip irrigation systems (i.e., high efficiency irrigation system) and quarter-cultivated plots. These strategies maintain adequate crop yield and conserve groundwater (< 0.5 m drawdown per year).
- In general, the best strategies under a dry climate and wet climate yield the same temporal pattern in water table elevation, but for corn, winter wheat, and sorghum, higher crop yields for the wet climate; for soybean, the trendline of yield fluctuates between the dry and wet climate conditions. In addition, for average crop yields over 30 years, yields of corn, soybean, winter wheat, and sorghum can be produced more 871 kg/ha, 92 kg/ha, 207 kg/ha, and 272 kg/ha, respectively, under the wet climate. The best strategy during a wet future climate, i.e., the scenario that provides the lowest use of groundwater for the

highest crop yield, still results in drawdowns of approximately 9.2 m (30.2 ft), 14.9 m (48.9 ft), 7.3 m (23.9 ft), and 8.2 m (26.9 ft) for areas of corn-related, soybean-related, winter wheat-related, and sorghum-related, respectively, during 2021-2050. Therefore, if crop yields are to be maintained in Finney County and similar regions in the High Plains Aquifer, groundwater storage can only be conserved, not sustained.

- Identifying management strategies should be focused on local (field-scale) conditions.

Climate change is markedly affecting the hydro-agronomic system (e.g., crop yields, water table elevation, groundwater storage, etc.), and this chapter implies that smaller crop areas/fields and higher irrigation efficiency is a useful combination to resist climate change, especially for future dry climate trends, and to have more crop yield and consume less groundwater regionally. Further, this chapter provides another implication that is a trade-off between plant levels (i.e., plant area) and irrigation system under different future climate patterns, which is conducive to solve the real-world issues since the ideal scenario cannot be achieved everywhere. Growers could refer to results of this chapter for their own troubleshooting through having a matchup of issues. This chapter could be used for other groundwater-based irrigated regions, and on condition that it is not available due to the limitations of model framework, researchers could re-build their own framework on a basis of the linked DSSAT-MODFLOW model.

REFERENCES

Abatzoglou, J. T. (2013). Development of gridded surface meteorological data for ecological applications and modelling. *International Journal of Climatology*, *33*(1), 121–131. https://doi.org/10.1002/joc.3413

Abatzoglou, J. T., & Brown, T. J. (2012). A comparison of statistical downscaling methods suited for wildfire applications. *International Journal of Climatology*, *32*(5), 772–780. https://doi.org/10.1002/joc.2312

Aeschbach-Hertig, W., & Gleeson, T. (2012). Regional strategies for the accelerating global problem of groundwater depletion. *Nature Geoscience*, *5*(12), 853–861. https://doi.org/10.1038/ngeo1617

Aliyari, F., Bailey, R. T., & Arabi, M. (2021). Appraising climate change impacts on future water resources and agricultural productivity in agro-urban river basins. *Science of the Total Environment*, *788*. https://doi.org/10.1016/j.scitotenv.2021.147717

Araya, A., Kisekka, I., Gowda, P. H., & Prasad, P. V. V. (2017). Evaluation of water-limited cropping systems in a semi-arid climate using DSSAT-CSM. *Agricultural Systems*, *150*, 86–98. https://doi.org/10.1016/j.agsy.2016.10.007

Arnold, J. G., Srinivasan, R., Muttiah, R. S., & Williams2, J. R. (1998). LARGE AREA HYDROLOGIC MODELING AND ASSESSMENT PART I: MODEL DEVELOPMENT. *JOURNAL OF THE AMERICAN WATER RESOURCES ASSOCIATION*, *34*, 73–89.

Audsley, E., Pearn, K. R., Simota, C., Cojocaru, G., Koutsidou, E., Rounsevell, M. D. A., et al. (2006). What can scenario modelling tell us about future European scale agricultural land use, and what not? *Environmental Science and Policy*, *9*(2), 148–162. https://doi.org/10.1016/j.envsci.2005.11.008

Bailey, R. T., Wible, T. C., Arabi, M., Records, R. M., & Ditty, J. (2016). Assessing regional-scale spatio-temporal patterns of groundwater–surface water interactions using a coupled SWAT-MODFLOW model. *Hydrological Processes*, *30*(23), 4420–4433. https://doi.org/10.1002/hyp.10933

Candela, L., Elorza, F. J., Jiménez-Martínez, J., & von Igel, W. (2012). Global change and agricultural management options for groundwater sustainability. *Computers and Electronics in Agriculture*, *86*, 120–130. https://doi.org/10.1016/j.compag.2011.12.012

Carter, R. C., & Parker, A. (2009). Climate change, population trends and groundwater in Africa. *Hydrological Sciences Journal*, *54*(4), 676–689. https://doi.org/10.1623/hysj.54.4.676

Cuthbert, M. O., Gleeson, T., Moosdorf, N., Befus, K. M., Schneider, A., Hartmann, J., & Lehner, B. (2019). Global patterns and dynamics of climate–groundwater interactions. *Nature Climate Change*, *9*(2), 137–141. https://doi.org/10.1038/s41558-018-0386-4

Deng, C., & Bailey, R. T. (2017). Assessing groundwater availability of the Maldives under future climate conditions. *Hydrological Processes*, *31*(19), 3334–3349. https://doi.org/10.1002/hyp.11246

Deryng, D., Sacks, W. J., Barford, C. C., & Ramankutty, N. (2011). Simulating the effects of climate and agricultural management practices on global crop yield. *Global Biogeochemical Cycles*, *25*(2), n/a-n/a. https://doi.org/10.1029/2009gb003765

Ewert, F., Rounsevell, M. D. A., Reginster, I., Metzger, M. J., & Leemans, R. (2005). Future scenarios of European agricultural land use: I. Estimating changes in crop productivity. *Agriculture, Ecosystems and Environment*, *107*(2–3), 101–116. https://doi.org/10.1016/j.agee.2004.12.003

Famiglietti, J. S. (2014). The global groundwater crisis. *Nature Climate Change*, *4*(11), 945–948. https://doi.org/10.1038/nclimate2425

Farhadi, S., Nikoo, M. R., Rakhshandehroo, G. R., Akhbari, M., & Alizadeh, M. R. (2016). An agent-based-nash modeling framework for sustainable groundwater management: A case study. *Agricultural Water Management*, *177*, 348–358. https://doi.org/10.1016/j.agwat.2016.08.018

Feng, W., Zhong, M., Lemoine, J. M., Biancale, R., Hsu, H. T., & Xia, J. (2013). Evaluation of groundwater depletion in North China using the Gravity Recovery and Climate Experiment (GRACE) data and ground-based measurements. *Water Resources Research*, *49*(4), 2110–2118. https://doi.org/10.1002/wrcr.20192

Foster, Timothy, Brozović, N., & Butler, A. P. (2014). Modeling irrigation behavior in groundwater systems. *Water Resources Research*, *50*(8), 6370–6389. https://doi.org/10.1002/2014WR015620

Gaisheng Liu, Brownie Wilson, Donald Whittemore, Wei Jin, and James Butler, J. (2011). *Ground-Water Model for Southwest Kansas Groundwater Management District No. 3* (Vol. 0110). Retrieved from http://www.kgs.ku.edu/Hydro/Publications/2010/OFR10_18/index.html

Gorelick, S. M., & Zheng, C. (2015). Global change and the groundwater management challenge. *Water Resources Research*, 3031–3051. https://doi.org/10.1002/2014WR016825

Grönwall, J., & Danert, K. (2020). Regarding Groundwater and Drinking Water Access through A Human Rights Lens: Self-Supply as A Norm. Water, 12, 419. https://doi.org/10.3390/w12020419

Grundy, M. J., Bryan, B. A., Nolan, M., Battaglia, M., Hatfield-Dodds, S., Connor, J. D., & Keating, B. A. (2016). Scenarios for Australian agricultural production and land use to 2050. *Agricultural Systems*, *142*, 70–83. https://doi.org/10.1016/j.agsy.2015.11.008

Haacker, E. M. K., Kendall, A. D., & Hyndman, D. W. (2016). Water Level Declines in the High Plains Aquifer: Predevelopment to Resource Senescence. *Groundwater*, *54*(2), 231–242. https://doi.org/10.1111/gwat.12350

Hadded, R., Nouiri, I., Alshihabi, O., Maßmann, J., Huber, M., Laghouane, A., et al. (2013). A Decision Support System to Manage the Groundwater of the Zeuss Koutine Aquifer Using the WEAP-MODFLOW Framework. *Water Resources Management*, *27*(7), 1981–2000. https://doi.org/10.1007/s11269-013-0266-7

Harbaugh, A. W. (2005). *MODFLOW-2005, the US Geological Survey modular ground-water model: the ground-water flow process*. US Department of the Interior, US Geological Survey Reston, VA.

Holman, I. P., Allen, D. M., Cuthbert, M. O., & Goderniaux, P. (2012). Towards best practice for assessing the impacts of climate change on groundwater. *Hydrogeology Journal*, *20*(1), 1–4. https://doi.org/10.1007/s10040-011-0805-3

Huang, Q., Wang, J., Rozelle, S., Polasky, S., & Liu, Y. (2013). The effects of well management and the nature of the aquifer on groundwater resources. *American Journal of Agricultural Economics*, *95*(1), 94–116. https://doi.org/10.1093/ajae/aas076

Jha, M. K., Chowdhury, A., Chowdary, V. M., & Peiffer, S. (2007). Groundwater management and development by integrated remote sensing and geographic information systems: Prospects and constraints. *Water Resources Management*, *21*(2), 427–467. https://doi.org/10.1007/s11269-006-9024-4

Jones, J. W., Hoogenboom, G., Porter, C. H., Boote, K. J., Batchelor, W. D., Hunt, L. A., et al. (2003). *The DSSAT cropping system model*. Retrieved from www.elsevier.com/locate/eja

Kadiyala, M. D. M., Nedumaran, S., Singh, P., S., C., Irshad, M. A., & Bantilan, M. C. S. (2015). An integrated crop model and GIS decision support system for assisting agronomic decision making under climate change. *Science of the Total Environment*, *521–522*, 123–134. https://doi.org/10.1016/j.scitotenv.2015.03.097

Kihara, J., Tamene, L. D., Massawe, P., & Bekunda, M. (2015). Agronomic survey to assess crop yield, controlling factors and management implications: a case-study of Babati in northern Tanzania. *Nutrient Cycling in Agroecosystems*, *102*(1), 5–16. https://doi.org/10.1007/s10705-014-9648-3

Klaas, D. K. S. Y., Imteaz, M. A., Sudiayem, I., Klaas, E. M. E., & Klaas, E. C. M. (2020). Assessing climate changes impacts on tropical karst catchment: Implications on groundwater resource sustainability and management strategies. *Journal of Hydrology*, *582*. https://doi.org/10.1016/j.jhydrol.2019.124426

Kløve, B., Ala-Aho, P., Bertrand, G., Gurdak, J. J., Kupfersberger, H., Kværner, J., et al. (2014). Climate change impacts on groundwater and dependent ecosystems. *Journal of Hydrology*, *518*(PB), 250–266. https://doi.org/10.1016/j.jhydrol.2013.06.037

Konikow, L. F. (2011). Contribution of global groundwater depletion since 1900 to sea-level rise. *Geophysical Research Letters*, *38*(17). https://doi.org/10.1029/2011GL048604

Konikow, L. F. (2015). Long-Term Groundwater Depletion in the United States. *Groundwater*, *53*(1), 2–9. https://doi.org/10.1111/gwat.12306

Konikow, L. F., & Kendy, E. (2005). Groundwater depletion: A global problem. *Hydrogeology Journal*, *13*(1), 317–320. https://doi.org/10.1007/s10040-004-0411-8

Kumar, C. P. (2012). Climate Change and Its Impact on Groundwater Resources. *RESEARCH INVENTY: International Journal of Engineering and Science*, *1*(5), 43–60. Retrieved from www.researchinventy.com

Lall, U., Josset, L., & Russo T. (2020). A Snapshot of the World's Groundwater Challenges. *Annual Review of Environment and Resources*, 45: 171-194. https://doi.org/10.1146/annurev-environ-102017-025800

Manghi, F., Williams, D., Safely, J., & Hamdi, M. R. (2012). Groundwater Flow Modeling of the Arlington Basin to Evaluate Management Strategies for Expansion of the Arlington Desalter Water Production. *Water Resources Management*, *26*(1), 21–41. https://doi.org/10.1007/s11269-011-9899-6

Masciopinto, C., & Liso, I. S. (2016). Assessment of the impact of sea-level rise due to climate change on coastal groundwater discharge. *Science of the Total Environment*, *569–570*, 672–680. https://doi.org/10.1016/j.scitotenv.2016.06.183

McCallum, J. L., Crosbie, R. S., Walker, G. R., & Dawes, W. R. (2010). Impacts of climate change on groundwater in Australia: A sensitivity analysis of recharge. *Hydrogeology Journal*, *18*(7), 1625–1638. https://doi.org/10.1007/s10040-010-0624-y

Mishra, N. (2014). Impact of Land Use Change on Groundwater-A Review. Retrieved from www.seipub.org/awrp

Motagh, M., Walter, T. R., Sharifi, M. A., Fielding, E., Schenk, A., Anderssohn, J., & Zschau, J. (2008). Land subsidence in Iran caused by widespread water reservoir overexploitation. *Geophysical Research Letters*, *35*(16). https://doi.org/10.1029/2008GL033814

Ni, X., & Parajuli, P. B. (2018). Evaluation of the impacts of BMPs and tailwater recovery system on surface and groundwater using satellite imagery and SWAT reservoir function. *Agricultural Water Management*, *210*, 78–87. https://doi.org/10.1016/j.agwat.2018.07.027

Parry, M. L., Rosenzweig, C., Iglesias, A., Livermore, M., & Fischer, G. (2004). Effects of climate change on global food production under SRES emissions and socio-economic

scenarios. *Global Environmental Change*, *14*(1), 53–67. https://doi.org/10.1016/j.gloenvcha.2003.10.008

Sekhar, M., Shindekar, M., Tomer, S. K., & Goswami, P. (2013). Modeling the vulnerability of an urban groundwater system due to the combined impacts of climate change and management scenarios. *Earth Interactions*, *17*(10). https://doi.org/10.1175/2012EI000499.1

Siebert, S., Burke, J., Faures, J. M., Frenken, K., Hoogeveen, J., Döll, P., & Portmann, F. T. (2010). Groundwater use for irrigation - A global inventory. *Hydrology and Earth System Sciences*, *14*(10), 1863–1880. https://doi.org/10.5194/hess-14-1863-2010

Singh, A. (2013). Groundwater modelling for the assessment of water management alternatives. *Journal of Hydrology*, *481*, 220–229. https://doi.org/10.1016/j.jhydrol.2012.12.042

Tang, J., Wang, J., Fang, Q., Dayananda, B., Yu, Q., Zhao, P., et al. (2019). Identifying agronomic options for better potato production and conserving water resources in the agro-pastoral ecotone in North China. *Agricultural and Forest Meteorology*, *272–273*, 91–101. https://doi.org/10.1016/j.agrformet.2019.04.001

Varela-Ortega, C., Blanco-Gutiérrez, I., Swartz, C. H., & Downing, T. E. (2011). Balancing groundwater conservation and rural livelihoods under water and climate uncertainties: An integrated hydro-economic modeling framework. *Global Environmental Change*, *21*(2), 604–619. https://doi.org/10.1016/j.gloenvcha.2010.12.001

Ventrella, D., Charfeddine, M., Moriondo, M., Rinaldi, M., & Bindi, M. (2012). Agronomic adaptation strategies under climate change for winter durum wheat and tomato in southern Italy: Irrigation and nitrogen fertilization. *Regional Environmental Change*, *12*(3), 407–419. https://doi.org/10.1007/s10113-011-0256-3

Voss, K. A., Famiglietti, J. S., Lo, M., de Linage, C., Rodell, M., & Swenson, S. C. (2013). Groundwater depletion in the Middle East from GRACE with implications for transboundary water management in the Tigris-Euphrates-Western Iran region. *Water Resources Research*, *49*(2), 904–914. https://doi.org/10.1002/wrcr.20078

Wada, Y., van Beek, L. P. H., van Kempen, C. M., Reckman, J. W. T. M., Vasak, S., & Bierkens, M. F. P. (2010). Global depletion of groundwater resources. *Geophysical Research Letters*, *37*(20). https://doi.org/10.1029/2010GL044571

Werner, A. D. (2010). A review of seawater intrusion and its management in AustraliaUne étude de l'intrusion d'eau de mer en Australie et de sa gestionUna revisión de la intrusión de agua de mar y su gestión en Australia**澳大利**亚海水入侵及其管理的综述Análise da intrusão salina e sua gestão na. *Hydrogeology Journal*, *18*(1), 281–285. https://doi.org/10.1007/s10040-009-0465-8

Williams, J. R., Jones, C. A., Kiniry, J. R., & Spanel, D. A. (1989). The EPIC Crop Growth Model. *Transactions of the ASAE*, *32*(2), 497–511.

Xiang, Z., Bailey, R. T., Nozari, S., Husain, Z., Kisekka, I., Sharda, V., & Gowda, P. (2020). DSSAT-MODFLOW: A new modeling framework for exploring groundwater conservation strategies in irrigated areas. *Agricultural Water Management*, *232*. https://doi.org/10.1016/j.agwat.2020.106033

Xiong, W., Conway, D., Lin, E., Xu, Y., Ju, H., Jiang, J., et al. (2009). Future cereal production in China: The interaction of climate change, water availability and socio-economic scenarios. *Global Environmental Change*, *19*(1), 34–44. https://doi.org/10.1016/j.gloenvcha.2008.10.006

Xu, X., Huang, G., Zhan, H., Qu, Z., & Huang, Q. (2012). Integration of SWAP and MODFLOW-2000 for modeling groundwater dynamics in shallow water table areas. *Journal of Hydrology*, *412–413*, 170–181. https://doi.org/10.1016/j.jhydrol.2011.07.002

Zhang, Y., Gong, H., Gu, Z., Wang, R., Li, X., & Zhao, W. (2014). Characterization of land subsidence induced by groundwater withdrawals in the plain of Beijing city, ChinaCaractérisation de la subsidence induite par les prélèvements d'eaux souterraines dans la plaine de Pékin, ChineCaracterización de la subsidencia del. *Hydrogeology Journal*, *22*(2), 397–409. https://doi.org/10.1007/s10040-013-1069-x

Zhao, Z., Qin, X., Zang, H., Chen, C., Zhang, Y., & Wang, Z. (2017). Value of groundwater used for producing extra grain in North China Plain. *Field Crops Research*, *210*, 47–51. https://doi.org/10.1016/j.fcr.2017.05.022

CHAPTER 5 – SUMMARY AND CONCLUSIONS

5.1 SUMMARY

This dissertation first presents a linked DSSAT-MODFLOW modeling framework and applied it to the Ogallala aquifer within Finney County, Kansas, a region experiencing significant groundwater depletion due to irrigation practices. The linkage between the models occurs on an annual time step, with irrigation depths from an ensemble of field-scale DSSAT simulations (DSSAT version 4.7) converted to pumping rates for the MODFLOW simulation (MODFLOW 2000). The MODFLOW simulates groundwater head, which can be used to update saturated thickness and thereby well capacities for each pumping well in the model domain. Well capacities are then used to constrain irrigation application in the DSSAT simulations during the following growing season. Python scripts are used to pass information between the two models and prepare input files. Batch files for DSSAT are used to run the ensemble of simulations for each year. Model results are tested against water table elevation and crop yield.

After the development of the linked hydro-agronomic modeling system, two sensitivity analyses (i.e., Morris screening method and Sobol' variance-based method) were applied to the groundwater-irrigated hydro-agronomic system to assess the governing system factors on crop yield and groundwater storage. The DSSAT-MODFLOW linked modeling system was used as the simulator. A combination of Python scripts and SimLab pre- and post-processing were used to generate parameter values, update model files for DSSAT and MODFLOW, run the model simulations, and calculate sensitivity indices for both the Morris method and the Sobol' method. 57 parameters were reduced to 24 parameters after the Morris screening method, and the sensitivity of 28 parameters (including 4 climate-related parameters) were analyzed on 10 model

responses (i.e., maize yield, soybean yield, winter wheat yield, sorghum yield, water table elevation, ET, recharge, irrigation pumping, river leakage, and aquifer seepage) using Sobol' variance-based sensitivity analysis.

Last, this dissertation uses a calibrated linked DSSAT-MODFLOW hydro-agronomic model to identify effective management strategies under future climate conditions in Finney County, Kansas, a semi-arid, groundwater-irrigated region of the High Plains Aquifer, USA. The DSSAT-MODFLOW model simulates crop growth, soil dynamics, and groundwater processes, with targeted state variables of crop yield (corn, soybean, winter wheat, sorghum) and groundwater drawdown. Strategies include irrigation type (surface, drip, sprinkler, center pivot) and planting level (full field, half field, quarter field). Climate conditions include wet, average, and dry trends, filtered from a set of 20 GCMs temporally downscaled to daily precipitation and temperature using the MACA dataset for both RCP 4.5 and RCP 8.5. Effective management strategies maximize crop yield while minimizing groundwater drawdown.

5.2 MAJOR FINDINGS

Major findings from this dissertation, as summarized in the last section of Chapters 2, 3, and 4, are:

1) climate-related parameters significantly affect crop yields, especially for maize and sorghum, and soybean and winter wheat yields are sensitive to a combination of cultivar genetic parameters, soil-related parameters, and climate-related parameters;

2) Climatic parameters account for 44%, 29%, 40%, and 36% variation in yield of maize, soybean, winter wheat, and sorghum;

3) Hydrogeologic parameters (aquifer hydraulic conductivity, aquifer specific yield, and riverbed conductance) have a relatively low influence on crop yields;

4) Water table elevation, recharge, and irrigation pumping are considerably sensitive to soil- and climate-related parameters, while ET, river leakage, and aquifer seepage are highly influenced by hydrogeological parameter (e.g., riverbed conductance, and specific yield);

5) Soil parameters accounted for 44%, 20%, 50%, and 34% variation in water table elevation, ET, recharge, and irrigation pumping;

6) For the dry and wet future climate conditions, the best management practice is the combination of the drip irrigation system (i.e., high efficiency irrigation system) and the plant level 3 (i.e., quarter-plots);

7) crop yields are to be maintained in Finney County and similar regions in the High Plains Aquifer, but groundwater storage can only be conserved, not sustained.

5.3 FUTURE RESEARCH

Currently, the linked model does not simulate water movement in the vadose zone, i.e., between the bottom of the soil layer and the top of water table. In the current system, deep percolation from the bottom of the soil profile, as simulated by DSSAT, and precipitation-based recharge, as simulated by a power function, are assumed to reach the water table instantaneously. Future versions of the modeling system could use the UZF (Unsaturated Zone Flow) package of MODFLOW to route the near-surface percolation water to the water table.

The linked hydro-agronomic modeling system can be applied to other groundwater-based irrigation regions to evaluate management practices under different climate conditions. In addition, the modeling framework can be linked with other models to create a novel tool to improve model performance and solve real-world issue, with comprehensive consideration of factor within a system. For example, the DSSAT-MODFLOW model can be linked with an

economic model that would simulate human planting decisions, considering available groundwater storage, weather patterns, and maximizing profit.

```
$BATCH(SPATIAL)
!
! Directory    : Finney
! Command Line : C:\DSSAT47\DSCSM047.EXE s DSSBatch_FC.v47
! Crop         : Spatial
! Experiment   : KSFY1701.GSX
! ExpNo        : 1
! Debug        : C:\DSSAT47\DSCSM047.EXE " S DSSBatch.v47"
!
@FILEX                                                                                  TRTNO     RP     SQ     OP     CO
Finney\KSFY1701.GSX                                                                         1      1      0      0      0
Finney\KSFY1701.GSX                                                                         2      1      0      0      0
Finney\KSFY1701.GSX                                                                         3      1      0      0      0
Finney\KSFY1701.GSX                                                                         4      1      0      0      0
Finney\KSFY1701.GSX                                                                         5      1      0      0      0
Finney\KSFY1701.GSX                                                                         6      1      0      0      0
Finney\KSFY1701.GSX                                                                         7      1      0      0      0
Finney\KSFY1701.GSX                                                                         8      1      0      0      0
Finney\KSFY1701.GSX                                                                         9      1      0      0      0
Finney\KSFY1701.GSX                                                                        10      1      0      0      0
Finney\KSFY1701.GSX                                                                        11      1      0      0      0
Finney\KSFY1701.GSX                                                                        12      1      0      0      0
Finney\KSFY1701.GSX                                                                        13      1      0      0      0
Finney\KSFY1701.GSX                                                                        14      1      0      0      0
Finney\KSFY1701.GSX                                                                        15      1      0      0      0
Finney\KSFY1701.GSX                                                                        16      1      0      0      0
Finney\KSFY1701.GSX                                                                        17      1      0      0      0
Finney\KSFY1701.GSX                                                                        18      1      0      0      0
Finney\KSFY1701.GSX                                                                        19      1      0      0      0
Finney\KSFY1701.GSX                                                                        20      1      0      0      0
Finney\KSFY1701.GSX                                                                        21      1      0      0      0
Finney\KSFY1701.GSX                                                                        22      1      0      0      0
Finney\KSFY1701.GSX                                                                        23      1      0      0      0
Finney\KSFY1701.GSX                                                                        24      1      0      0      0
Finney\KSFY1701.GSX                                                                        25      1      0      0      0
Finney\KSFY1701.GSX                                                                        26      1      0      0      0
Finney\KSFY1701.GSX                                                                        27      1      0      0      0
Finney\KSFY1701.GSX                                                                        28      1      0      0      0
Finney\KSFY1701.GSX                                                                        29      1      0      0      0
Finney\KSFY1701.GSX                                                                        30      1      0      0      0
Finney\KSFY1701.GSX                                                                        31      1      0      0      0
Finney\KSFY1701.GSX                                                                        32      1      0      0      0
Finney\KSFY1701.GSX                                                                        33      1      0      0      0
Finney\KSFY1701.GSX                                                                        34      1      0      0      0
Finney\KSFY1701.GSX                                                                        35      1      0      0      0
Finney\KSFY1701.GSX                                                                        36      1      0      0      0
Finney\KSFY1701.GSX                                                                        37      1      0      0      0
Finney\KSFY1701.GSX                                                                        38      1      0      0      0
Finney\KSFY1701.GSX                                                                        39      1      0      0      0
Finney\KSFY1701.GSX                                                                        40      1      0      0      0
Finney\KSFY1701.GSX                                                                        41      1      0      0      0
Finney\KSFY1701.GSX                                                                        42      1      0      0      0
Finney\KSFY1701.GSX                                                                        43      1      0      0      0
Finney\KSFY1701.GSX                                                                        44      1      0      0      0
Finney\KSFY1701.GSX                                                                        45      1      0      0      0
Finney\KSFY1701.GSX                                                                        46      1      0      0      0
Finney\KSFY1701.GSX                                                                        47      1      0      0      0
Finney\KSFY1701.GSX                                                                        48      1      0      0      0
Finney\KSFY1701.GSX                                                                        49      1      0      0      0
Finney\KSFY1701.GSX                                                                        50      1      0      0      0
Finney\KSFY1701.GSX                                                                        51      1      0      0      0
Finney\KSFY1701.GSX                                                                        52      1      0      0      0
Finney\KSFY1701.GSX                                                                        53      1      0      0      0
Finney\KSFY1701.GSX                                                                        54      1      0      0      0
Finney\KSFY1701.GSX                                                                        55      1      0      0      0
Finney\KSFY1701.GSX                                                                        56      1      0      0      0
Finney\KSFY1701.GSX                                                                        57      1      0      0      0
Finney\KSFY1701.GSX                                                                        58      1      0      0      0
Finney\KSFY1701.GSX                                                                        59      1      0      0      0
Finney\KSFY1701.GSX                                                                        60      1      0      0      0
```

Fig. 2-S1 The structure of a batch file to run DSSAT model using .GSX input file.

```
*CULTIVARS
@C CR INGENO CNAME
 1 WH IB0491 FINNEY

*FIELDS
@L  ID_FIELD WSTA....   FLSA   FLOB   FLDT   FLDD   FLDS   FLST SLTX  SLDP   ID_SOIL     FLNAME
 1  KSFY0001 GRGR         -99      0 DR000      0      0 00000 -99    180   KSFC000002 -99
 2  FLSC0002 GRGR         -99      0 DR000      0      0 00000 -99    180   KSFC000007 -99
 3  FLSC0003 GRGR         -99      0 DR000      0      0 00000 -99    180   KSFC000002 -99
 4  FLSC0004 GRGR         -99      0 DR000      0      0 00000 -99    180   KSFC000002 -99
 5  FLSC0005 GRGR         -99      0 DR000      0      0 00000 -99    180   KSFC000007 -99
 6  FLSC0006 GRGR         -99      0 DR000      0      0 00000 -99    180   KSFC000002 -99
 7  FLSC0007 GRGR         -99      0 DR000      0      0 00000 -99    180   KSFC000002 -99
 8  FLSC0008 GRGR         -99      0 DR000      0      0 00000 -99    180   KSFC000002 -99
 9  FLSC0009 GRGR         -99      0 DR000      0      0 00000 -99    180   KSFC000007 -99
10  FLSC0010 GRGR         -99      0 DR000      0      0 00000 -99    180   KSFC000004 -99
11  FLSC0011 GRGR         -99      0 DR000      0      0 00000 -99    180   KSFC000001 -99
12  FLSC0012 GRGR         -99      0 DR000      0      0 00000 -99    180   KSFC000007 -99
13  FLSC0013 GRGR         -99      0 DR000      0      0 00000 -99    180   KSFC000006 -99
14  FLSC0014 GRGR         -99      0 DR000      0      0 00000 -99    180   KSFC000006 -99
15  FLSC0015 GRGR         -99      0 DR000      0      0 00000 -99    180   KSFC000007 -99
16  FLSC0016 GRGR         -99      0 DR000      0      0 00000 -99    180   KSFC000002 -99
17  FLSC0017 GRGR         -99      0 DR000      0      0 00000 -99    180   KSFC000002 -99
18  FLSC0018 GRGR         -99      0 DR000      0      0 00000 -99    180   KSFC000004 -99
19  FLSC0019 GRGR         -99      0 DR000      0      0 00000 -99    180   KSFC000001 -99
20  FLSC0020 GRGR         -99      0 DR000      0      0 00000 -99    180   KSFC000001 -99

*INITIAL CONDITIONS
@C    PCR ICDAT  ICRT  ICND  ICRN  ICRE  ICWD ICRES ICREN ICREP ICRIP ICRID ICNAME
 1     WH 01280  1200     0     1     1   -99  6500  1.14     0   100    15 -99
@C   ICBL   SH2O  SNH4  SNO3
 1     15   .205   3.4   9.8
 1     30    .17   3.2   7.3
 1     60   .092   2.5   5.1
 1     90   .065   2.2   4.7
 1    120   .066   2.7   4.3
 1    150   .066   2.7   4.3
 1    180   .066   2.7   4.3

*PLANTING DETAILS
@P PDATE EDATE  PPOP  PPOE  PLME  PLDS  PLRS  PLRD  PLDP  PLWT  PAGE  PENV  PLPH  SPRL
 1 01290   -99   162   162     S     R    16     0   5.5   -99   -99   -99   -99     0

*IRRIGATION AND WATER MANAGEMENT
@I  EFIR  IDEP  ITHR  IEPT  IOFF  IAME  IAMT IRNAME
 1     0   -99   -99   -99   -99   -99   -99
@I IDATE  IROP IRVAL
 1 02096 IR001    65
 1 02110 IR001    78
 1 02117 IR001    70

*FERTILIZERS (INORGANIC)
@F FDATE  FMCD  FACD  FDEP  FAMN  FAMP  FAMK  FAMC  FAMO  FOCD FERNAME
 1 01290 FE001 AP001    15     0     0     0     0     0   -99 -99
 2 01290 FE001 AP001    15    60     0     0     0     0   -99 -99
 3 01290 FE001 AP001    15    90     0     0     0     0   -99 -99
 3 02156 FE001 AP001     1    90     0     0     0     0   -99 -99

*SIMULATION CONTROLS
@N GENERAL     NYERS NREPS START SDATE RSEED SNAME.................... SMODEL
 1 GE              1     1     S 01125  2150 Wheat Simulation Options
@N OPTIONS     WATER NITRO SYMBI PHOSP POTAS DISES  CHEM  TILL   CO2
 1 OP              Y     N     N     N     N     N     N     N     D
@N METHODS     WTHER INCON LIGHT EVAPO INFIL PHOTO HYDRO NSWIT MESOM MESEV MESOL
 1 ME              M     M     E     F     S     L     R     1     G     S     2
@N MANAGEMENT  PLANT IRRIG FERTI RESID HARVS
 1 MA              R     F     N     N     M
@N OUTPUTS     FNAME OVVEW SUMRY FROPT GROUT CAOUT WAOUT NIOUT MIOUT DIOUT VBOSE CHOUT OPOUT FMOPT
 1 OU              F     N     Y     1     N     N     Y     N     N     N     Y     N     N     A

@  AUTOMATIC MANAGEMENT
@N PLANTING    PFRST PLAST PH2OL PH2OU PH2OD PSTMX PSTMN
 1 PL          00001 00001    40   100    30    40    10
@N IRRIGATION  IMDEP ITHRL ITHRU IROFF IMETH IRAMT IREFF AVWAT IFREQ AIName
 1 IR             30    50   100 GS000 IR001    25     1  -99   0.01  Sowing date
@N NITROGEN    NMDEP NMTHR NAMNT NCODE NAOFF
 1 NI             30    50    25 IB001 IB001
@N RESIDUES    RIPCN RTIME RIDEP
 1 RE              0     0     0
@N HARVEST     HFRST HLAST HPCNP HPCNR
 1 HA              0 00001   100     0
```

Fig. 2-S2 The structure of the .GSX input file, including soil type, cultivar type, planting schedule, and irrigation method.

*SOIL WATER DAILY OUTPUT FILE

*DSSAT Cropping System Model Ver. 4.7.1.001 -release DEC 30, 2019; 13:33:29

*RUN 1 : 301 MZCER047 KSFY0121 1
MODEL : MZCER047 - Maize
EXPERIMENT : KSFY0121 GS SPATIAL ANALYSES CORN
DATA PATH : Finney\
TREATMENT 1 : 301 MZCER047

														Soil water content (mm3/mm3) by soil depth (cm):								
!														0-5	5-15	15-20	20-28	28-36	36-48	48-59	59-71	71-136	136-201
@YEAR	DOY	DAS	SWTD	SWXD	ROFC	DRNC	PREC	IR#C	IRRC	DTWT	MWTD	TDFD	TDFC	ROFD	SW1D	SW2D	SW3D	SW4D	SW5D	SW6D	SW7D	SW8D	SW9D	SW10
2001	124	0	474	121	0	0	0	0	0	0	0.00	0.0	0.0	0.00	0.203	0.203	0.203	0.203	0.262	0.282	0.282	0.228	0.232	0.236
2001	125	1	474	120	0	0	0	0	0	51	0.00	0.0	0.0	0.00	0.195	0.202	0.203	0.203	0.262	0.282	0.282	0.228	0.232	0.236
2001	126	2	497	144	0	0	0	1	25	201	0.00	0.0	0.0	0.00	0.398	0.337	0.202	0.203	0.262	0.282	0.282	0.228	0.232	0.236
2001	127	3	519	165	0	0	2	2	50	201	0.00	0.0	0.0	0.00	0.394	0.410	0.414	0.276	0.259	0.279	0.280	0.227	0.231	0.235
2001	128	4	514	161	0	0	2	2	50	201	0.00	0.0	0.0	0.00	0.390	0.401	0.403	0.284	0.257	0.277	0.277	0.225	0.229	0.233
2001	129	5	510	156	0	0	2	2	50	201	0.00	0.0	0.0	0.00	0.387	0.398	0.399	0.282	0.255	0.274	0.275	0.223	0.227	0.231
2001	130	6	508	155	0	0	2	2	50	201	0.00	0.0	0.0	0.00	0.354	0.395	0.399	0.282	0.255	0.274	0.275	0.223	0.227	0.231
2001	131	7	506	153	0	0	2	2	50	201	0.00	0.0	0.0	0.00	0.325	0.393	0.398	0.281	0.254	0.274	0.275	0.223	0.227	0.231
2001	132	8	504	151	0	0	2	2	50	201	0.00	0.0	0.0	0.00	0.299	0.391	0.397	0.281	0.254	0.274	0.275	0.223	0.227	0.231
2001	133	9	503	150	0	0	2	2	50	201	0.00	0.0	0.0	0.00	0.275	0.389	0.396	0.281	0.254	0.274	0.275	0.223	0.227	0.231
2001	134	10	501	148	0	0	2	2	50	201	0.00	0.0	0.0	0.00	0.254	0.387	0.396	0.281	0.254	0.274	0.275	0.223	0.227	0.231
2001	135	11	500	147	0	0	2	2	50	201	0.00	0.0	0.0	0.00	0.234	0.384	0.395	0.280	0.254	0.274	0.275	0.223	0.227	0.231
2001	136	12	500	147	0	0	3	2	50	201	0.00	0.0	0.0	0.00	0.245	0.382	0.394	0.280	0.254	0.274	0.274	0.223	0.227	0.231
2001	137	13	510	157	0	0	15	2	50	201	0.00	0.0	0.0	0.00	0.395	0.404	0.403	0.282	0.254	0.274	0.274	0.223	0.227	0.231
2001	138	14	506	153	0	0	15	2	50	201	0.00	0.0	0.0	0.00	0.391	0.400	0.399	0.279	0.252	0.271	0.272	0.221	0.225	0.229
2001	139	15	540	187	7	0	59	2	50	201	0.00	0.0	0.0	6.62	0.409	0.414	0.416	0.423	0.424	0.325	0.271	0.220	0.224	0.229
2001	140	16	545	192	7	0	70	2	50	201	0.00	0.0	0.0	0.22	0.393	0.408	0.412	0.419	0.421	0.377	0.290	0.219	0.223	0.228
2001	141	17	543	189	7	0	72	2	50	201	0.00	0.0	0.0	0.00	0.395	0.399	0.408	0.406	0.411	0.375	0.306	0.218	0.223	0.227
2001	142	18	538	185	7	0	72	2	50	201	0.00	0.0	0.0	0.00	0.391	0.395	0.400	0.398	0.399	0.367	0.319	0.216	0.221	0.225
2001	143	19	533	180	7	0	72	2	50	201	0.00	0.0	0.0	0.00	0.387	0.391	0.396	0.394	0.396	0.363	0.316	0.214	0.219	0.223
2001	144	20	531	178	7	0	72	2	50	201	0.00	0.0	0.0	0.00	0.353	0.388	0.395	0.393	0.395	0.363	0.316	0.214	0.219	0.223
2001	145	21	529	176	7	0	72	2	50	201	0.00	0.0	0.0	0.00	0.324	0.386	0.394	0.393	0.395	0.363	0.316	0.214	0.219	0.223
2001	146	22	527	174	7	0	72	2	50	201	0.00	0.0	0.0	0.00	0.297	0.383	0.393	0.392	0.395	0.363	0.316	0.214	0.219	0.223
2001	147	23	538	185	7	0	88	2	50	201	0.00	0.0	0.0	0.01	0.418	0.415	0.415	0.415	0.406	0.367	0.318	0.212	0.217	0.222
2001	148	24	532	179	7	0	88	2	50	201	0.00	0.0	0.0	0.00	0.379	0.396	0.399	0.399	0.396	0.363	0.341	0.211	0.216	0.221
2001	149	25	573	220	17	0	142	2	50	201	0.00	0.0	0.0	10.20	0.405	0.413	0.415	0.422	0.423	0.406	0.407	0.374	0.218	0.220
2001	150	26	568	215	17	0	142	2	50	201	0.00	0.0	0.0	0.00	0.379	0.396	0.401	0.402	0.404	0.380	0.380	0.368	0.231	0.220
2001	151	27	563	209	17	0	142	2	50	201	0.00	0.0	0.0	0.00	0.374	0.392	0.396	0.396	0.397	0.369	0.369	0.364	0.233	0.218
2001	152	28	557	204	17	0	142	2	50	201	0.00	0.0	0.0	0.00	0.368	0.386	0.391	0.391	0.393	0.365	0.365	0.361	0.231	0.216
2001	153	29	555	202	17	0	142	2	50	201	0.00	0.0	0.0	0.00	0.335	0.382	0.388	0.390	0.392	0.365	0.365	0.361	0.231	0.216
2001	154	30	553	200	17	0	142	2	50	201	0.00	0.0	0.0	0.00	0.307	0.378	0.387	0.389	0.392	0.365	0.365	0.361	0.231	0.216
2001	155	31	551	198	17	0	143	2	50	201	0.00	0.0	0.0	0.00	0.291	0.375	0.385	0.388	0.391	0.365	0.365	0.361	0.231	0.216
2001	156	32	550	197	17	0	143	2	50	201	0.00	0.0	0.0	0.00	0.276	0.372	0.384	0.387	0.391	0.365	0.365	0.361	0.231	0.216
2001	157	33	549	196	17	0	144	2	50	201	0.00	0.0	0.0	0.00	0.262	0.369	0.381	0.386	0.390	0.365	0.365	0.361	0.231	0.216
2001	158	34	587	234	21	0	190	2	50	201	0.00	0.0	0.0	4.22	0.419	0.415	0.415	0.422	0.422	0.406	0.406	0.400	0.239	0.215
2001	159	35	596	242	22	0	205	2	50	201	0.00	0.0	0.0	0.69	0.394	0.407	0.411	0.419	0.421	0.405	0.406	0.406	0.256	0.214
2001	160	36	589	236	22	0	205	2	50	201	0.00	0.0	0.0	0.00	0.386	0.396	0.398	0.401	0.402	0.378	0.379	0.379	0.270	0.212
2001	161	37	583	229	22	0	205	2	50	201	0.00	0.0	0.0	0.00	0.378	0.388	0.390	0.395	0.394	0.368	0.368	0.368	0.272	0.211
2001	162	38	575	222	22	0	205	2	50	201	0.00	0.0	0.0	0.00	0.367	0.377	0.380	0.387	0.388	0.363	0.365	0.365	0.269	0.209
2001	163	39	571	218	22	0	205	2	50	201	0.00	0.0	0.0	0.00	0.329	0.369	0.373	0.384	0.384	0.362	0.365	0.365	0.269	0.209

Fig. 2-S3 The soil water daily output file of DSSAT, which contains the column named as 'DRNC' and 'IRRC' used for linkage phase 1.

```
set startTime=%time%

:: 2000 Simulation
"A" s B.v47
xcopy /y "C\2000.wel" "D\2000*.wel*"
"E\python.exe" "D\Linkage_Script_for_Phase1_2000.py"
xcopy /y "C\gv18.glo" "D\gv18*.glo*"
xcopy /y "C\gv18_new.lst" "D\gv18_new*.lst*"
xcopy /y "C\step.bas" "D\step*.bas*"
xcopy /y "C\2000.dis" "D\2000*.dis*"
xcopy /y "C\steptr.lpf" "D\steptr*.lpf*"
xcopy /y "C\gv18.zone" "D\gv18*.zone*"
xcopy /y "C\2000.RCH" "D\2000*.RCH*"
xcopy /y "C\2000.chd" "D\2000*.chd*"
xcopy /y "C\GV18.evt" "D\GV18*.evt*"
xcopy /y "C\GMD3.gmg" "D\GMD3*.gmg*"
xcopy /y "C\gv181head.oc" "D\gv181head*.oc*"
xcopy /y "C\2000.hob" "D\2000*.hob*"
xcopy /y "C\2000.obs" "D\2000*.obs*"
xcopy /y "C\2000.str" "D\2000*.str*"
xcopy /y "C\2000._os" "D\2000*._os*"
xcopy /y "C\Base.asp" "D\Base*.asp*"
xcopy /y "C\gv18.cbb" "D\gv18*.cbb*"
xcopy /y "C\KZ.dat" "D\KZ*.dat*"
xcopy /y "C\iniH6.dat" "D\iniH6*.dat*"
xcopy /y "C\kst6.dat" "D\kst6*.dat*"
xcopy /y "C\Sys6.DAT" "D\Sys6*.DAT*"
"C\mf2k_GMS.exe" "C\2000.mfn"
xcopy /y "D\2000.hds" "D\Head values from Linkage Model\2000*.hds*"
xcopy /y "D\2000._os._ww" "D\One to One Plot\2000*._os._ww*"
Del "D\iniH6*.DAT*"
"E\python.exe" "D\Linkage_Script_for_Phase2_2000.py"
xcopy /y "D\KSFY0111.GSX" "F\KSFY0111*.GSX*"
xcopy /y "D\KSFY0121.GSX" "F\KSFY0121*.GSX*"
xcopy /y "D\KSFY0131.GSX" "F\KSFY0131*.GSX*"
xcopy /y "D\KSFY0141.GSX" "F\KSFY0141*.GSX*"
xcopy /y "D\KSFY0151.GSX" "F\KSFY0151*.GSX*"
Del "D\gv18*.glo*"
Del "D\gv18_new*.lst*"
Del "D\step*.bas*"
Del "D\steptr*.lpf*"
Del "D\gv18*.zone*"
Del "D\GV18*.evt*"
Del "D\GMD3*.gmg*"
Del "D\gv181head*.oc*"
Del "D\Base*.asp*"
Del "D\gv18*.cbb*"
Del "D\KZ*.dat*"
Del "D\kst6*.dat*"
Del "D\Sys6*.DAT*"

echo Start Time: %startTime%
echo Finish Time:%time%
pause

Notations:
A - The directory that DSSAT engine is stored.
B - The directory that DSSAT batch file is stored.
C - The directory that MODFLOW input files and an executable file are stored.
D - The directory that all files relative the the linked model are stored.
E - The directory that python language is stored.
F - The directory that DSSAT input files are stored.
```

Fig. 2-S4 A batch file to simulate multiple-year linked modeling system (DSSAT-MODFLOW).

LAT – Latitude Degrees, (decimals)
LONG – Longitude Degrees, (decimals)
ELEV – Elevation, (m)
TAV – Air Temperature Average, (°C)
AMP – Air Temperature Amplitude, monthly average, (°C)
REFHT – Height of Temperature Measurement, (m)
WNDHT – Height of Wind Measurement, (m)
SRAD – Solar Radiation (MJ/m^2*d)
TMAX – Air Temperature Maximum (°C)
TMIN – Air Temperature Minimum (°C)
RAIN – Precipitation (mm)
DEWP – Dew-point Temperature (°C)
WIND – Wind Run (km/day)
PAR – Photosynthetic Active Radiation ($mole/m^2*day$)
RHUM – Relative Humidity

Fig. 2-S5 Definition, Units of weather-related parameters.

```
0
570
56
0
296.875 1.626875 725 615 11.1875 34.375 4.8125 171.875 91.25 13.8125 56.25 537.5 137.5 53.125 418.75 71.25 9.375
121.875 1.626875 725 615 11.1875 34.375 4.8125 171.875 91.25 13.8125 56.25 537.5 137.5 53.125 418.75 71.25 9.375
121.875 1.626875 725 615 11.1875 34.375 4.8125 171.875 91.25 13.8125 56.25 537.5 137.5 53.125 418.75 71.25 9.375
121.875 1.626875 725 615 11.1875 34.375 4.8125 171.875 91.25 13.8125 56.25 537.5 137.5 53.125 418.75 71.25 9.375
121.875 1.626875 725 615 11.1875 34.375 4.8125 171.875 91.25 13.8125 56.25 537.5 137.5 53.125 418.75 71.25 9.375
121.875 1.626875 725 615 11.1875 34.375 4.8125 171.875 91.25 13.8125 56.25 537.5 137.5 53.125 418.75 41.25 9.375
121.875 1.626875 725 615 11.1875 34.375 4.8125 171.875 91.25 13.8125 56.25 537.5 137.5 53.125 418.75 41.25 9.375
121.875 1.626875 725 615 11.1875 34.375 4.8125 171.875 91.25 13.8125 56.25 537.5 137.5 53.125 418.75 41.25 9.375
121.875 1.626875 725 615 11.1875 34.375 4.8125 171.875 91.25 13.8125 56.25 537.5 137.5 53.125 418.75 41.25 9.375
121.875 1.626875 725 615 11.1875 34.375 4.8125 171.875 91.25 13.8125 56.25 537.5 137.5 53.125 418.75 41.25 9.375
121.875 0.631875 725 615 11.1875 34.375 4.8125 171.875 91.25 13.8125 56.25 537.5 137.5 53.125 418.75 41.25 9.375
121.875 0.631875 725 615 11.1875 34.375 4.8125 171.875 101.25 13.8125 56.25 537.5 137.5 53.125 418.75 41.25 9.375
121.875 0.631875 725 615 11.1875 34.375 4.8125 346.875 101.25 13.8125 56.25 537.5 137.5 53.125 418.75 41.25 9.375
121.875 0.631875 725 615 11.1875 34.375 4.8125 346.875 101.25 13.8125 56.25 537.5 137.5 53.125 418.75 41.25 9.375
121.875 0.631875 725 615 11.1875 34.375 4.8125 346.875 101.25 13.8125 56.25 537.5 137.5 53.125 418.75 41.25 9.375
121.875 0.631875 725 615 11.1875 34.375 4.8125 346.875 101.25 13.8125 56.25 537.5 137.5 53.125 418.75 41.25 9.375
121.875 0.631875 725 615 11.1875 34.375 4.8125 346.875 101.25 13.8125 56.25 537.5 137.5 53.125 418.75 41.25 9.375
121.875 0.631875 725 615 11.1875 34.375 4.8125 346.875 101.25 13.8125 56.25 537.5 137.5 53.125 418.75 41.25 9.375
121.875 0.631875 725 615 11.1875 34.375 3.3125 346.875 101.25 13.8125 56.25 537.5 137.5 53.125 418.75 41.25 9.375
121.875 0.631875 725 615 11.1875 34.375 3.3125 346.875 101.25 13.8125 56.25 537.5 137.5 53.125 418.75 41.25 9.375
121.875 0.631875 725 615 11.1875 34.375 3.3125 346.875 101.25 13.8125 56.25 537.5 137.5 53.125 418.75 41.25 9.375
121.875 0.631875 725 615 11.1875 34.375 3.3125 346.875 101.25 13.8125 56.25 537.5 37.5 53.125 418.75 41.25 9.375
121.875 0.631875 725 615 11.1875 34.375 3.3125 346.875 101.25 13.8125 56.25 537.5 37.5 53.125 418.75 41.25 9.375
121.875 0.631875 725 615 11.1875 34.375 3.3125 346.875 101.25 13.8125 56.25 537.5 37.5 53.125 418.75 41.25 9.375
121.875 0.631875 725 615 11.1875 59.375 3.3125 346.875 101.25 13.8125 56.25 537.5 37.5 53.125 418.75 41.25 9.375
121.875 0.631875 725 615 11.1875 59.375 3.3125 346.875 101.25 13.8125 56.25 537.5 37.5 53.125 418.75 41.25 9.375
121.875 0.631875 725 615 11.1875 59.375 3.3125 346.875 101.25 13.8125 56.25 637.5 37.5 53.125 418.75 41.25 9.375
121.875 0.631875 725 615 11.1875 59.375 3.3125 346.875 101.25 13.8125 56.25 637.5 37.5 53.125 418.75 41.25 9.375
121.875 0.631875 725 615 11.1875 59.375 3.3125 346.875 101.25 13.8125 56.25 637.5 37.5 53.125 418.75 41.25 9.375
121.875 0.631875 725 615 11.1875 59.375 3.3125 346.875 101.25 13.8125 56.25 637.5 37.5 53.125 418.75 41.25 9.375
121.875 0.631875 725 615 11.1875 59.375 3.3125 346.875 101.25 13.8125 56.25 637.5 37.5 53.125 418.75 41.25 9.375
121.875 0.631875 725 615 11.1875 59.375 3.3125 346.875 101.25 13.8125 56.25 637.5 37.5 53.125 418.75 41.25 9.375
121.875 0.631875 725 615 11.1875 59.375 3.3125 346.875 101.25 13.8125 56.25 637.5 37.5 53.125 418.75 41.25 9.375
121.875 0.631875 725 615 11.1875 59.375 3.3125 346.875 101.25 13.8125 56.25 637.5 37.5 53.125 418.75 41.25 9.375
121.875 0.631875 925 615 11.1875 59.375 3.3125 346.875 101.25 13.8125 56.25 637.5 37.5 53.125 418.75 41.25 9.375
121.875 0.631875 925 615 11.1875 59.375 3.3125 346.875 101.25 13.8125 56.25 637.5 37.5 53.125 568.75 41.25 9.375
Correlation Matrix:
1 0 0 0 0 0 0 0 0 0 0 0 0 0 0 0 0
0 1 0 0 0 0 0 0 0 0 0 0 0 0 0 0 0
0 0 1 0 0 0 0 0 0 0 0 0 0 0 0 0 0
0 0 0 1 0 0 0 0 0 0 0 0 0 0 0 0 0
0 0 0 0 1 0 0 0 0 0 0 0 0 0 0 0 0
0 0 0 0 0 1 0 0 0 0 0 0 0 0 0 0 0
0 0 0 0 0 0 1 0 0 0 0 0 0 0 0 0 0
0 0 0 0 0 0 0 1 0 0 0 0 0 0 0 0 0
0 0 0 0 0 0 0 0 1 0 0 0 0 0 0 0 0
0 0 0 0 0 0 0 0 0 1 0 0 0 0 0 0 0
0 0 0 0 0 0 0 0 0 0 1 0 0 0 0 0 0
0 0 0 0 0 0 0 0 0 0 0 1 0 0 0 0 0
0 0 0 0 0 0 0 0 0 0 0 0 1 0 0 0 0
0 0 0 0 0 0 0 0 0 0 0 0 0 1 0 0 0
0 0 0 0 0 0 0 0 0 0 0 0 0 0 1 0 0
0 0 0 0 0 0 0 0 0 0 0 0 0 0 0 1 0
0 0 0 0 0 0 0 0 0 0 0 0 0 0 0 0 1
0 0 0 0 0 0 0 0 0 0 0 0 0 0 0 0 0
0 0 0 0 0 0 0 0 0 0 0 0 0 0 0 0 0
0 0 0 0 0 0 0 0 0 0 0 0 0 0 0 0 0
0 0 0 0 0 0 0 0 0 0 0 0 0 0 0 0 0
0 0 0 0 0 0 0 0 0 0 0 0 0 0 0 0 0
0 0 0 0 0 0 0 0 0 0 0 0 0 0 0 0 0
0 0 0 0 0 0 0 0 0 0 0 0 0 0 0 0 0
0 0 0 0 0 0 0 0 0 0 0 0 0 0 0 0 0
0 0 0 0 0 0 0 0 0 0 0 0 0 0 0 0 0
Stein Information:

0
0
0
2
4
Morris
8
10
570
56
200000000
Elementary effects
-1
0
26
46
37
15
31
17
52
27
1
8
7
21
39
22
42
51
6
33
19
12
```

Fig. 3-S1 An example of a sample file for Morris screening method.

The primary MACA statistically downscaled variable outputs directly obtained by University of Idaho for each model are described below:

- tasmax (daily near-surface maximum temperature in Kelvin)
- tasmin (daily near-surface minimum temperature in Kelvin)
- prec (daily accumulated precipitation in millimeters)
- uas (daily mean 10m eastward wind in meters per second)
- vas (daily mean 10m northward wind in meters per second)
- rhsmax (daily near-surface maximum relative humidity (%))
- rhsmin (daily near-surface minimum relative humidity (%))
- rsds (daily mean surface downwelling shortwave radiation flux in Watts per meter squared)

Fig. 4-S1 The definition and unit of variables derived by MACA.

Calculation for primary variables:

- Wind speed (m/s): to derive daily wind speed, the square root of the added values of the squares of uas and vas was calculated (e.g. sqrt (uas^2 + vas^2). Wind speed was estimated at 2 meters using FAO wind profile relationship approximation (Allen et al., 1998).
- Wind run (km/day): wind speed was multiplied by a factor of 86.4
- Solar radiation (mJ/m2-day): to derive daily solar radiation in mJ per meters squared per day, daily rsds was multiplied by a factor of 0.0864.
- Elevation (m): the elevation raster was used from the METDATA climatology lab (http://www.climatologylab.org/gridmet.html). METDATA elevation coordinates were linearly interpolated to the MACA grid coordinates.
- Relative humidity (fraction or %) and dewpoint temperature (deg. C): to derive daily relative humidity and dew point temperature, the average of the daily minimum and maximum humidity were calculated, and then daily average dew point temperature was computed using the daily average temperature and relative humidity.
- Potential Evapotranspiration (PET in mm): the Penman-Monteith methodology was used in the manual "The ASCE Standardized Reference Evapotranspiration Equation". The short crop reference equation and the ET-methodology which uses the maximum and minimum relative humidities since these variables were downscaled.

Fig. 4-S2 Details of computation of downscaled variables.

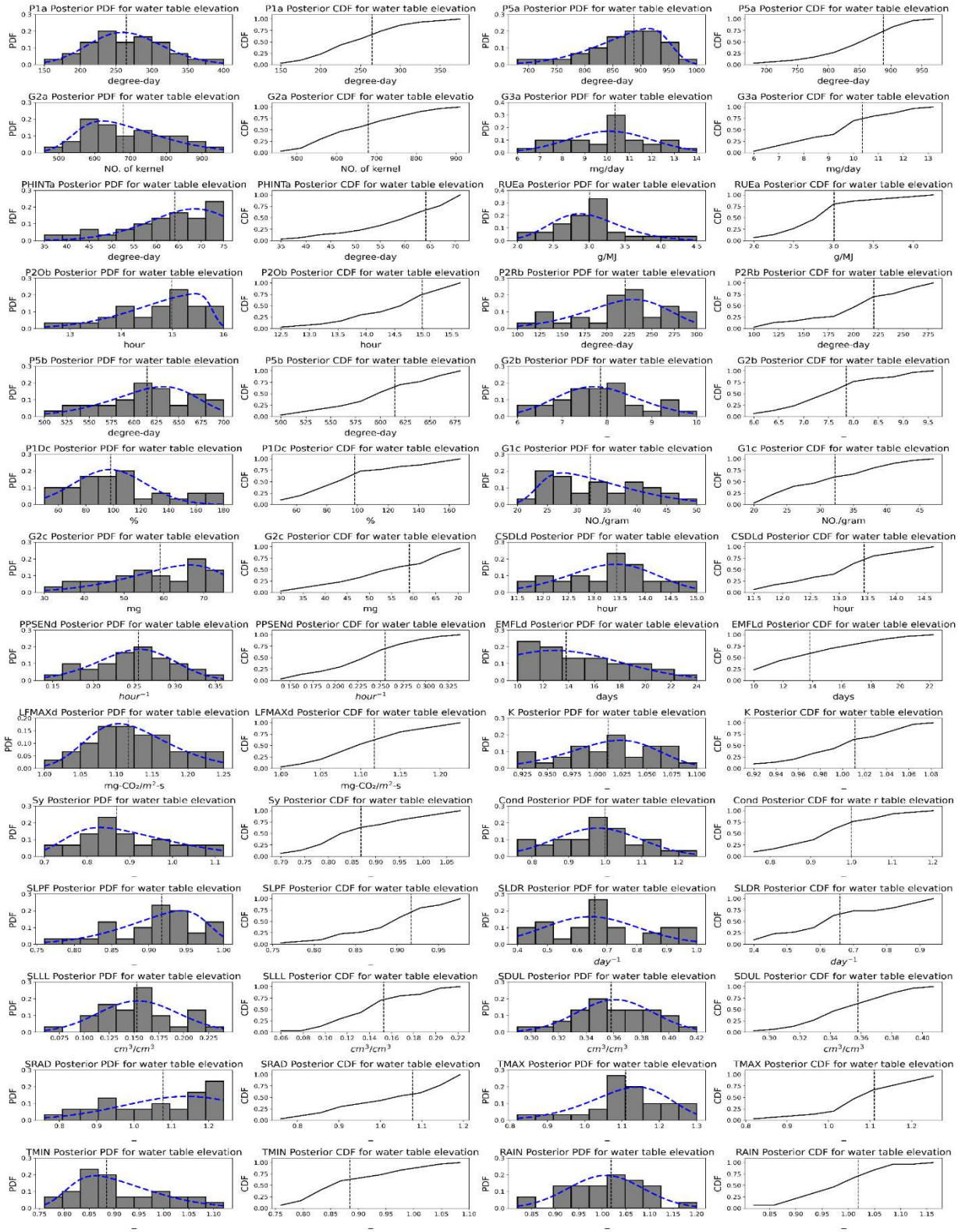

Fig. 4-S3 Posterior distributions of PDFs and CDFs for 28 parameters for water table elevation for the top 1% of the 14,848 simulations.

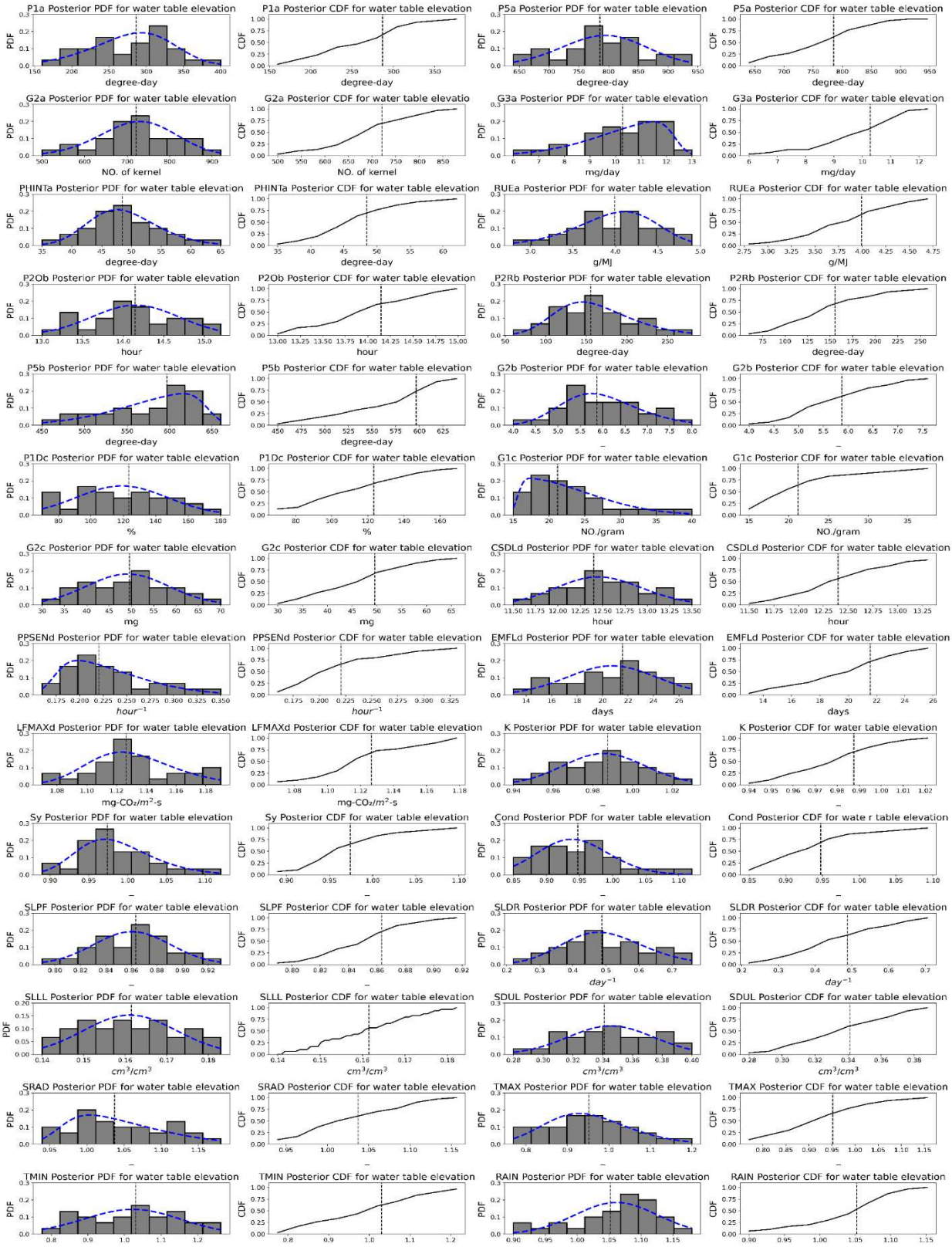

Fig. 4-S4 Posterior distributions of PDFs and CDFs for 28 parameters for maize for the top 1% of the 14,848 simulations.

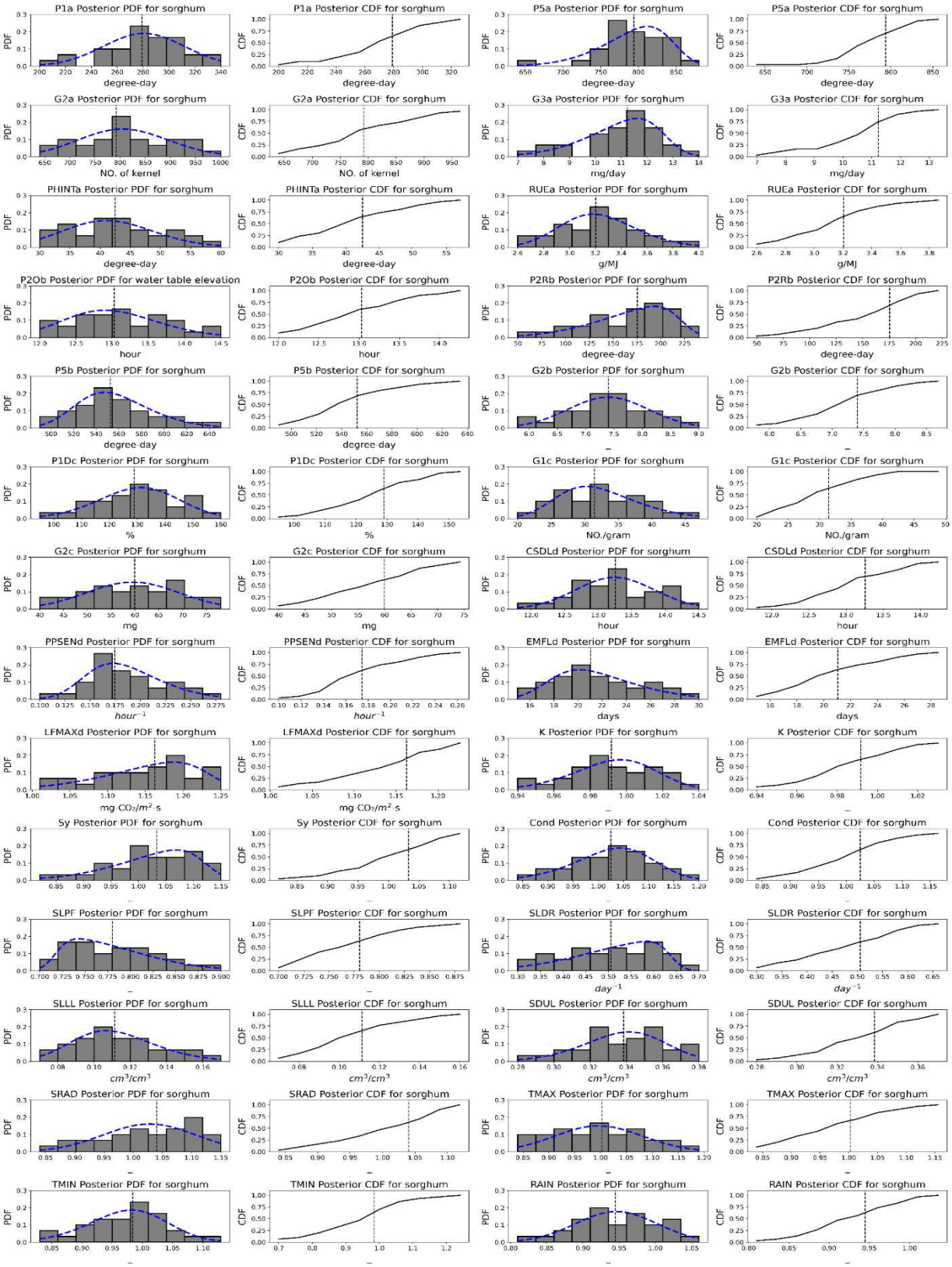

Fig. 4-S5 Posterior distributions of PDFs and CDFs for 28 parameters for sorghum for the top 1% of the 14,848 simulations.

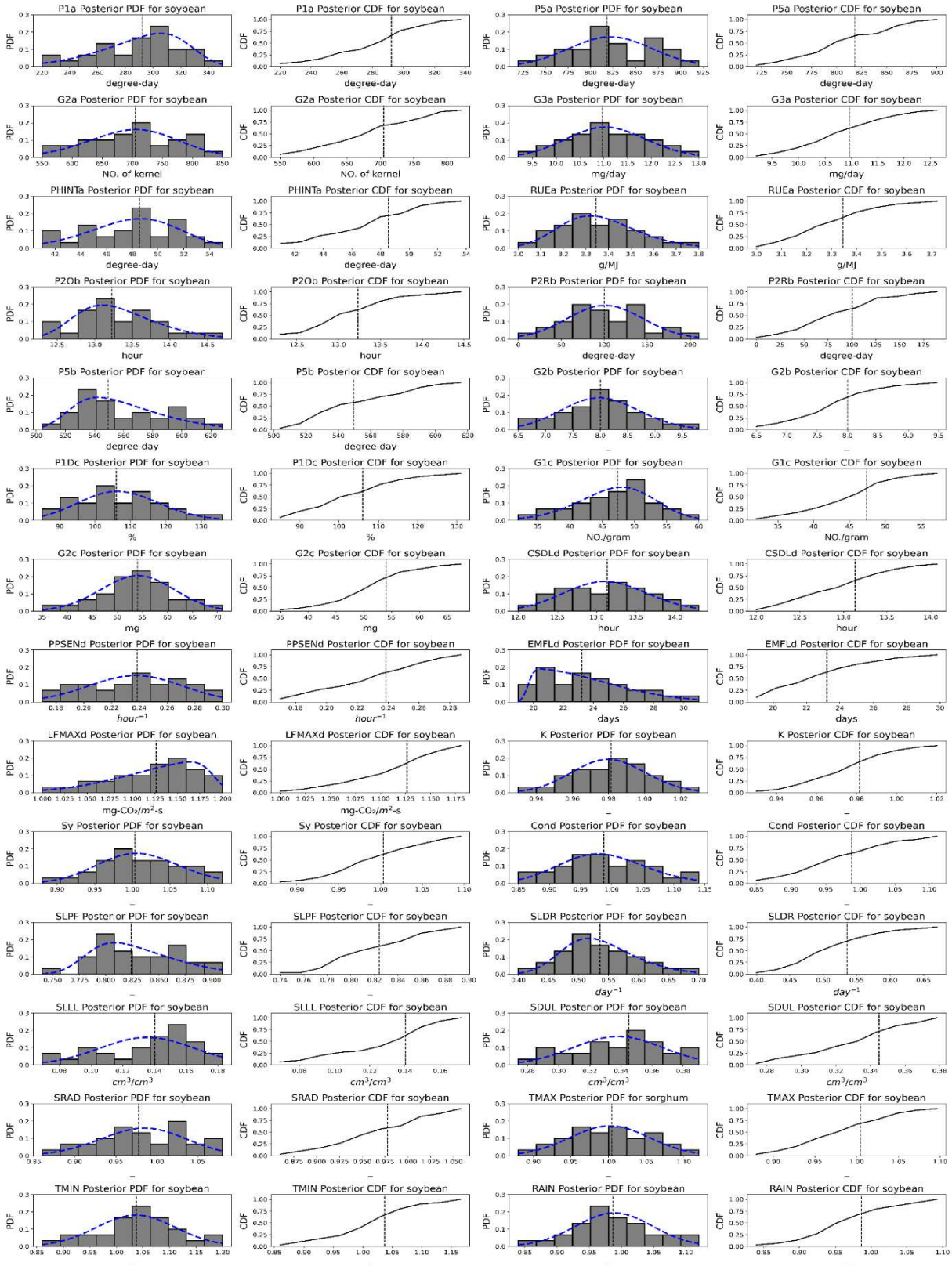

Fig. 4-S6 Posterior distributions of PDFs and CDFs for 28 parameters for soybean for the top 1% of the 14,848 simulations.

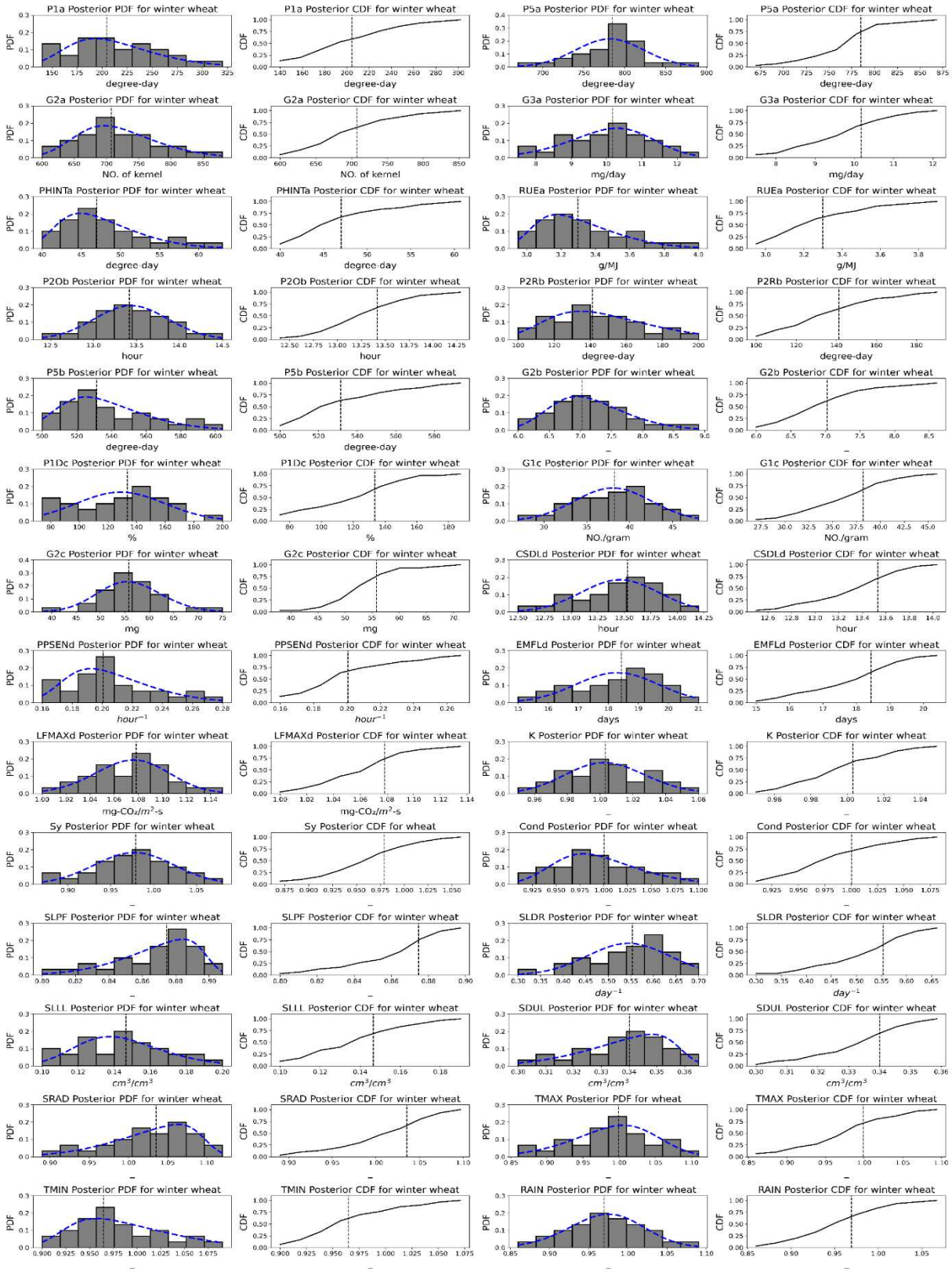

Fig. 4-S7 Posterior distributions of PDFs and CDFs for 28 parameters for winter wheat for the top 1% of the 14,848 simulations.

Tab. 4-S1 Water Use Profit (WUP) (x10^8 U.S. Dollars of crop yield per m of groundwater drawdown) for maize, soybean, winter wheat, and sorghum under future wet climate conditions.

Crop Type and Climate Conditions	Water Use Profit for 12 combinations of management scenarios (*x10^8* ***U.S. Dollar/m***)											
	1	2	3	4	5	6	7	8	9	10	11	12
Corn_wet_RCP4.5	0.9789	1.6958	2.4396	0.9489	1.6963	2.9917	0.9886	1.7627	3.1187	1.0184	1.8183	3.2297
Corn_wet_RCP8.5	0.4073	0.7687	1.4508	0.4998	0.9327	1.7861	0.528	0.9768	1.8833	0.5507	1.0287	2.0006
Soybean_wet_RCP4.5	0.042	0.0704	0.0958	0.0401	0.0679	0.1144	0.0415	0.0704	0.1183	0.0425	0.0723	0.1217
Soybean_wet_RCP8.5	0.0269	0.0494	0.0899	0.0323	0.0596	0.1109	0.0332	0.0621	0.1158	0.0347	0.065	0.1222
Winter Wheat_wet_RCP4.5	0.3819	1.1545	1.5916	0.4518	1.1698	1.7969	0.5086	1.2129	1.8392	0.5452	1.2779	1.8777
Winter Wheat_wet_RCP8.5	0.0683	0.4941	1.1163	0.1791	0.727	1.3511	0.2064	0.7707	1.4311	0.2503	0.8114	1.4835
Sorghum_wet_RCP4.5	0.1365	0.3208	0.6481	0.1394	0.3525	0.8591	0.1483	0.3773	0.9112	0.1648	0.3953	0.9706
Sorghum_wet_RCP8.5	0.0437	0.204	0.6085	0.081	0.2958	0.7925	0.093	0.3134	0.861	0.106	0.3316	0.9418

1- surface, full; 2 – surface, half; 3 – surface, quarter; 4 – sprinkler, full; 5 – sprinkler, half; 6 – sprinkler, quarter; 7 – center pivot, full; 8 – center pivot, half; 9 – center pivot, quarter; 10 – drip, full; 11 – drip, half; 12 – drip, quarter. Light blue means only acceptable for crop yield; light red means only acceptable for groundwater drawdown; light purple means acceptable for both.

Tab. 4-S2 Water Use Profit (WUP) (x10^8 U.S. Dollars of crop yield per m of groundwater drawdown) for maize, soybean, winter wheat, and sorghum under future average climate conditions.

Crop Type and Climate Conditions	Water Use Profit for 12 combinations of management scenarios (*x10^8* ***U.S. Dollar/m***)											
	1	2	3	4	5	6	7	8	9	10	11	12
Corn_avg._RCP4.5	0.4508	0.8895	1.9523	0.6035	1.0751	2.4333	0.6298	1.3717	2.005	0.6537	1.1676	2.0804
Corn_avg._RCP8.5	0.539	0.9947	1.7594	0.6683	1.199	2.162	0.7159	1.2436	2.2641	0.726	1.3201	2.1538
Soybean_avg._RCP4.5	0.0279	0.0489	0.107	0.0332	0.0586	0.1315	0.0342	0.0753	0.1056	0.0357	0.0626	0.1085
Soybean_avg._RCP8.5	0.0254	0.0459	0.0797	0.0308	0.0538	0.0968	0.0327	0.0562	0.1007	0.0332	0.0596	0.0948
Winter Wheat_avg._RCP4.5	0.0999	0.5354	1.3183	0.2198	0.7731	1.4895	0.2613	1.0808	1.4671	0.3036	0.8567	1.534
Winter Wheat_avg._RCP8.5	0.2181	0.68	1.4343	0.35	0.8864	1.6214	0.3773	1.024	1.6317	0.4081	1.0369	1.6653
Sorghum_avg._RCP4.5	0.0377	0.1269	0.6726	0.0615	0.1932	0.6894	0.0673	0.2365	0.6954	0.0759	0.2184	0.744
Sorghum_avg._RCP8.5	0.0795	0.3021	0.6327	0.1632	0.3838	0.8115	0.1867	0.4116	0.8641	0.1961	0.4405	0.8218

1- surface, full; 2 – surface, half; 3 – surface, quarter; 4 – sprinkler, full; 5 – sprinkler, half; 6 – sprinkler, quarter; 7 – center pivot, full; 8 – center pivot, half; 9 – center pivot, quarter; 10 – drip, full; 11 – drip, half; 12 – drip, quarter. Light blue means only acceptable for crop yield; light red means only acceptable for groundwater drawdown; light purple means acceptable for both.

Tab. 4-S3 Water Use Profit (WUP) (x10^8 U.S. Dollars of crop yield per m of groundwater drawdown) for maize, soybean, winter wheat, and sorghum under future dry climate conditions.

Crop Type and Climate Conditions	Water Use Profit for 12 combinations of management scenarios (*x10^8* ***U.S. Dollar/m***)											
	1	2	3	4	5	6	7	8	9	10	11	12
Corn_dry_RCP4.5	0.6	1.096	1.8767	0.7412	1.3067	2.2878	0.7727	1.5871	2.3809	0.8004	1.4072	2.4689
Corn_dry_RCP8.5	0.4571	0.803	1.265	0.5847	0.8879	1.5494	0.6258	0.9219	1.6155	0.6483	0.8912	1.6831
Soybean_dry_RCP4.5	0.0274	0.0464	0.0782	0.0323	0.0552	0.0938	0.0332	0.0674	0.0972	0.0342	0.0591	0.1007
Soybean_dry_RCP8.5	0.0313	0.0445	0.0738	0.0367	0.0528	0.0899	0.0376	0.0542	0.0928	0.0391	0.0557	0.0963
Winter Wheat_dry_RCP4.5	0.0723	0.5384	1.2203	0.2007	0.763	1.4633	0.2624	1.0347	1.5029	0.3025	0.8458	1.5526
Winter Wheat_dry_RCP8.5	0.0046	0.291	0.8791	0.1016	0.5053	1.0934	0.1368	0.5602	1.1261	0.1633	0.6069	1.1622
Sorghum_dry_RCP4.5	0.0329	0.0971	0.29	0.0497	0.1367	0.4251	0.0543	0.1817	0.4621	0.0596	0.1663	0.5176
Sorghum_dry_RCP8.5	0.0704	0.2026	0.2788	0.1122	0.2838	0.4114	0.1245	0.298	0.464	0.1447	0.2987	0.5368

1- surface, full; 2 – surface, half; 3 – surface, quarter; 4 – sprinkler, full; 5 – sprinkler, half; 6 – sprinkler, quarter; 7 – center pivot, full; 8 – center pivot, half; 9 – center pivot, quarter; 10 – drip, full; 11 – drip, half; 12 – drip, quarter. Light blue means only acceptable for crop yield; light red means only acceptable for groundwater drawdown; light purple means acceptable for both.